

Analytical and Testing Methods for Rating Longitudinal Laminated Timber Slab Bridges

Justin Dahlberg, PE
Zhengyu Liu, PhD, PE
Brent Phares, PhD, PE
James Wacker

Bridge Engineering Center
Iowa State University
Ames, Iowa

WisDOT ID no. 0092-20-01

December 2021



RESEARCH & LIBRARY UNIT



WISCONSIN HIGHWAY RESEARCH PROGRAM

WISCONSIN DOT
PUTTING RESEARCH TO WORK

Technical Report Documentation Page

1. Report No. WisDOT ID no. 0092-20-01		2. Government Accession No		3. Recipient's Catalog No	
4. Title and Subtitle Analytical and Testing Methods for Rating Longitudinal Laminated Timber Slab Bridges				5. Report Date December 2021	
				6. Performing Organization Code	
7. Authors Justin Dahlberg, Zhengyu Liu, Brent M. Phares, and James Wacker				8. Performing Organization Report No.	
9. Performing Organization Name and Address Bridge Engineering Center Iowa State University 2711 South Loop Drive, Suite 4700 Ames, IA 50010-8664				10. Work Unit No. (TRAIS)	
				11. Contract or Grant No.	
12. Sponsoring Agency Name and Address Wisconsin Department of Transportation Research & Library Unit 4802 Sheboygan Ave. Rm 104 Madison, WI 53707				13. Type of Report and Period Covered Final Report	
				14. Sponsoring Agency Code	
15. Supplementary Notes					
16. Abstract The Wisconsin Department of Transportation recognizes the importance of accurately assessing the timber deck slab bridge inventory within the state. Of the 571 timber bridges in Wisconsin, 450 bridges are timber slab bridges. Current methods of load rating employ equations first developed in the later 1980s and early 1990s for determining the equivalent strip width. These equations often produce results that unnecessarily penalize the bridge by requiring a posted weight limit. Through a program of bridge live load tests and analytical modeling, the researchers in this study have both measured and modeled the bridge behavior with more accuracy and have shown the current equivalent strip width calculation methodologies to be conservative, as was originally speculated. Ten unique bridges were tested a part of this study. Three of them were tested twice; once before and once after bridge strengthening measures were employed. An equation to calculate the equivalent strip width was developed with numerous variables in mind.					
17. Key Words Timber slab bridge, load distribution			18. Distribution Statement		
18. Security Classif.(of this report) Unclassified		19. Security Classif. (of this page) Unclassified		20. No. of Pages 113	21. Price

Disclaimer

This research was funded through the Wisconsin Highway Research Program by the Wisconsin Department of Transportation and the Federal Highway Administration under Project 0092-20-01. The contents of this report reflect the views of the authors who are responsible for the facts and accuracy of the data presented herein. The contents do not necessarily reflect the official views of the Wisconsin Department of Transportation or the Federal Highway Administration at the time of publication.

This document is disseminated under the sponsorship of the Department of Transportation in the interest of information exchange. The United States Government assumes no liability for its contents or use thereof. This report does not constitute a standard, specification or regulation.

The United States Government does not endorse products or manufacturers. Trade and manufacturers' names appear in this report only because they are considered essential to the object of the document.

1 TABLE OF CONTENTS

Executive Summary.....	xi
1 Introduction	1
1.1 Background.....	1
1.2 Research Objective.....	2
1.3 Research Plan	2
1.4 Interim Report.....	2
1.5 Final Report	2
2 Literature Review	3
2.1 Wheel Load Distribution Width on Timber Slab Bridges.....	3
2.2 Retrofit Techniques for Longitudinal Timber Slab Bridge	5
2.2.1 Spreader beam.....	5
2.2.2 Post-tensioning	7
2.2.3 Transverse spreader deck panels.....	8
2.3 FE Modeling of Longitudinal Timber Slab Bridge	8
3 Summary of DOT Practices	11
3.1 State DOT Practice.....	11
3.1.1 Identification of states of interests.....	11
3.1.2 Results for the state practice review	12
3.1.3 Conclusions from the state practice review	16
3.2 Use of Timber Slab Bridges in Wisconsin	17
4 Field Evaluation Program.....	20
4.1 Load Test Program.....	20
4.1.1 Bridge candidates.....	20
4.1.2 Load test procedures	24
4.1.3 Instrumentation plan	28
4.2 Load Test Results.....	30
4.2.1 Basic theory on calculation of equivalent wheel load width	30
4.2.2 Equivalent wheel load width from field tests	31
4.2.3 Multiple Lanes Loaded	34
4.2.4 Retrofit Effectiveness	37
4.2.5 Bridges Designed by AASHTO LRFD.....	39
4.3 In-Situ Timber Inspection	47
4.3.1 Visual Observation	47
4.3.2 Moisture Results	49
4.3.3 Comparison with AASHTO and WisDOT policy	50
4.3.4 Timber Evaluation using Micro-drill.....	50
4.3.5 Micro-drill Procedure	50
4.3.6 Micro-drill results.....	51
5 Numerical Modeling	62
5.1 Model Development.....	62
5.2 Model Validation	64
5.3 Parametric Study	69
5.3.1 Parameters of interests.....	69
5.3.2 Parametric study results	71

6	Development of Recommendations	74
	6.1 Comparison with Current AASHTO Code and Wisconsin Specification	74
	6.2 Development of the ESW Equation	75
	6.2.1 Spreader Beam	76
	6.2.2 Spreader Beam Material	79
	6.2.3 Transverse Spreader Deck	79
	6.2.4 Multiple Lanes Loaded	80
	6.3 Validation of Proposed Equation	80
	6.4 Recommendations	82
	6.4.1 Summary	82
	6.4.2 Limitations	82
7	Load Testing Process	83
	7.1.1 Introduction	83
	7.1.2 Load Testing Procedure	84
8	Summary	87
9	References	88
10	Appendix	91
	10.1 Appendix A: Bridge Information	92
	10.1.1 Appendix A.1 B030174 BARRON COUNTY	92
	10.1.2 Appendix A.2 P030079 BARRON COUNTY	93
	10.1.3 Appendix A.3 P320064 LA CROSSE COUNTY	94
	10.1.4 Appendix A.4 P320083 LA CROSSE COUNTY	95
	10.1.5 Appendix A.5 P320110 LA CROSSE COUNTY	96
	10.1.6 Appendix A.6 P410140 MONROE COUNTY	97
	10.1.7 Appendix A.7 P410923 MONROE COUNTY	98
	10.1.8 Appendix A.8 P410953 MONROE COUNTY	99
	10.1.9 Appendix A.9 B410315 MONROE COUNTY	100
	10.1.10 Appendix A.10 P410948 MONROE COUNTY	101
	10.2 Appendix B: ESW Calculation Example	102

2 LIST OF FIGURES

Figure 2-1 Types of transverse stiffener beam connections (Wipf 1986)	6
Figure 2-2 Post-tensining anchorage systems (Ekholm 2013)	8
Figure 2-3 Cross-section view of timber slab bridge with transverse timber deck on top.....	8
Figure 3-1 Nationwide distribution of timber slab bridge	11
Figure 3-2 Prestressing detail for rehabilitation of existing decks (USFS 1990)	15
Figure 3-3 Timber slab bridge locations in Wisconsin	17
Figure 3-4 Timber slab bridge distribution by county in Wisconsin	18
Figure 3-5 Timber slab bridges in Wisconsin disributed by year of construction.....	18
Figure 3-6 Posted capacity of timber slab bridges in Wisconsin	19
Figure 3-7 Timber slab bridges in Wisconsin distributed by main span length	19
Figure 3-8 Timber slab bridges in Wisconsin distributed by bridge deck width	19
Figure 4-1 Locations for the bridges selected for the field test.....	20
Figure 4-2 Typical superstructure cross-section view.....	21
Figure 4-3 La Crosse County – P320064.....	23
Figure 4-4 La Crosse County – P320083.....	23
Figure 4-5 La Crosse County – P320110.....	23
Figure 4-6 Barron County – P030079.....	23
Figure 4-7 Barron County – B030174.....	23
Figure 4-8 Monroe County – B410315.....	23
Figure 4-9 Monroe County – P410140.....	24
Figure 4-10 Monroe County – P410923.....	24
Figure 4-11 Monroe County – P410948.....	24
Figure 4-12 Monroe County – P410953.....	24
Figure 4-13 Load truck crossing the bridge.....	25
Figure 4-14 Transverse position of the truck for each load case.....	26
Figure 4-15 Truck parked at position of maximum strain response for survey data collection.....	26
Figure 4-16 Axle and tire dimensions for each load truck	27
Figure 4-17 Cross-section view of general instrumentation plan.....	29
Figure 4-18 Side view of typical bridge instrumentation.....	29
Figure 4-19 Data collection locations by surveying equipment.....	29
Figure 4-20 Typcial bridge instrumentation	30
Figure 4-21 Strain distribution	31
Figure 4-22 Typical Strain Time History	31
Figure 4-23 Equivalent Strip Width Superimposed on Strain Time History.....	32
Figure 4-24 Example of Range formed by Discrete ESW Calculations.....	32
Figure 4-25 Example of Cumulative Distribution Function.....	33
Figure 4-26 Example of Single Bridge Cumulative Distribution Functions for Each Load Case	33
Figure 4-27 Combined CDFs for All Load Cases	34
Figure 4-28 Combined CDFs by Load Case.....	34
Figure 4-29 Two lanes loaded.....	35
Figure 4-30 Idealized transverse strain distribution for multiple lanes loaded.....	35
Figure 4-31 ESW Comparison for Combined Load Cases 2 and 4 for Bridge P410948.....	36
Figure 4-32 ESW Comparison for Combined Load Cases 2 and 4 for Bridge P320064.....	36
Figure 4-33 ESW Comparison for Combined Load Cases 2 and 4 for Bridge B030174.....	37
Figure 4-34 La Crosse County Deck Retrofit	37
Figure 4-35 Transverse Timber Slab Retrofit under Construction	38

Figure 4-36 CDFs for Bridge P320064 Before and After Retrofit	38
Figure 4-37 CDFs for Bridge P320083 Before and After Retrofit	39
Figure 4-38 CDFs for Bridge P320110 Before and After Retrofit	39
Figure 4-39 Monroe County Bridge B410315.....	40
Figure 4-40 AASHTO LRFD Designed Bridge Cross-section	40
Figure 4-41 CDFs for Bridge B410315	41
Figure 4-42 Monroe County Bridge B410315	42
Figure 4-43 Sauk County Bridge B560224.....	42
Figure 4-44 Monroe County Bridge B410315 Plan View	43
Figure 4-45 Monroe County Bridge B410315 Section View	43
Figure 4-46 Sauk County Bridge B560224 Plan View	44
Figure 4-47 Sauk County Bridge B560224 Section View	44
Figure 4-48 Monroe County Bridge B410315 Spreader Beams.....	45
Figure 4-49 Sauk County Bridge B560224 Spreader Beam	45
Figure 4-50 LRFD Bridge Load Vehicles.....	46
Figure 4-51 CDF Comparison of Monroe (grey) and Sauk County (black) LRFD Bridges	46
Figure 4-52 Missing shims or gapping between spreader beam and bottom side of deck (La Crosse Co. P320083).....	47
Figure 4-53 Cracked Lamination (La Crosse Co. P320083)	48
Figure 4-54 Cracked Lamination (La Crosse Co. P320083)	48
Figure 4-55 Vegetation in Curb Gutters (Barron Co. B030174)	49
Figure 4-56 Delamination near edge of slab (Monroe Co. P410953)	49
Figure 4-57 Micro-drill Assessment (La Crosse Co. P320110).....	50
Figure 4-58 Example Plot of Micro-drill Results.....	51
Figure 5-1 FE model detailing	63
Figure 5-2 Model calibration results from LC1 (La Crosse Co. P320110).....	65
Figure 5-3 Model calibration results from LC3 (La Crosse Co. P320110).....	66
Figure 5-4 Exaggerated deformed shape (La Crosse Co. P320110)	67
Figure 6-1 Comparison between the field data and codified values	75
Figure 6-2 ESW with respect to <i>ELIL /ESIS</i>	78
Figure 6-3 ESW with respect to <i>ELIL /ESIS × HLHS</i>	78
Figure 6-4 Validation of equation by field test data	81
Figure 6-5 Validation of equation by parametric study results	81
Figure 7-1 Deflection data collected via LVDTs.....	83
Figure 7-2 Deflection data collected via total station.....	84
 APPENDIX FIGURES	
Figure A. 1 Bridge photos for B030174.....	92
Figure A. 2 Bridge photos for P320079	93
Figure A. 3 Bridge photos for P320064	94
Figure A. 4 Bridge photos for P320083	95
Figure A. 5 Bridge photos for P320110	96
Figure A. 6 Bridge photos for P410140	97
Figure A. 7 Bridge photos for P410923	98
Figure A. 8 Bridge photos for P410953	99
Figure A. 9 Bridge photos for B410315.....	100
Figure A. 10 Bridge photos for P410948	101

3 LIST OF TABLES

Table 2-1 AASHTO multiple presence “m” factors.....	5
Table 2-2 FE model details.....	10
Table 3-1 Summary of design practices.....	13
Table 3-2 Summary of practice on retrofit and strengthening methods.....	14
Table 4-1 Bridges selected for the field testing.....	22
Table 5-1 Modeling details.....	64
Table 5-2 Model calibration results.....	68
Table 5-3 Model matrix for parametric study of La Crosse Co. P320110.....	70
Table 5-4 Parametric study results.....	71
Table 6-1 Model calibration results of spreader beam variations.....	77
Table 6-2 Value of αT	79

EXECUTIVE SUMMARY

The Wisconsin Department of Transportation recognizes the importance of accurately assessing the timber deck slab bridge inventory within the state. Of the 571 timber bridges in Wisconsin, 450 bridges are timber slab bridges. Current methods of load rating employ equations first developed in the later 1980s and early 1990s for determining the equivalent strip width. These equations often produce results that unnecessarily penalize the bridge by requiring a posted weight limit.

Through a program of bridge live load tests and analytical modeling, the researchers in this study have both measured and modeled the bridge behavior with more accuracy and have shown the current equivalent strip width calculation methodologies to be conservative, as was originally speculated. Ten unique bridges were tested a part of this study. Three of them were tested twice; once before and once after bridge strengthening measures were employed. An equation to calculate the equivalent strip width was developed with numerous variables in mind.

The equivalent strip width is shown to be a function of the ratio of longitudinal and transverse stiffness of the timber slab deck. Accordingly, where bridge strengthening or rehabilitation methods are being considered, it is to the benefit of the structural capacity to be mindful of this relationship. Ways to increase the transverse stiffness are provided within this report.

Load testing has proven to be extremely beneficial in developing the models and recommendations. The resulting equation for calculating the equivalent strip width is considered to be a good representation of actual structural behavior. Nonetheless, the steps required to complete additional live load testing are provided so any bridge can be tested in the future if deemed necessary.

1 INTRODUCTION

1.1 Background

The Wisconsin Department of Transportation (WisDOT) has an important responsibility to provide safe and efficient transportation infrastructure for the travelling public. This is achieved by ensuring that assets operate reliably while also limiting unnecessary restrictions to bridge traffic. As such, any decision to load post a bridge must ensure safety while also not being overly restrictive. WisDOT has recognized that there are many challenges in assessing bridge condition/performance and, as a result, has been updating their bridge load-rating program to include more data analytics, especially for their timber bridge inventory.

Of the 571 timber bridges in Wisconsin, 450 bridges are timber slab bridges. The most prevalent type of timber deck slab bridges are a nail- or spike-laminated bridge system. Traditional codified load rating methods continue to be the most prominent method used for load rating bridges including these types of bridges. However, in the last 10 to 15 years there has been notable research and implementation related to using load testing of bridges to either perform or improve a bridge rating. While a conventional load rating is less expensive, the load testing method has been proven much more accurate and shown to reduce the number of bridges that are unnecessarily embargoed (Hosteng et al., 2009). Empirical equations in relevant AASHTO bridge design and rating specifications provide details for completing a conventional load rating that characterizes global behaviors. For timber slab bridges, specifically, these specifications define the live load distribution on the deck system. However, questions regarding parameters such as deck overburden (overlay) and the influence of tire width on load distribution remain unanswered. Even more, there is a lack of guidance as to how to handle spreader beams (a component of deck slab bridges) and their inclusion in the load rating process.

Research has shown that the process of inspecting, load testing, and modeling representative bridge structures provides a means to accurately calibrate analytical bridge models for purposes such as load ratings (Fanous et al., 2010; Hosteng et al., 2009; Wipf et al., 1986). Furthermore, once a baseline performance metric is attained from the live load testing, various retrofit techniques can be implemented into the analytical model to evaluate their efficacy at improving load distribution. Combined analytical and experimental research helps better understand critical bridge behavior and contributes to more effective and accurate load rating computations.

A previous analytical and field-testing study completed by the Iowa State University (ISU) team for multiple longitudinal glue-laminated deck slab bridges compared the calculated live load distribution from the LRFD AASHTO Specification to distribution from field-testing (Fanous, et al., 2010). The lane load distribution factors from the field-testing were typically improved when compared to the codified specifications. The analytical comparisons with the AASHTO specifications showed similar results. The analytical study also investigated the effect of spreader beams spacing and found that the lane load distribution factor improves with more stiffener beams. The ISU team has tested multiple bridges on secondary roads in Iowa to determine load distribution for heavy agriculture vehicles (Phares 2017), which resulted in recommendations for updated distribution factor equations. Additionally, more than ten embargoed bridges were load tested on the secondary roads system in Iowa for the Iowa DOT (Hosteng 2009). In 2004, the research team conducted live load tests and load distribution calculations for numerous timber bridges across the country (Hosteng 2005). In all cases considered in these studies, live load tests verified the safe load capacity of the bridges and more often than not resulted in removal of the load posting, or at a minimum increase in the posted load capacity.

1.2 Research Objective

The primary focus of this research project is to develop data-driven wheel-load distribution width recommendations for use in load rating of timber slab deck bridges. The major goals of the work include:

- 1) developing updated wheel load distribution width equations through physical load testing and analytical modeling of longitudinal timber slab bridges,
- 2) investigating various retrofit techniques for potentially increasing the live load capacity of timber slab bridges, communicating a procedure for conducting future load testing and establishing proof legal load capacity of similar bridges,
- 3) reducing the number of timber slab bridges with over conservative load postings.

1.3 Research Plan

In order to achieve the objectives mentioned above, multiple tasks were proposed at the beginning of the research work. The title of each task was listed as below:

Task A: Literature Review and Assessment of Current Practices

Task B: Summary of Other DOT Practices

Task C: Formulate and Present Analytical and Technical Field Evaluation Program

Task D: Conduct Analytical Evaluation Program

Task E: Conduct Field Testing Program

Task F: Conduct In-Situ Timber Inspection

Task G: Develop Wheel Load Distribution Width Recommendations

Task H: Evaluate Longitudinal Timber Slab Retrofit Techniques

Task I: Develop Recommendations, Guidelines and Presentation Materials for WisDOT

Task J: Develop Process/Specification for Load Testing Timber Slab Bridges

Task K: Final Reporting

1.4 Interim Report

The first phase of the research including Tasks A, B, and C, was conducted to collect the relative information from past literature and national and statewide bridge design and maintenance manuals. This interim report was drafted at the end of Task C to deliver the information to WisDOT. In addition, this interim report included a detailed research plan for the future field testing and analytical modeling work based on the collected data.

1.5 Final Report

In this report the results from the Task A are presented in Chapter 2 for the literature review and a summary of state DOT practices in Chapter 3. The field evaluation program is discussed in Chapter 4. In Chapter 5, the analytical modeling of timber bridges is presented. Chapter 6 presents recommendations and guidelines for timber slab assessment. Finally, in Chapter 7 the load testing procedures are presented for any future load testing that may be necessary.

2 LITERATURE REVIEW

To ensure that the research team has a full understanding of the scope of the project, a literature review was conducted to gather the related information from national bridge design manuals as well as academic papers and technical reports. This review was conducted with a focus on three topics: 1) current wheel load distribution width evaluation method for these structures; 2) past and present methods for the retrofit of these structures for improvement of the load distribution; 3) finite element (FE) modeling of longitudinal timber slab bridges.

2.1 Wheel Load Distribution Width on Timber Slab Bridges

The live load distribution equations for longitudinal glued-laminated timber deck panel bridges have been included in the AASHTO Standard Bridge Design Specifications for many years.

For plank and nail laminated longitudinal flooring, AASHTO Standard Specifications 16th Edition (AASHTO 1996) prescribes:

- In the direction of the span, the wheel load shall be considered a point load (3.25.2.1).
- Normal to the direction of the span the wheel load shall be distributed as follows (3.25.2.2):
 - Plan floor: width of plank;
 - Non-interconnected nail laminated floor: width of tire plus thickness of floor, but not to exceed panel width. Continuous nail laminated floor and interconnected nail laminated floor, with adequate shear transverse between panels, not less than 6 in. thick: width of tire plus twice thickness of floor.

AASHTO Standard Specifications 17th Edition (AASHTO 2002) prescribes load distribution for plank and nail laminated longitudinal flooring in nearly the same way with some slight differences:

- In the direction of the span, the wheel load shall be distributed over 10 in. (3.25.2.2).
- Normal to the direction of the span the wheel load shall be distributed as follows:
 - Plan floor: 20 in.;
 - Non-interconnected nail laminated floor: width of tire plus thickness of floor, but not to exceed panel width. Continuous nail laminated floor and interconnected nail laminated floor, with adequate shear transverse between panels, not less than 6 in. thick: width of tire plus twice thickness of floor (3.25.2.2).

Furthermore, the current Manual for Bridge Evaluation references AASHTO 2002 for Allowable Stress Rating method of existing slabs, which utilizes the same equations.

AASHTO 1996 and AASHTO 2002 (3.25.3.1) calculate the live load distribution factors for flexure design of longitudinal glued-laminated timber deck bridges utilizing Eq.1 for a single traffic lane and Eq.2 for two traffic lanes. These equations are presented based on wheel loads, or half of the total axle load, carried by a single panel.

$$\text{Load Fraction} = \frac{W_p}{4.25 + \frac{L}{28}} \text{ or } \frac{W_p}{5.50} \text{ whichever is greater} \quad \text{Eq.1}$$

$$\text{Load Fraction} = \frac{W_p}{3.75 + \frac{L}{28}} \text{ or } \frac{W_p}{5.00} \text{ whichever is greater} \quad \text{Eq.2}$$

where W_p is width of panel (ft) ($3.5 \leq W_p \leq 4.5$), and L is the length of bridge (ft).

AASHTO (2004) introduced a major revision for the evaluation of the live load distribution provisions. AASHTO (2004) provides equivalent strip width equations for slab-type bridges based on lane loads, or full axle loads. Eq.3 and Eq.4 are used to calculate the equivalent strip width for the timber slab bridge. These equations were originally derived from the testing of, and are also used for, reinforced concrete slab bridges.

$$E = 10.0 + 5.0\sqrt{(L_1)(W_1)} \quad \text{Eq.3}$$

$$E = 84.0 + 1.44\sqrt{(L_1)(W_1)} \leq \frac{12.0 W}{N_L} \quad \text{Eq.4}$$

where E is the equivalent width (in.); L_1 is the modified span length taken to the lesser of the actual span or 60.0 ft, W_1 is the modified width of the bridge taken to be equal to the lesser of the actual width, or 60.0 for multi-lane loading, or 30.0 for single-lane loading (ft), W is the physical edge-to-edge width of bridge (ft), and N_L is the number of design lanes. This method is still being used in the current AASHTO (2020) design manual with no significant changes in the equations. Fanous (2010) indicated the live load distribution equations documented in the NCHRP 12-26 report (Zokaie and others, 1991) were the basis for the load-distribution provisions presented in AASHTO (2004). These equations were developed using 130 reinforced concrete slab bridges, and longitudinal glued/spike-laminated timber deck bridges were not included.

In the NCHRP 12-26 report, the load distribution factors were determined for each of the longitudinal beam elements, similar to the method used for girder-slab bridges. Dividing the load distribution factor by the width of the deck represented by the longitudinal beam element in the grillage model produces a moment distribution factor per unit width. The load distribution design width, or equivalent strip width, is determined by taking the inverse of this factor. Simply, the equivalent strip-width values can be determined using Eq.5.

$$E_i = \frac{W_E}{DF_i} \quad \text{Eq.5}$$

where, DF_i is the lane load distribution factor of the i^{th} longitudinal beam; E_i is the equivalent strip width of the i^{th} longitudinal beam (in.), and W_E is the tributary width of longitudinal beam element. This equation is used to relate live load distribution factors to equivalent strip widths (Zokaie and others, 1991).

The multiple presence factors are utilized in the AASHTO code to account for uncertainties associated with the number of loaded lanes. Table 2-1 lists the multiple presence factors in AASHTO (2020). Fanous (2010) indicated that for bridges with multiple design lanes, it is unlikely that three adjacent lanes will be loaded at the same time. Therefore, the design load is decreased. For the single design lane condition, the multiple presence factor is greater than one to account for an overload condition.

Table 2-1 AASHTO multiple presence “m” factors

Number of Loaded Lanes	AASHTO 2020
1	1.2
2	1.0
3	0.85
>3	0.65

The AASHTO live load distribution provisions for longitudinal glued/spike-laminated timber deck bridges were based on the assumption that the bridge deck behaves as one slab and ignores the discontinuity of the bridge deck panels. Fanous (2010) investigated this assumption by using analytical models that validated field test data from several in-service bridges and data from a full-scale laboratory test bridge. The result indicated that the assumption that panelized structure behaves as a single-panel bridge appears to be valid based on the performance of the in-service bridges. However, to assure that the panelized structure performs as a single panel, additional research was recommended to be performed on the panel-to-panel connections.

2.2 Retrofit Techniques for Longitudinal Timber Slab Bridge

To date, methods used to improve load capacity of timber slab bridges include tightening the connections to existing spreader beams, adding spreader beams, using transverse post-tensioning and using 4 in. thick laminated spreader deck panels placed transversely on top of the existing slab. These methods are meant to increase the effective wheel width. The effective width is directly proportional to load rating (allowable live load). Further research is required to more reliably quantify the effective wheel distribution width of these retrofit methods (AASHTO, 2018; MN Bridge design manual, 2020; Fanous et al., 2010).

2.2.1 Spreader beam

Placement of a spreader beam perpendicular to the deck panel is the most common practice on timber slab bridges to improve the live load distribution and increase the live-load capacity of the superstructure. Timber and steel are two commonly used materials for the spreader beams.

The AASHTO LRFD Specification indicates placement of spreader beams be attached to the underside of the timber deck. AASHTO (2018) states the distance between spreader beams shall not exceed 8.0 ft and the rigidity, EI , of each spreader beam shall not be less than 80,000 kip-in². In addition, the spreader beams are required to attach to each deck panel near the panel edges at an interval not exceeding 15.0 in. It should be noted that all timber slab bridges in Wisconsin designed and built prior to LRFD design specifications being used do not meet these spreader beam spacing and fastening requirements. Therefore, the applicability of LRFD effective slab width calculations is unknown.

Wipf (1986) summarized that four types of stiffener beam connectors are commonly used to attach spreader beams: aluminum brackets, thru-bolts, steel plates, and C-clips (shown in Figure 2-1). Currently, the most common types of connectors being used are the aluminum brackets and thru-bolts.

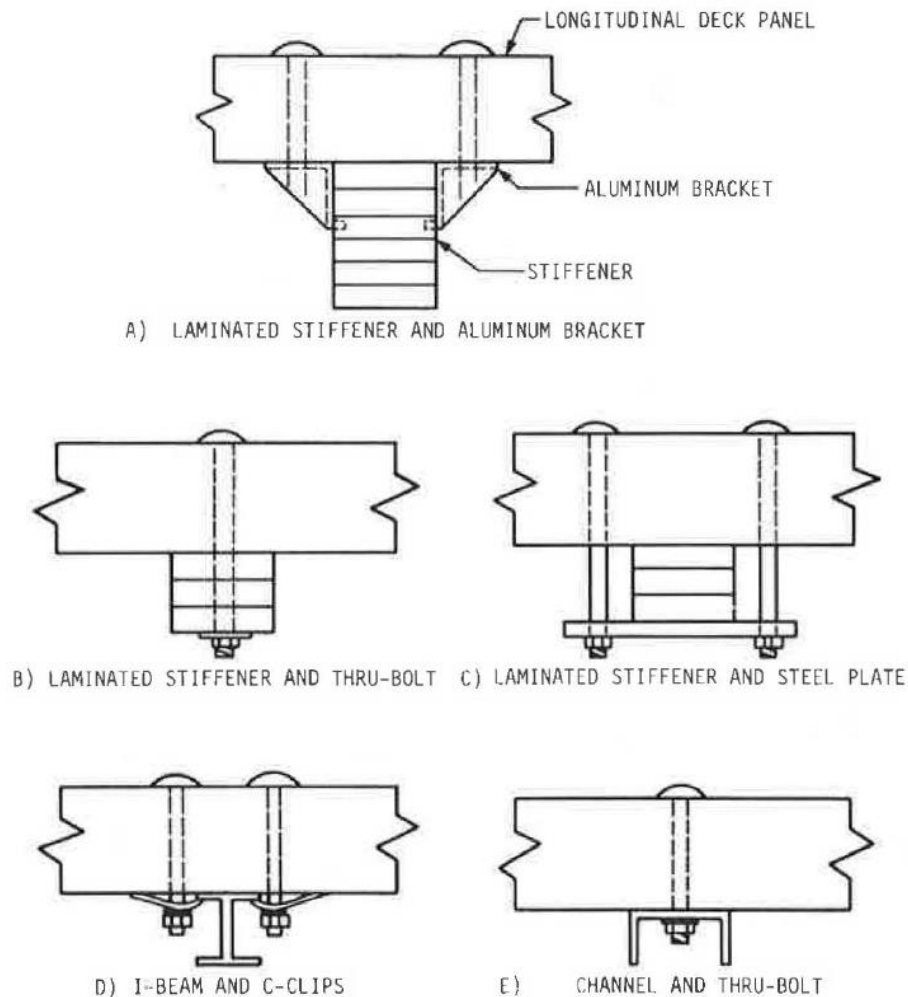


Figure 2-1 Types of transverse stiffener beam connections (Wipf 1986)

Funke (1986) conducted laboratory testing and analytical study to verify the applicability of the live load distribution equations created by Sanders and others (1985). Various stiffener beam, deck panel, and load-positioning arrangements were investigated during the study. The results indicated that favorable live load distribution behavior occurred when using at least three stiffener beams. The results of these tests were not adopted into AASHTO Standard Specifications or AASHTO LRFD and are not widely used.

Kurian (2001) conducted finite element analyses to investigate the effects of several design parameters on the overall structural behavior of many in-service bridges. It was concluded that the modulus of elasticity of the deck material had a significant influence on bridge response when comparing the deflections attained from the analytical models with the field-test results. It was also found that the influence of edge stiffening becomes insignificant to the panel deflections and stresses move away from the exterior panels to the interior panels. Fanous (2010) found that the effects of edge stiffening were observed at the in-service bridges. However, further study of the curb and guardrail should be conducted to aid in better understanding the edge-stiffening effects.

2.2.2 Post-tensioning

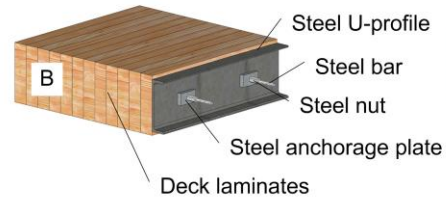
One particular strengthening method for the timber slab bridge that has become popular in North America, as well as in Australia and Europe, is the application of post-tensioning force. With this method, the decks are constructed using longitudinal timber laminations side by side and post tensioned transverse to the traffic direction. As a result of pre-stressing, a resisting frictional force between the timber laminations produces a deck that exhibits orthotropic plate behavior.

Ekholm (2011) indicated that the post-tensioning force on the timber laminations should be sufficient to generate a compressive stress between the laminations larger than the tensile stress from transverse bending of the deck panels. A gap could be induced when the tensile stresses from bending are greater than the compressive stresses from pre-stressing, and eventually decrease the durability of the structure. In addition, the transverse shear force from concentrated loads should be smaller than the resisting friction between the lamination generated by the pre-stressing to ensure that the distributed load can be transferred to the neighboring laminates. Insufficient post-tensioning force could induce vertical interlaminar slip and gaps between the laminations, resulting in an increased level of stress in single laminate and deflections larger than expected. Horizontal slip and twisting was found during the study.

A review of the past literature and records for field practice revealed that the post-tensioning force is typically applied through post-tensioning tendons placed either through a pre-drilled hole through the timber laminations or outside and underneath the deck panels. Selection of the anchorage systems depends on the location of the post-tensioning force application and the timber material properties. The steel channel (shown in Figure 2-2-a and -b) enabled the prestress to be more evenly distributed through the laminated deck (Sarisbury and Accorsi 1990). However, based on the research results from Oliva et al. (1990), it was found that the use of a continuous steel profile was not as favorable as previously thought. AASHTO (2010) still recommends continuous steel profiles be used along the edges of the deck when softwood beams are used for laminated deck panels. Ekholm (2011) summarized that four anchorage systems are commonly used on timber slab deck panel bridges as shown in Figure 2-2. Comparing Figure 2-2-a to 2-b, the two steel bars, over and under the deck in Figure 2-2-a enables an external application of the posttensioning force, while the one in Figure 2-2-b requires drilling a hole through the deck before the placement of the laminated deck panels. If the deck is constructed using hardwood laminations, or if at least the two beams closest to the edge are a hardwood species, the prestress can be anchored using a system of discrete steel plates as shown in Figure 2-2-c. Figure 2-2-d shows an anchorage system used in Sweden that consists of wood, aluminum and steel plates to distribute the prestressing force to the beams.



a) Measure of repair of nail-laminated decks;



b) Continuous steel profile used for softwood decks according to AASHTO;



c) Bearing plates used for hardwood decks according to AASHTO;



d) Prestressing system normally used in Sweden

Figure 2-2 Post-tensing anchorage systems (Ekholm 2013)

2.2.3 Transverse spreader deck panels

Transverse spreader deck panels have been used in the recent past, including in the State of Wisconsin. Several examples of this system are accessible through the WisDOT bridge inventory. One example is shown in the cross-section provided in Figure 2-3. Despite the system's more common use recently, a literature search revealed no appreciable related information could be found within past academic papers or technical reports. This indicates a detailed study of transverse spreader deck panels is warranted.

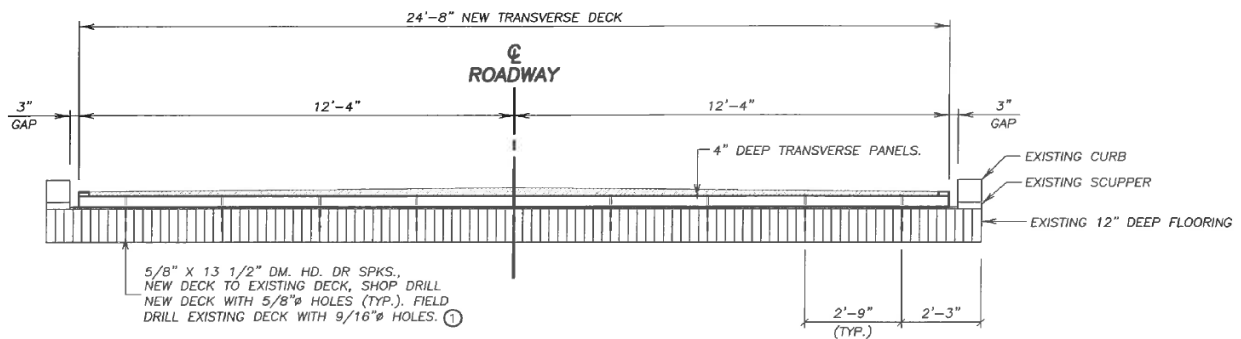


Figure 2-3 Cross-section view of timber slab bridge with transverse timber deck on top

2.3 FE Modeling of Longitudinal Timber Slab Bridge

Sanders (1985) performed analytical studies to determine the load distribution characteristics of longitudinal glued-laminated timber deck bridges. The analytical models were created using the finite element software SAP IV. Plate elements were used to model the deck panels and beam elements were used to model the stiffener beam. Rigid links were used to connect the stiffener beam to the deck panels. A parametric study was performed on bridges with various span lengths, roadway widths, deck thickness and stiffener-beam arrangements.

Funke (1986) conducted laboratory testing and analytical study to verify the applicability of the live load distribution equations created by Sanders and others (1985). The analytical study was performed on a series of finite element models created utilizing SAP IV. Various stiffener beam, deck panel, and load-positioning arrangements were investigated during the study.

Wipf (1990) developed finite element models to study the behavior of a glued-laminated, longitudinal-deck highway bridges. Experimental tests of a full-scale laboratory test bridge were performed to validate the analytical model, which had been used in the development of design criteria for the longitudinal deck bridge. The model was developed using SAP IV. The glued-laminated panels of the longitudinal bridge were modeled as thin plate/shell elements. The stiffener beams were modeled using a three-dimensional beam element. It was pointed out that the behavior of the connection depends on whether the connection is in compression or tension. When the connection is in compression, the panel bears against the stiffener beam and the panel load is transferred directly to the stiffener beam. However, when the connection is in tension, load is transferred through the panel connection. Beam elements were selected to model the connections, and since they are assumed to be incapable of transferring significant moment or shear, the beam elements were assigned very small flexural stiffness.

Kurian (2001) conducted finite element analyses to investigate the effects of several design parameters on the overall structural behavior of many in-service bridges. The parametric analyses were performed to examine the effects of edge stiffening, boundary conditions, and the change in the timber modulus of elasticity. The results indicated that the modulus of elasticity of the deck material had a significant influence on bridge response when comparing the deflections attained from the analytical models with the field-test results. It was found that the influence of edge stiffening becomes insignificant to the panel deflections and stresses move away from the exterior panels to the interior panels.

May (2008) conducted a finite element analysis to determine the truck loads distribution on the glued-laminated timber bridge. The full-scale finite element bridge models were developed utilizing ANSYS and calibrated with field data. Solid elements, which incorporate the orthotropic timber material properties, were used to model the deck panel and stiffener beam. The compression-only spring elements were used to idealize the interface between the panels and the stiffener beam. Tension-compression spring elements were utilized to model the through bolt, or aluminum bracket, connections that are required to connect the stiffener beam to the deck panels. At the end of the work, simplified live load distribution equations were developed following methods established for other bridge types where needed to improve the accuracy of determining how truck loads are distributed to structural members of glued-laminated timber bridges.

Table 2-2 summarizes the modeling details for all the reviewed publications listed above. It was found that as the development of the computation technology progressed, the analytical models were developed with more advanced elements (3D solid) and more realistic material properties (nonlinear/elastic-plastic).

Table 2-2 FE model details

Research	Retrofit method	Software	Elements				Material
			Deck	Stiffener beam	Beam-deck connection	Beam-deck contact	
Sanders 1985	Spreader beam	SAP IV	Plate	Beam	Rigid link		Elastic
Funke 1985	Spreader beam	SAP IV	Plate	Beam	Rigid link		Elastic
Wipf 1990	Spreader beam	SAP IV	Plate	Beam	Rigid link		Elastic
May 2008	Spreader beam	ANSYS	Solid	Solid	Beam	Contact element	Elastic
Fanous 2011	Spreader beam	ANSYS	Solid	Solid	Beam	Contact element	Elastic
Kliger 2011	Posttensioning	ABAQUS	Solid				Nonlinear
Ekholm 2013	Posttensioning	ABAQUS	Solid				Elastic-Plastic

3 SUMMARY OF DOT PRACTICES

In this chapter, the current methods of predicting the wheel load distribution width and retrofit/strengthening methods for the timber slab bridges used by various DOTs were investigated. In addition, the implementation on timber slab bridges in Wisconsin was studied.

3.1 State DOT Practice

The objective of this task was to review the practices currently implemented by State DOTs for the estimation of the wheel load distribution and strengthening/enhancing load distribution on timber slab bridges. In order to achieve that, various manuals and specifications created and adopted by nine state DOTs were reviewed. The review work was conducted with a focus on the states with large numbers of timber bridges. These states include Oregon, Minnesota, Wisconsin, Michigan, Iowa, Indiana, New York, New Jersey and Delaware. The specific language from these manuals and specifications were extracted and presented. Similarities and differences between policies were compared and discussed.

3.1.1 Identification of states of interests

In order to identify the states/organizations that have tremendous experience on the design, construction and maintenance of timber slab bridges, the Long-Term Bridge Performance (LTBP) InfoBridge data base provided by the Federal Highway Administration (FHWA) was used. The criteria that used to locate the timber slab bridges in the system includes “Timber-43A” for Main Span Material and “Slab Bridge-43B” for Main Span Design as shown on the left in Figure 3-1.

The results indicated the timber slab bridges are mainly distributed in three regions within the United States shown Figure 3-1: northwest, upper midwest and northeast. Among these areas, most of the timber slab bridges are located in the upper midwest states of Minnesota, Wisconsin, Michigan, Iowa, Indiana. In the northeast, the timber slab bridges were mainly located in the states of New York, New Jersey and Delaware. A smaller number of bridges were found in the northwest in the state of Oregon. The review work was conducted using the state bridge design and maintenance manuals from these states.

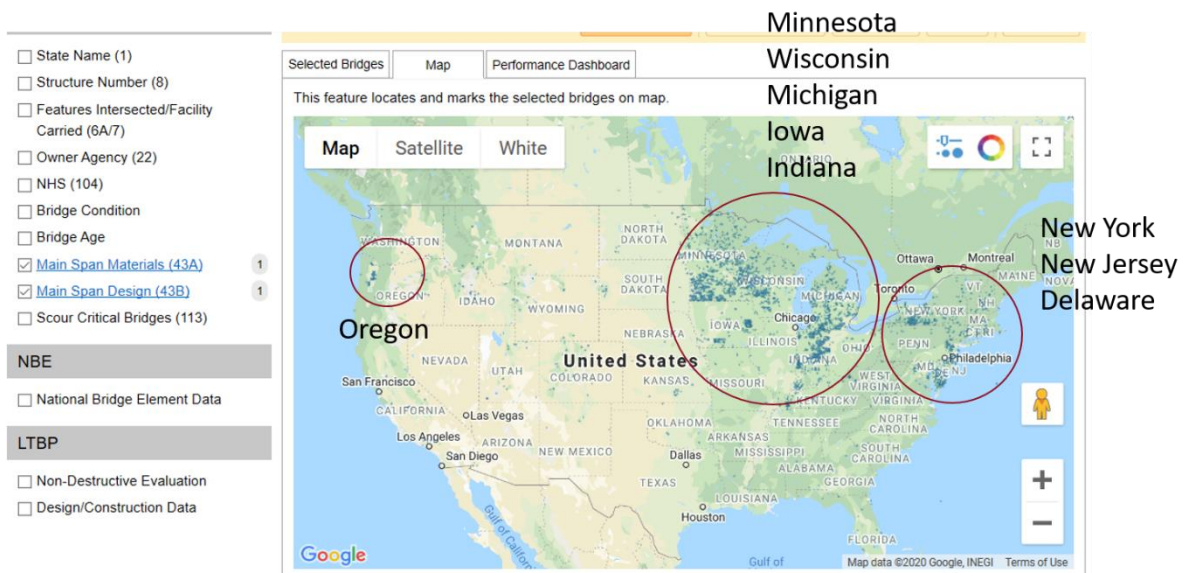


Figure 3-1 Nationwide distribution of timber slab bridge

3.1.2 Results for the state practice review

Prior to the review of state practice, the related national specifications were reviewed for federal guidance with respect to the determination of the design wheel load distribution and enhancing the transverse load distribution on a timber slab bridge. Two national specifications were reviewed: American Association of State Highway Officials Load and Resistance Factor Design (AASHTO LRFD) Bridge Design Specification - referred to as AASHTO 2018 - and American Association of State Highway Officials Standard Design Specifications 17th Edition (AASHTO 2002) from which the load distribution equations were an adaptation of United States Forest Products Service (USFS) Timber Bridge Manual - referred to as USFS 1990 (Ritter, 1990).

AASHTO (2018) provides the design guidance for three specific timber slab bridges: spike laminated deck panel; glued laminated timber panel deck and stress-laminated decks. The wheel load distribution for each type of timber slab bridge was calculated using Eq.3 and Eq. 4 as shown in Chapter 2. It was pointed out by Fanous (2010) that these live load distribution equations were developed by NCHRP 12-26 report (Zokaie and others 1991) based on a series of experiments conducted on concrete slab bridges. No specific equation was provided by AASHTO (2018) to predict the wheel load distribution for the timber slab bridge. With respect to the enhancing/strengthening of the existing timber slab, AASHTO did not provide any specific recommendations. However, the design guidelines do provide little detailing for each type of bridge. For example, a transverse stiffener beam was required to be used underneath the laminated deck panel and glued laminated timber panel deck. It was stated that the distance between stiffener beams shall not exceed 8.0 ft, and the rigidity, EI , of each stiffener beam shall not be less than 80,000 kip-in.². The beams shall be attached to each deck panel near the panel edges and at intervals not exceeding 15.0 in. The use of transverse post-tensioning was recommended only for the bridges with a skew less than 45 degrees to create a stress laminated timber deck.

Table 3-1 and Table 3-2 present the key points from the national and state design and maintenance guides.

Table 3-1 Summary of design practices

	Bridge types	Wheel load distribution
AASHTO LRFD	<ul style="list-style-type: none"> • Spike laminated deck • Glued laminated timber panel deck • Stress-laminated decks [9.9.4; 9.9.5; 9.9.6] 	<ul style="list-style-type: none"> • $E = 10.0 + 5.0\sqrt{(L_1)(W_1)}$ (S) • $E = 84.0 + 1.44\sqrt{(L_1)(W_1)} \leq \frac{12.0 W}{N_L}$ (M) [4.6.2.3]
AASHTO Standard/USFS	<ul style="list-style-type: none"> • Glue-laminated deck panels • Nail-laminated lumber Deck • Longitudinal glulam deck on transverse floor beams [8.3; 8.4; 8.5] 	<ul style="list-style-type: none"> • Glue-laminated deck panels: $WLF = \frac{W_p}{4.25+L/28}$ or $\frac{W_p}{5.5}$, whichever is greater (S) $WLF = \frac{W_p}{4.25+L/28}$ or $\frac{W_p}{5.00}$, whichever is greater (M) • Nail-laminated timber deck : $D_w = b_t + 2t$ • Longitudinal glulam deck on transverse floor beams: $D_w = b_t + t$ [8.3; 8.4; 8.5]
Wisconsin	<ul style="list-style-type: none"> • Spike "laminated deck" [23.1.1] 	<ul style="list-style-type: none"> • Follow AASHTO LRFD
Oregon	<ul style="list-style-type: none"> • Glued laminated longitudinal deck 	Not mentioned
Minnesota	<ul style="list-style-type: none"> • Spike laminated deck • Glued laminated timber deck • Stress-laminated decks [8.2.3] 	<ul style="list-style-type: none"> • Follow AASHTO [8.7.1 Example]
New York	<ul style="list-style-type: none"> • Nail-laminated plank decks • Nail-laminated decks panels with interconnecting transverse stiffener beams • Glue-laminated deck panels • Stress-laminated decks. [10.5.3] 	<ul style="list-style-type: none"> • Follow AASHTO Standard/USFS [10.1]
Indiana	<ul style="list-style-type: none"> • Spike laminated deck (panel) • Glued laminated timber deck (panel) • Transverse prestressed decks [65-3.03; 65-3.04;65-3.05] 	<ul style="list-style-type: none"> • Follow AASHTO [65-3.03; 65-3.04; 65-3.05]
Iowa	Not mentioned	Not mentioned
Michigan	Not mentioned	Not mentioned
New Jersey	Not mentioned	Not mentioned
Delaware	Not mentioned	Not mentioned

Table 3-2 Summary of practice on retrofit and strengthening methods

	Transverse beam	Transverse deck panel	Post-tensioning
AASHTO LRFD	<ul style="list-style-type: none"> • 8ft • 15in. • 80,000 kip-in² [9.9.4.3.1] 	Not mentioned	<ul style="list-style-type: none"> • Shall not be used where the skew exceeds 45 degree [9.9.5.1]
AASHTO Standard/USFS	<ul style="list-style-type: none"> • Analytical and experimental data from ISU 	Not mentioned	<ul style="list-style-type: none"> • External posttensioning with plank surface on top
Wisconsin	<ul style="list-style-type: none"> • Follow AASHTO [23.4.15] 	Not mentioned	Not mentioned
Oregon	Not mentioned	Not mentioned	Not mentioned
Minnesota	<ul style="list-style-type: none"> • Follow AASHTO; • 6in. by 12in. beam is commonly used as a standard [8.2.3] 		<ul style="list-style-type: none"> • Follow AASHTO [8.2.3]
New York	<ul style="list-style-type: none"> • Generally, follow AASHTO Standard/USFS [10.1] 	<ul style="list-style-type: none"> • Generally, follow AASHTO Standard/USFS [10.1] 	<ul style="list-style-type: none"> • Generally, follow AASHTO Standard/USFS [10.1]
Indiana	<ul style="list-style-type: none"> • Used with glued-laminated longitudinal deck • Follow AASHTO [65-3.04] 	Not mentioned	<ul style="list-style-type: none"> • Follow AASHTO [65-3.05]
Iowa	<ul style="list-style-type: none"> • Transverse timber beam • Transverse timber planks topped with longitudinally boards 	Not mentioned	<ul style="list-style-type: none"> • “Hollywood” timber deck • Nail laminated timber deck [2.1.3]
Michigan	Not mentioned	Not mentioned	Not mentioned
New Jersey	Not mentioned	Not mentioned	Not mentioned
Delaware	Not mentioned	Not mentioned	Not mentioned

USFS (1990) also provide the design guidance for three types of timber slab bridges: glued-laminated deck panels; nail-laminated lumber deck and longitudinal glulam deck on transverse floor beams. Although both AASHTO LRFD and USFS Timber Bridge Manual give guidance on the design of glued-laminated deck panels and nailed (spiked) laminated timber deck, the design equations used to estimate the wheel load distribution are quite different. Unlike AASHTO (2018) which provides the same equation for all the slab bridges, USFS (1990) provides a unique equation for each type of timber slab bridge. For example, for the glued-laminated deck panels, Eq.1 was recommended for the single lane traffic load and the Eq.2 was recommended for multi-lane traffic. These equations are the same as those provided in AASHTO (1996). For the nail-laminated lumber deck, the wheel load distribution is predicted based on the width of the wheel and the thickness of the deck as shown in Eq.6.

$$D_w = b_t + 2t \tag{Eq.6}$$

where D_w is the wheel load distribution width; b_t is the tire width and t is the deck thickness. For the longitudinal glulam deck on transverse floor beams, the wheel load distribution was calculated utilizing Eq. 7.

$$D_w = b_t + t \tag{Eq.7}$$

With respect to the use of stiffener beams, there is no specific requirement in USFS (1990) but in research conducted by Iowa State University it is referenced. Although the detailed design guidelines for the stress-laminated slab bridge was not provided, a repairing method that uses external post-tensioning on the deck top and bottom was presented. Figure 3-2 shows the prestressing detail for rehabilitation of existing decks. A number of bridges repaired using this method were loaded tested. The results demonstrate the benefits of rehabilitating nail-laminated decks by this method. It was pointed out this method improves the load distribution thus improving on the original design.

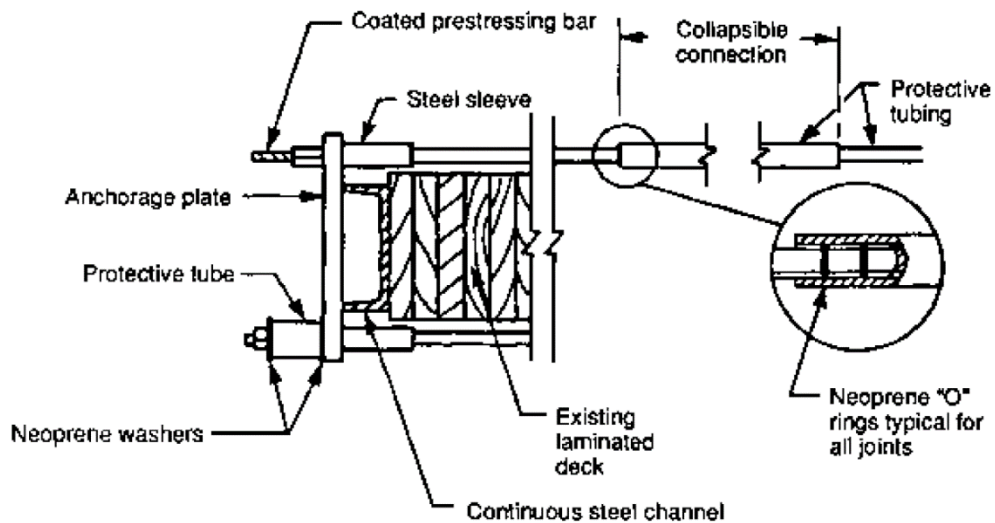


Figure 3-2 Prestressing detail for rehabilitation of existing decks (USFS 1990)

Although nine bridge design manuals published by different state DOTs were reviewed, only three of them (Minnesota, New York and Indiana) have detailed information regarding timber slab bridges. Two of these nine manuals (Wisconsin and Oregon) show little information, while no related information can be found

from the other four state bridge design manuals (Iowa, Michigan, New Jersey, Delaware). (Iowa 2020; Michigan 2020; New Jersey 2020; Delaware 2020)

Wisconsin's bridge design manual mentions the use of a "spike laminated deck". However, little additional information could be found. An equation for wheel load distribution was not provided. The use of a stiffener beam was recommended following the corresponding criteria in AASHTO (2018). (Wisconsin 2020)

Oregon's bridge design manual mentions the use of glued laminated longitudinal deck; however, no further detailing was given. (Oregon 2020)

Minnesota's bridge design manual indicates use of three types of laminated timber slab bridges: spike laminated deck, glued laminated timber deck, stress-laminated decks. The calculation of the wheel load distribution is that shown in Eq.3 and Eq.4 following the AASHTO (2018). The use of a transverse stiffener beam and post-tensioning force were recommended strategies following the corresponding criteria in AASHTO (2018). However, it was pointed out that a 6 in. by 12 in. beam is commonly used as a standard in State of Minnesota.

New York's bridge design manual indicates use of four types of a laminated timber slab bridge: nail-laminated plank decks, nail-laminated decks panels with interconnecting transverse stiffener beams, glue-laminated deck panels, and stress-laminated decks. However, the detail guidelines for the design of each type bridge was not provided. A general suggestion to follow USFS (1990) was provided at the beginning of the chapter for timber structure design. (New York 2020)

Indiana's bridge design manual recommends the use of three types of laminated timber slab bridge: spike laminated deck (panel), glued laminated timber deck (panel), transverse prestressed decks. The manual provides the similar equation/criteria as AASHTO (2018) for the prediction of the wheel load distribution. It also suggests the use of post-tensioning force. It should be noted that in the Indiana's bridge design manual, the transverse stiffener beam was recommended only for glued-laminated longitudinal deck. (Indiana 2020)

A literature search was also conducted on the state bridge maintenance/preservation manuals from the nine states identified above. It was found that only the Iowa Bridge Maintenance Manual proposed the use of a transverse timber beam and transverse timber deck. However, detailed information was not presented. The search revealed that the other state DOTs either do not have a maintenance/preservation manual or have nothing related to timber slab bridges in their manuals.

3.1.3 Conclusions from the state practice review

The results from the review of State Practice indicate that the timber slab population primarily exists in nine states. A review of the bridge manual from these states indicates that all of them have either no specific guidance or very similar guidance to AASHTO and USFS (1990) with respect to the calculation of wheel load distribution and strengthening/enhancing methods. Minnesota, New York and Indiana were the three states that have the most information in their bridge design manuals regarding to the design of timber slab bridges, but all of them generally follow the national specification (New York follows USFS; Minnesota and Indiana follow AASHTO LRFD).

It was also found that the state bridge preservation manuals do not have detailed guidance on how to strengthen existing timber slab bridges, although the national specification USFS (1990) does provide a

case study for the use of external post-tensioning as a strengthening method. The search indicated that a transverse stiffener beam is the most commonly used method to enhance the transverse load distribution. Only one state-Minnesota-provides guidance for the use of transverse deck panels. Use of external post-tensioning force as a strengthening method was proposed by USFS (1990) and the performance of it was approved.

3.2 Use of Timber Slab Bridges in Wisconsin

The current status on the use of the timber slab bridges in State of Wisconsin was investigated in this chapter. The objective of this step is to identify candidate bridges for the field-testing program detailed below. To achieve this objective, a review of WisDOT’s inventory of timber slab bridges was conducted.

Data within WisDOT’s bridge inventory system indicates there are currently 439 timber slab bridges in State of Wisconsin. A general geographical distribution of these bridges is shown in Figure 3-3. It was found a majority of these bridges are distributed in the western portions of the state. Figure 3-4 Timber slab bridge distribution by county in Wisconsin shows the distributions of timber slab bridges in each county.

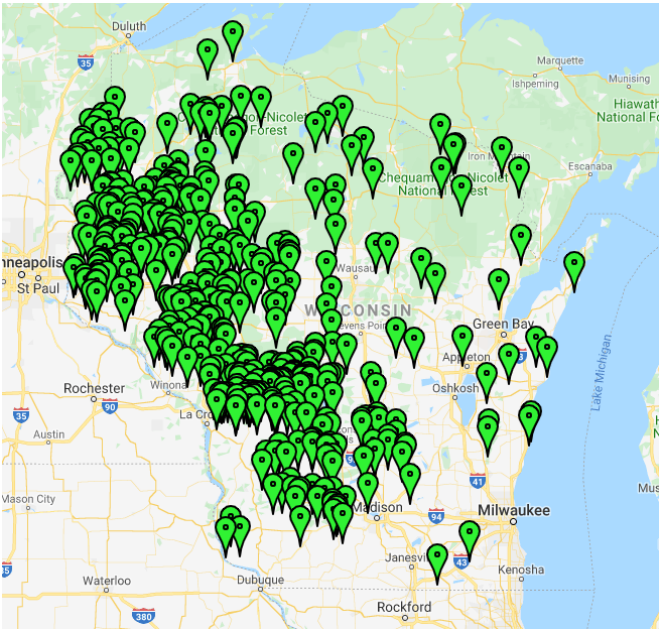


Figure 3-3 Timber slab bridge locations in Wisconsin

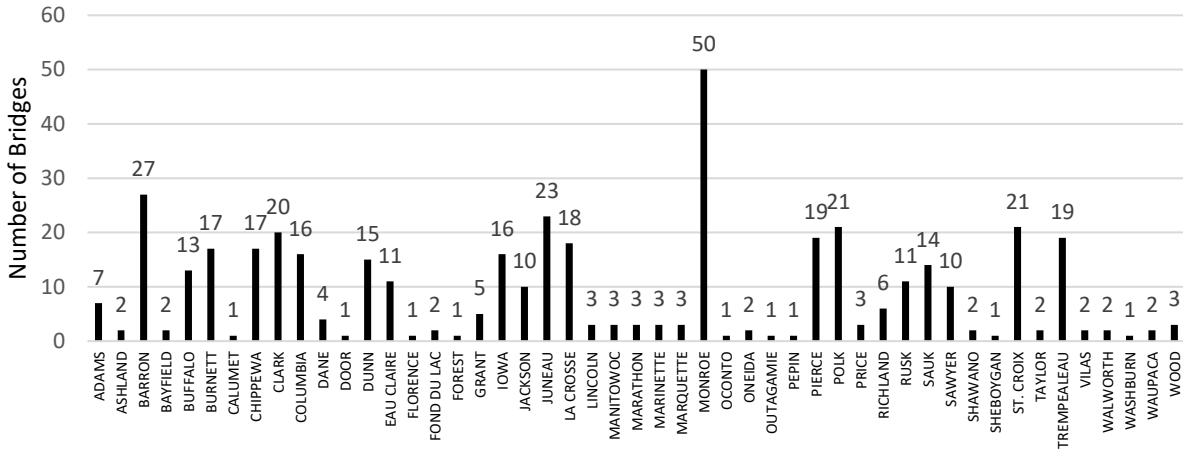


Figure 3-4 Timber slab bridge distribution by county in Wisconsin

A majority of these bridges were built between 1964 and 1994 as shown in Figure 3-5, which indicates a significant number of these bridges are between 30 and 60 years old at the time of publication, an aging fleet to say the least. It was found that 86 bridges are posted for weight limits with 73 verified as Wheeler bridges.

and show the data for the bridge main span length and bridge width. Most of these bridges have a relatively short span length between 21 and 33 ft and a deck width from 23.6 to 33.6 ft.

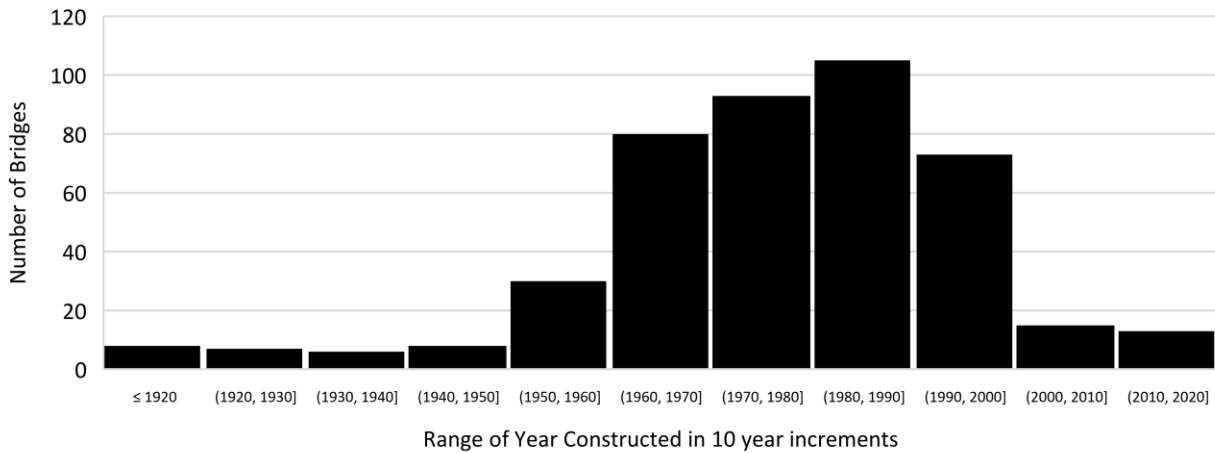


Figure 3-5 Timber slab bridges in Wisconsin distributed by year of construction

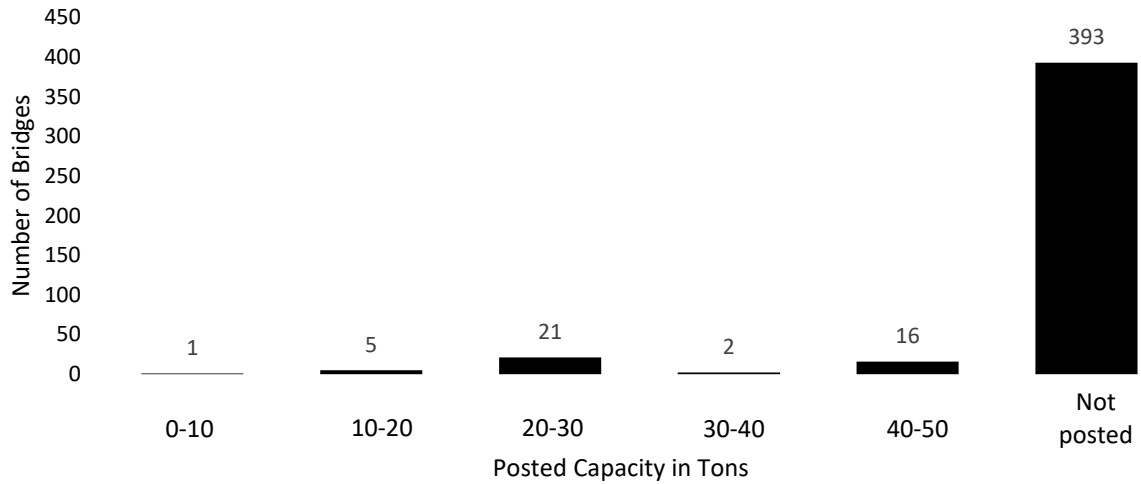


Figure 3-6 Posted capacity of timber slab bridges in Wisconsin

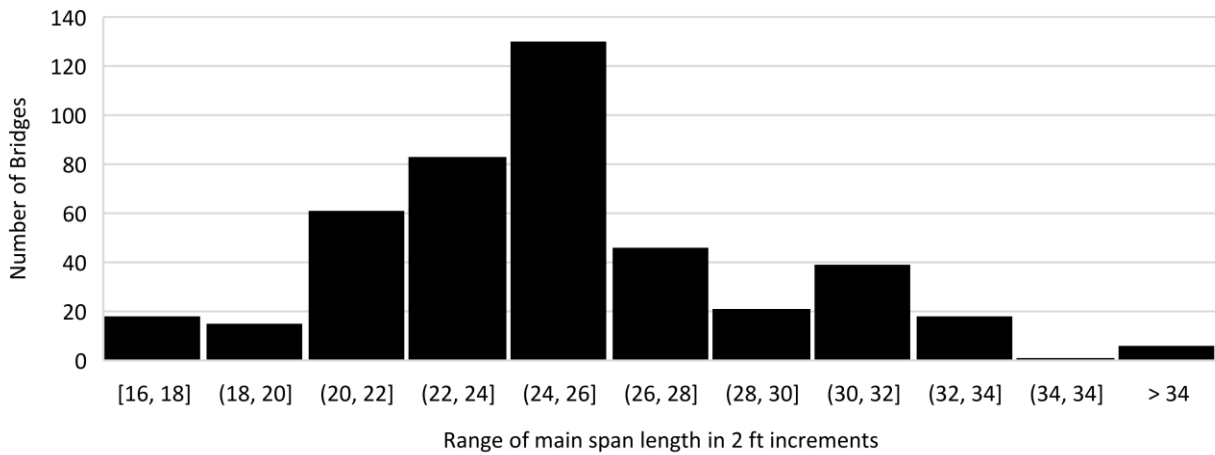


Figure 3-7 Timber slab bridges in Wisconsin distributed by main span length

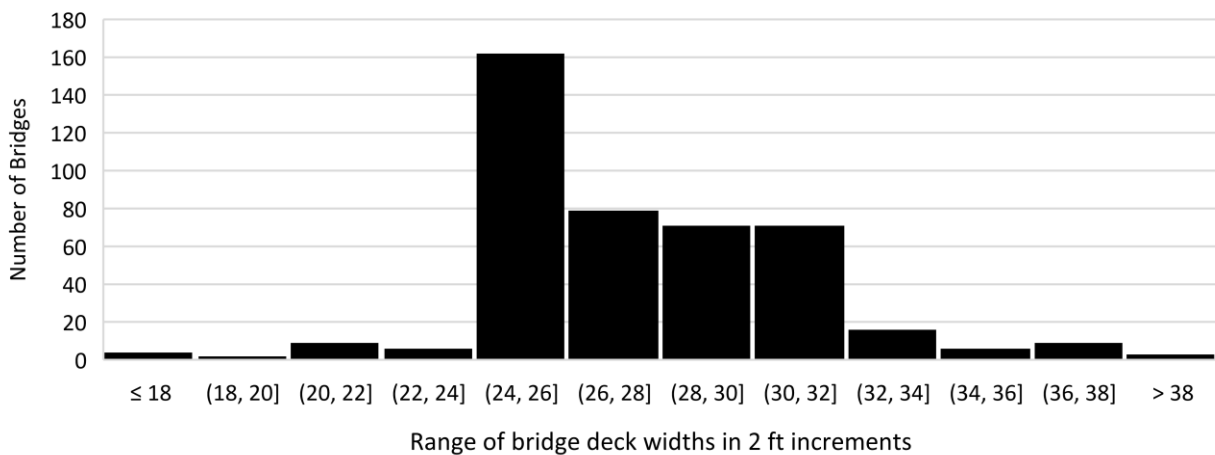


Figure 3-8 Timber slab bridges in Wisconsin distributed by bridge deck width

4 FIELD EVALUATION PROGRAM

The field evaluation work was conducted with a major objective to investigate the wheel load distribution and study the effect of various retrofit methods. The field work also provides the data for the calibration of the FE models developed in the next chapter and refines the step-by-step process for conducting load testing on similar bridges that could be used by the DOT engineers.

4.1 Load Test Program

The field test program was developed based on the previous experience of the research team and shaped by the literature review. The program was designed to collect pertinent data needed to effectively evaluate wheel load distribution and other general performance indices.

4.1.1 Bridge candidates

The selection of the bridges for the field testing considered multiple parameters including bridge type, year built, main span length, deck width, and posting information. In total, nine bridges from three counties: Barron County, La Crosse County and Monroe County were identified. The locations for these three counties are shown in Figure 4-1. Additionally, per the request of the oversight committee, one additional recently-constructed bridge in Monroe County which was designed using LRFD methods was selected for testing to compare its performance to non-LRFD-designed bridges. Three bridges in La Crosse County were tested twice: before and after the strengthening measures in order to study the effect of the retrofit method. The other seven bridges in Barron and Monroe Counties were tested once each.

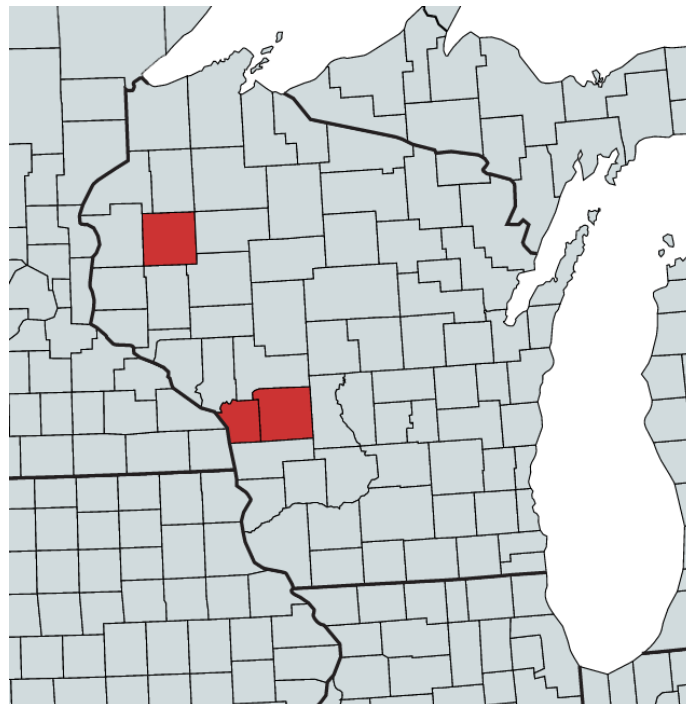


Figure 4-1 Locations for the bridges selected for the field test

In Barron County, the two bridges identified for the testing include one which has spreader beam retightened in 2018 and the other one which had a spreader deck previously added. The two Barron county bridges were tested in September 2020.

In La Crosse County, three bridges were selected for field testing. They were specifically selected knowing strengthening measures (spreader deck) would be completed in the fall of 2020. Since one of the objectives in this project is to evaluate the performance of the strengthening methods, two load tests, one before strengthening work and one after the strengthening work, were planned for each of these bridges. A comparison of the two data sets before and after the strengthening work provides direct observation of the efficacy of the strengthening method. The tests before the retrofit work were performed in August 2020 and the after-retrofit tests were performed in November 2020.

In Monroe County, three Wheeler bridges were selected for the field testing. Wheeler bridges comprise at least 73 of 439 timber slab bridges in Wisconsin with hundreds more having a similar system, thus this bridge type is of particular interest. Of those selected bridges, one of them was built in 1945 and the other two were built in the 1990s. These bridges were tested in October 2020.

All the bridges selected are timber slab bridges with a span length of 23 to 31 ft and a width of 25.5 to 32 ft. All of the identified bridges consist of four to five deck panels with a width of 4 to 6 ft each. Each panel was built with 3 to 4 in. wide and 10 to 14 in. deep laminates. These laminates were assembled using transverse dowels with each dowel crossing four laminates. The dowel connection was placed near the top and bottom of the laminate with a spacing of 2 ft in the longitudinal direction. Figure 4-2 shows a typical cross-section view of the superstructure of the timber slab bridge. A ship lap connection detail was used at adjoining deck panels. The connection was completed using a vertical spike spaced at approximately 3 ft in the bridge longitudinal direction. Detailed information for each bridge is presented in Table 4-1. Each of the bridges are pictured in Figure 4-3 through Figure 4-12.

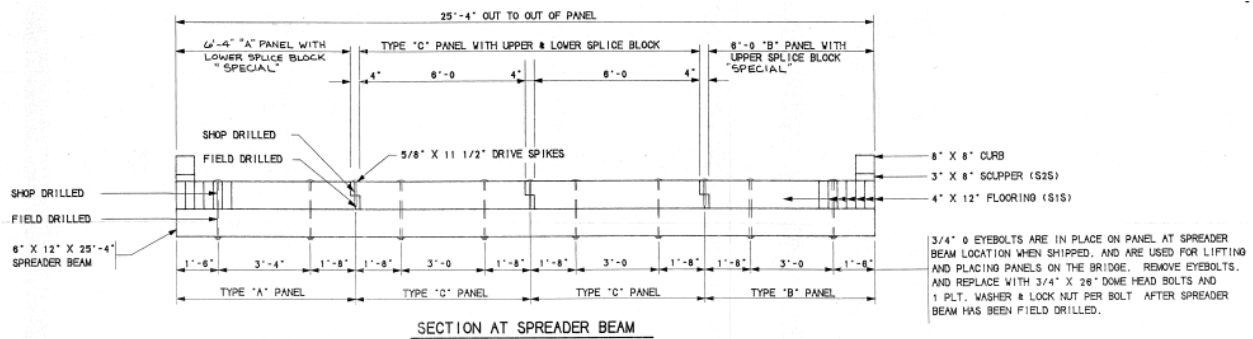


Figure 4-2 Typical superstructure cross-section view

Table 4-1 Bridges selected for the field testing

Bridge		Basic information				Deck laminates			Posting/Rehabilitation	
Bridge ID	County	Year Built	Main Span Length (ft)	Deck Width (ft)	No. of spans	Width (in.)	Height (in.)	No. of laminates	Posting	Recent Strengthening
B030174	Barron	2001	24	25.9	2	3	12	104	Not given	Retighten spreader beam (2018)
P030079	Barron	1969	25.2	26.5	2	3	12	106	Not given	Spreader deck
P320064	La Crosse	1973	24.6	32.2	3	3	12 (middle spans) & 10 (end spans)	129	45 Ton Load Limit	None
P320083	La Crosse	1976	26	31.9	3	3	12	128	45 Ton Load Limit	None
P320110	La Crosse	1971	26	31.9	2	3	12	128	20 Ton Load Limit	None
P410140	Monroe	1991	31	25.3	1	4*	14	76	25 Ton Load Limit	Unknown
P410923	Monroe	1945	23	25.5	1	4	14	77	25 Ton Load Limit	Unknown
P410953	Monroe	1990	24	31.3	1	4	12	94	Not given	Unknown
B410315	Monroe	2018	28.0	26.0	28.0	4	14	78	Not given	None
P410948	Monroe	1970	25.0	25.8	25.0	3	12	100	Not given	Unknown



Figure 4-3 La Crosse County – P320064



Figure 4-4 La Crosse County – P320083



Figure 4-5 La Crosse County – P320110



Figure 4-6 Barron County – P030079



Figure 4-7 Barron County – B030174



Figure 4-8 Monroe County – B410315



Figure 4-9 Monroe County – P410140



Figure 4-10 Monroe County – P410923



Figure 4-11 Monroe County – P410948



Figure 4-12 Monroe County – P410953

4.1.2 Load test procedures

The field test procedures were prescribed to generally follow a commonly operated live load test procedure. A truck with known weight was driven across the instrumented bridge at a walking pace (< 5 mph) to generate the equivalent static truck load behavior. At the same time, various types of gauges were used to collect desired data through a data acquisition system. After the test, the data collected are processed to assess the deck behavior with respect to the wheel load distribution. Similarly, the effect of different retrofit methods will be assessed where they exist.

Since one of the tasks was to develop a step-by-step process for conducting load testing on similar bridges that could be used by the DOT engineers to evaluate load wheel distribution for each individual bridge, the field test procedures conducted in this project were enhanced to explore the potential testing methods/equipment that could be most simply employed. In order to do this, in addition to collecting data with strain gages and deflection transducers (through the data acquisition system), the research team collected data using surveying equipment (total station) that can be easily obtained by WisDOT for a relatively low initial investment. With that, a general test procedure was developed and is presented below:

1. Install strain gauges and displacement transducers, and set up the data acquisition station.
2. Drive a truck of known weight and configuration across the bridge at a walking pace along one of five designated paths. Maintain continuous data acquisition during this period, marking the longitudinal truck position within the data.
3. Repeat Step 1 for each of the five load paths.
4. Drive the truck across the bridge stopping at the point of maximum load response to manually survey the deck deflection at various transverse locations. The position is typically when the center of gravity of the truck is positioned at midspan.
5. Repeat Step 4 for each of the five load paths.

For each bridge, the truck was driven across (see Figure 4-13) while maintaining the transverse position of one of five designated load paths. The load paths, or load cases (LCs) are shown in Figure 4-14. LC1 and LC5 are near the curb line of the bridge with the driver's-side wheel (LC1) or passenger's-side wheel (LC5) centered 2ft from the face of the curb. LC2 and LC4 centers the passenger's-side wheel (LC2) or driver's-side wheel (LC4) 2 ft from the centerline of the bridge. The truck is centered on the bridge for LC3. Figure 4-15 shows the truck positioned near midspan for purposes of survey data collection.



Figure 4-13 Load truck crossing the bridge

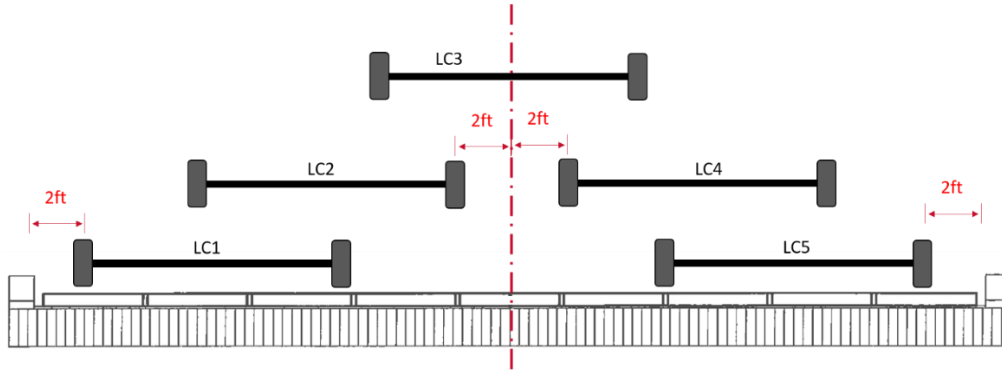
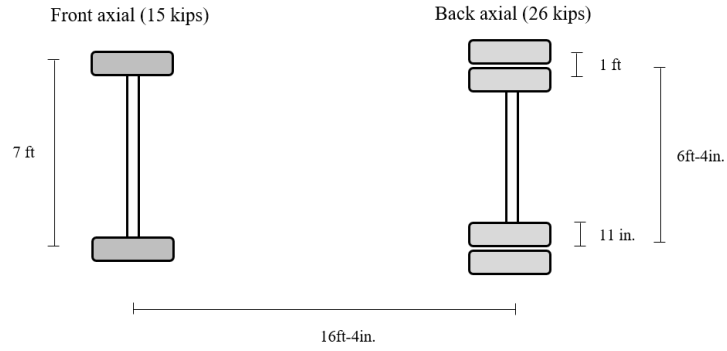


Figure 4-14 Transverse position of the truck for each load case

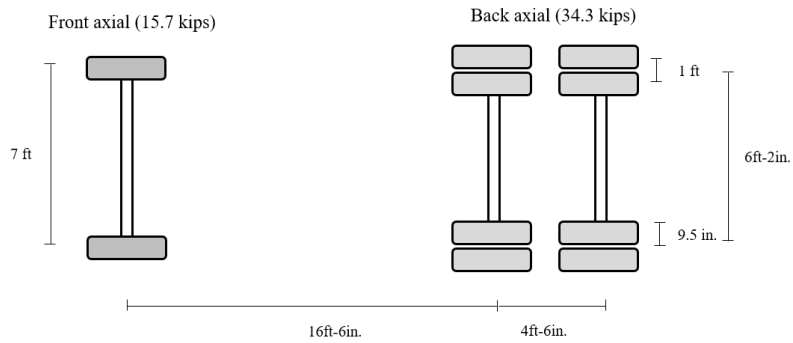


Figure 4-15 Truck parked at position of maximum strain response for survey data collection

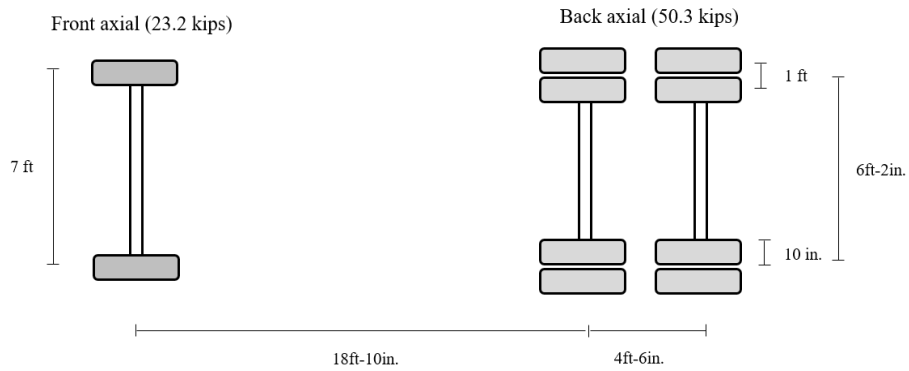
Three different size of trucks were used during the tests. The wheel width, spacing and the weight of each axle were measured before the test. Figure 4-16 shows the detail truck information. Truck A was driven on all the La Crosses County bridges. Note the same truck was used during the tests before and after the retrofit work for these three bridges. Truck B was driven on Barron County bridges and Truck C was used on the Monroe County bridges.



a) Truck A used on bridges La Crosse County Bridges: P320064; P320083; P320110



b) Truck B used on Barron County Bridges: B030174; P030079



c) Truck C used on bridges Monroe County Bridges: P410140; P410923; P410953; B410315; P410948

Figure 4-16 Axle and tire dimensions for each load truck

4.1.3 Instrumentation plan

Data were collected in two different ways. The first was using a conventional approach through the use of strain gages and deflection transducers connected to a data acquisition system. The data collected helped the research team gain a comprehensive understanding of the timber deck behavior. The second way was to collect deflection data using surveying equipment. This approach aimed to obtain the same or similar deflection data as that obtained from the first approach, albeit reduced to only the longitudinal truck position where the maximum load response was realized. The data collected from the first approach is used to validate the data collected from the second approach thereby proving or disproving the efficacy of using surveying equipment to provide usable data.

In the conventional data collection approach, both strain and displacement data were collected at two cross-sections (mid-span and quarter span) on each bridge. Although each bridge has a different length and width, a typical instrumentation plan was designed for all the bridges and is presented in Figure 4-17 and Figure 4-18. In the cases of bridges having multiple spans, only one span was instrumented.

The strain gages at the mid-span were attached along the bottom of the deck to collect longitudinal strain. These strain gages were spaced 2 ft apart near midspan to fully detect the wheel load distribution. At the quarter span, the strain gages were placed with a lesser spacing of approximately one-fourth of the bridge width. These data are generally used for finite element model validation in the subsequent tasks.

The displacement transducers were installed at both mid-span and the quarter span with a spacing of one-fourth of the bridge width. These data were not only used for the model validation but also used for validating deflection results from survey equipment. A total station was used to collect the deflection data from those locations of interests (see targets in Figure 4-19).

Figure 4-20 is a photograph of a typical instrumentation setup.

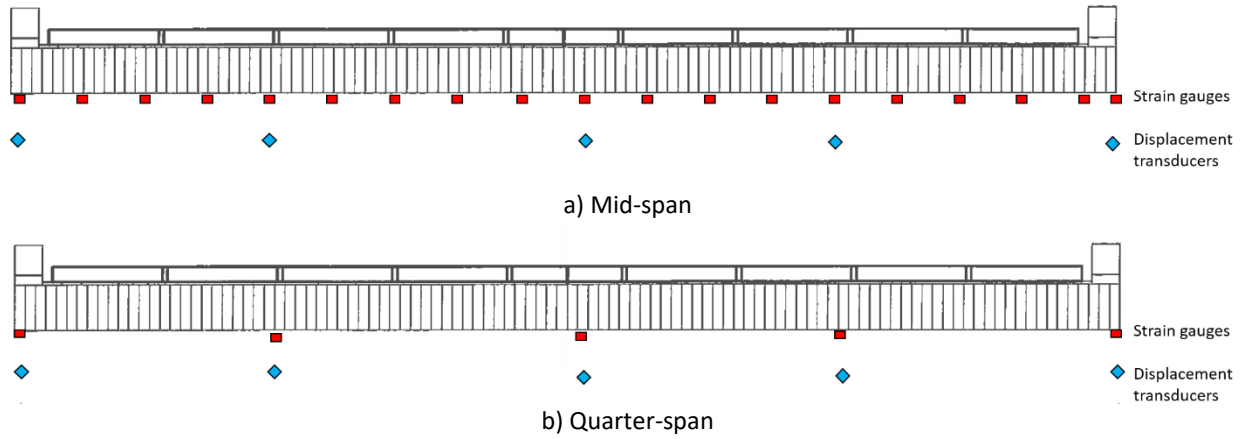


Figure 4-17 Cross-section view of general instrumentation plan

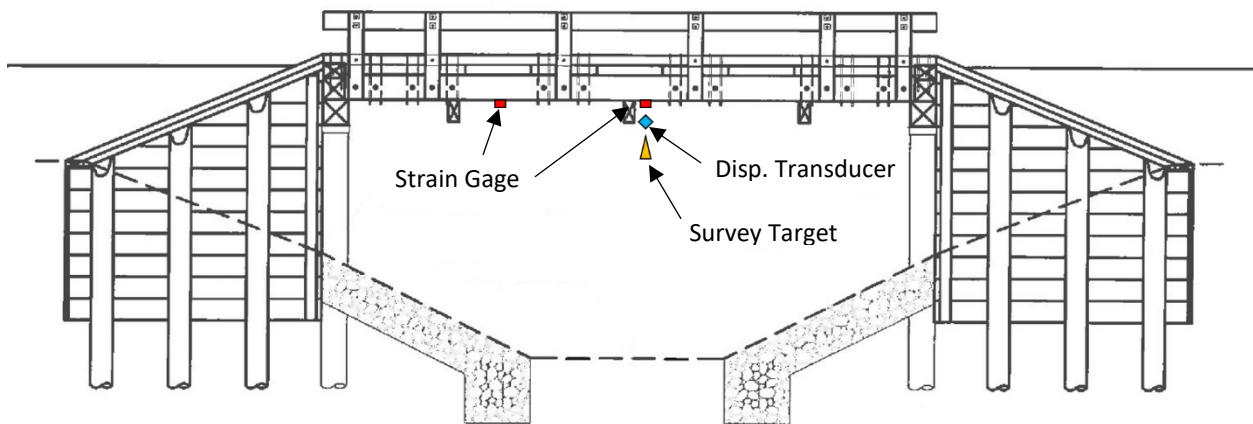


Figure 4-18 Side view of typical bridge instrumentation

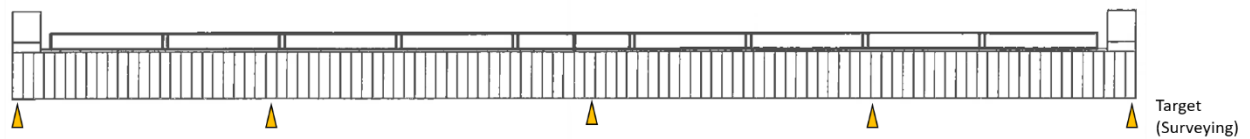


Figure 4-19 Data collection locations by surveying equipment

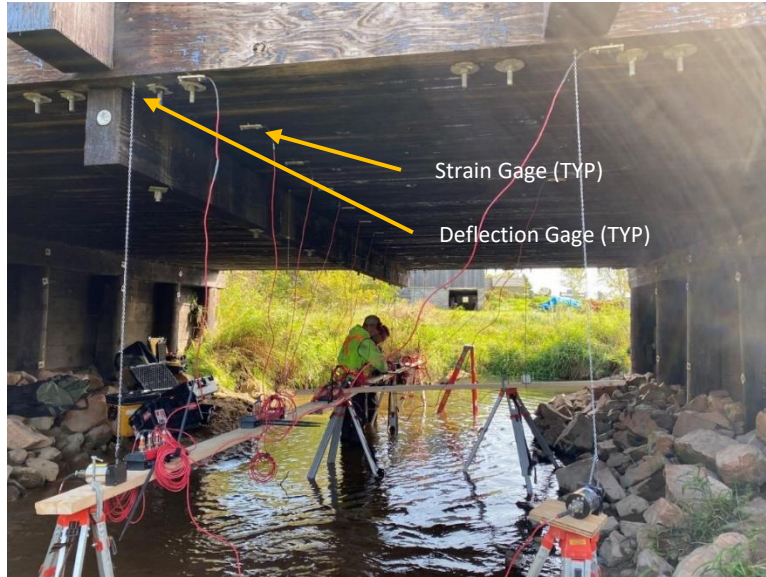


Figure 4-20 Typical bridge instrumentation

4.2 Load Test Results

The strain data collected from the field were used to calculate the equivalent wheel load width. The theory behind the calculation of the equivalent wheel load width, or equivalent strip width (ESW), utilizing field-collected strain data is represented in Section 4.2.1 and the calculated results are shown in Section 4.2.2.

4.2.1 Basic theory on calculation of equivalent wheel load width

Calculation of the equivalent wheel load width using field tests data could be achieved by the following general procedures: 1) numerically integrating the area under the moment distribution curve, and 2) dividing the summation by the estimated maximum moment.

The field test results provide strain and displacement data, instead of moments. However, these strain and displacements are directly related to the moment. The relation between the strain and moment is illustrated in Eq.8 at the i -th measurement location.

$$Strain_i = \frac{Moment_i}{ES_i} \Rightarrow Moment_i = Strain_i \times ES_i \quad \text{Eq. 8}$$

where, E is the Young's modulus, and S_i is the Section Modulus at the location where the i -th sensor is installed. If one assumes that the section modulus at all strain measurements are equal, the strip width may be calculated as:

$$E \text{ (Equivalent strip width)} = \frac{\sum_{i=1}^n (strain_i \times d_i)}{strain_{max}} \quad \text{Eq. 9}$$

where, n is the total number of strain sensors, $strain_i$ is the strain reading of the i -th sensor, $strain_{max}$ is the maximum strain measured by the sensors, and d_i is the spacing of adjacent strain gages. Figure 4-21 shows a graphical representation of the procedure.

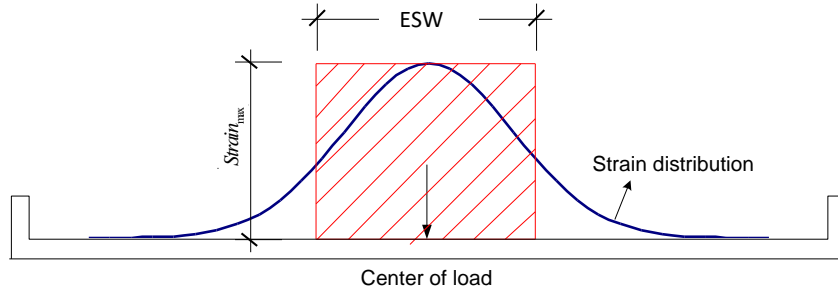


Figure 4-21 Strain distribution

A similar relationship exists between the displacement and the moment, and between the displacement and the equivalent strip width. In collecting displacement data in two ways, the goal was to determine the equivalent strip width using deflection data. If the survey station deflection results proved to have sufficient similarity to the deflection gages, it would be proposed as a simpler alternative to collecting data and thus calculating the equivalent strip width.

4.2.2 Equivalent wheel load width from field tests

Data were continuously collected for each truck path while the truck was on the bridge. A typical strain signature of all gages at mid-span observed for each bridge is shown in Figure 4-22. The first peak represents when the front axle crossed over the gage line and the second peak represents when the rear axle(s) crossed over the gage line. Using the procedure for calculating the equivalent strip width given above, the ESW was calculated and plotted with respect to truck position. An example is shown in Figure 4-23. This process was completed for all load passes and the resulting data, plots, and their statistical summaries are presented with recommendations appropriately formulated.

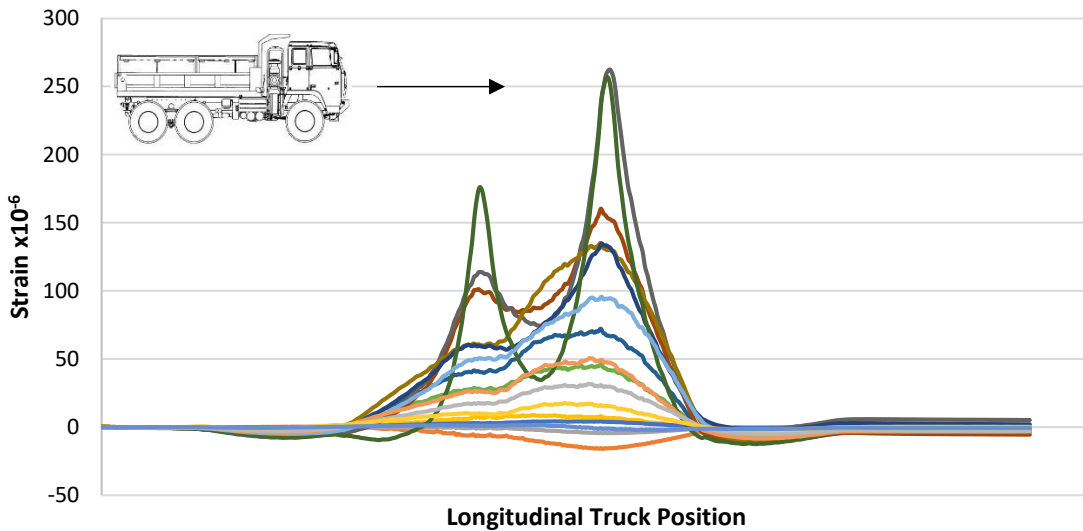


Figure 4-22 Typical Strain Time History

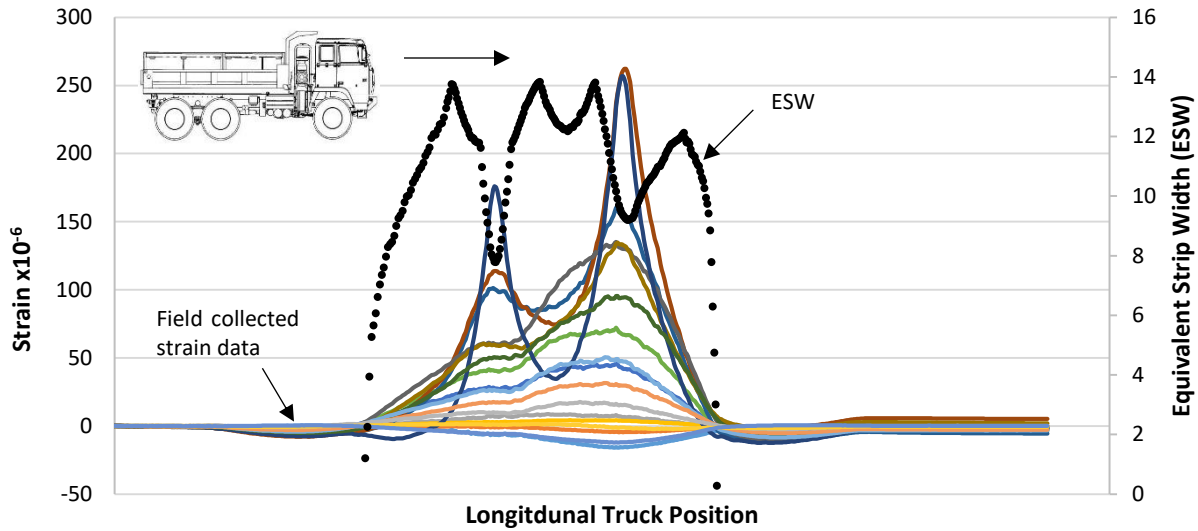


Figure 4-23 Equivalent Strip Width Superimposed on Strain Time History

When combined, the calculated discrete equivalent strip width values form a visible range that proposes the lower and higher ESW bounds. An example is shown in Figure 4-24. One should note the “tails” are omitted from the range based on the associated strain values at that point in time being very small. That is, the truck is just entering or leaving the bridge with very little load actually being applied to the bridge.

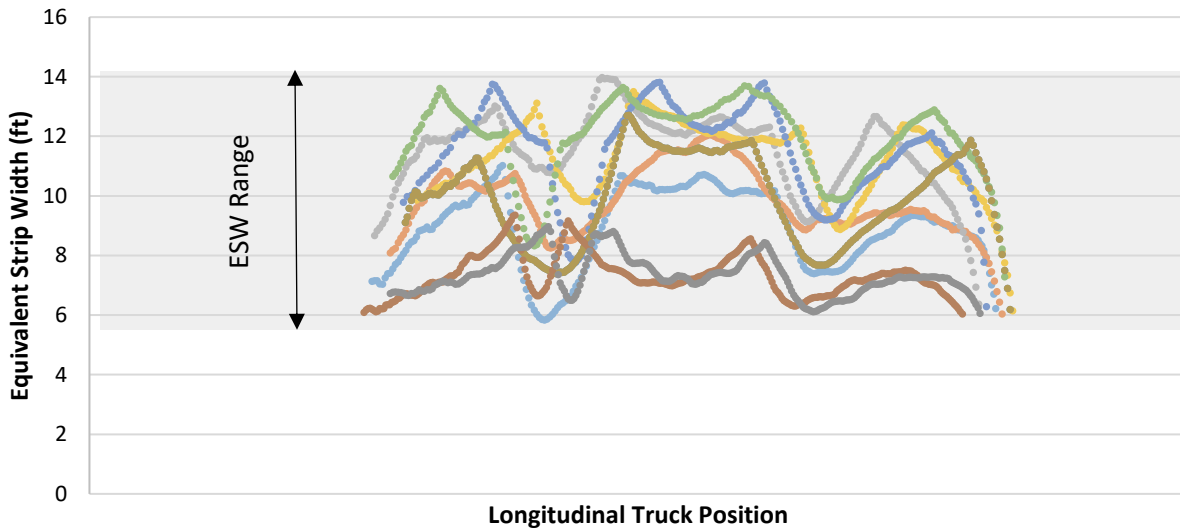


Figure 4-24 Example of Range formed by Discrete ESW Calculations

Furthermore, the statistical cumulative distribution function (CDF) can be calculated on these discrete values. The CDF provides the total probability of the equivalent strip width being at or below a given number. As an example, in Figure 4-25, the probability of the ESW being 10 ft or less is approximately 0.6. That is, there is a 60 percent probability the ESW is less than 10 ft.

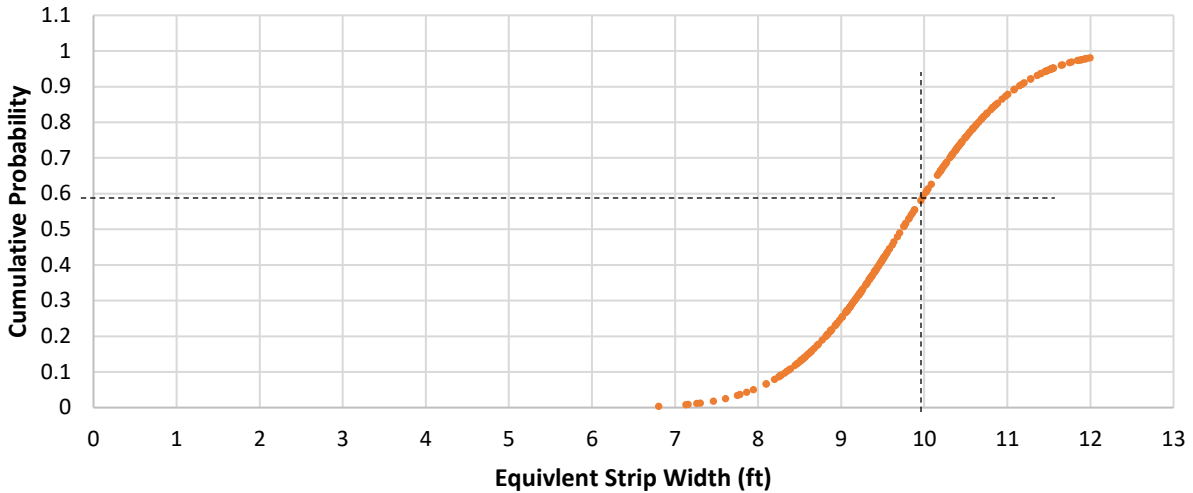


Figure 4-25 Example of Cumulative Distribution Function

A combined plot of the CDF for each load case shows the variation in ESW cumulative probability with respect to the transverse position of the truck. Figure 4-26 provides an example the trends of which generally prove true for each load tested bridge. When the truck is positioned closer to the curb the ESW tends to be lower (LC1 and LC5). When the truck is positioned closer to the center of the bridge the ESW tends to be higher (LC 2, LC3, and LC 4).

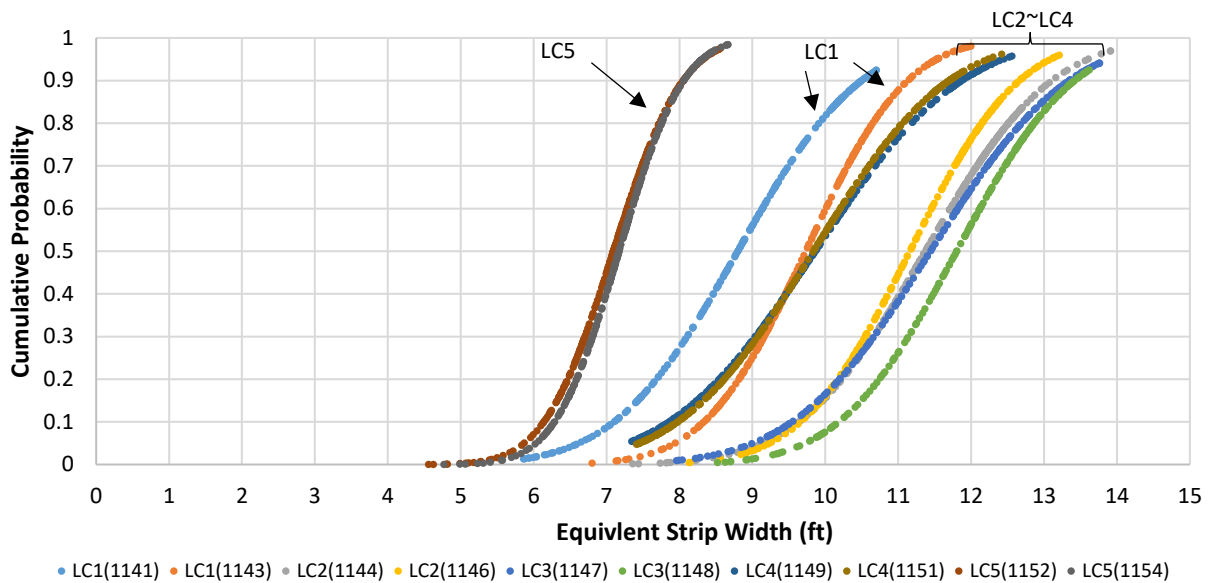


Figure 4-26 Example of Single Bridge Cumulative Distribution Functions for Each Load Case

Furthermore, a plot of the CDFs for all load cases and all tested bridges is provided to show the range of equivalent strip widths as shown in Figure 4-27. Superimposed on this plot (dashed vertical lines) are the calculated widths prescribed in Chapter 45 of the Wisconsin Load Rating Manual for poor condition (left) and good condition (right) bridges. It can be observed that the probability of being below these values is relatively low in comparison to the probability of exceeding them.

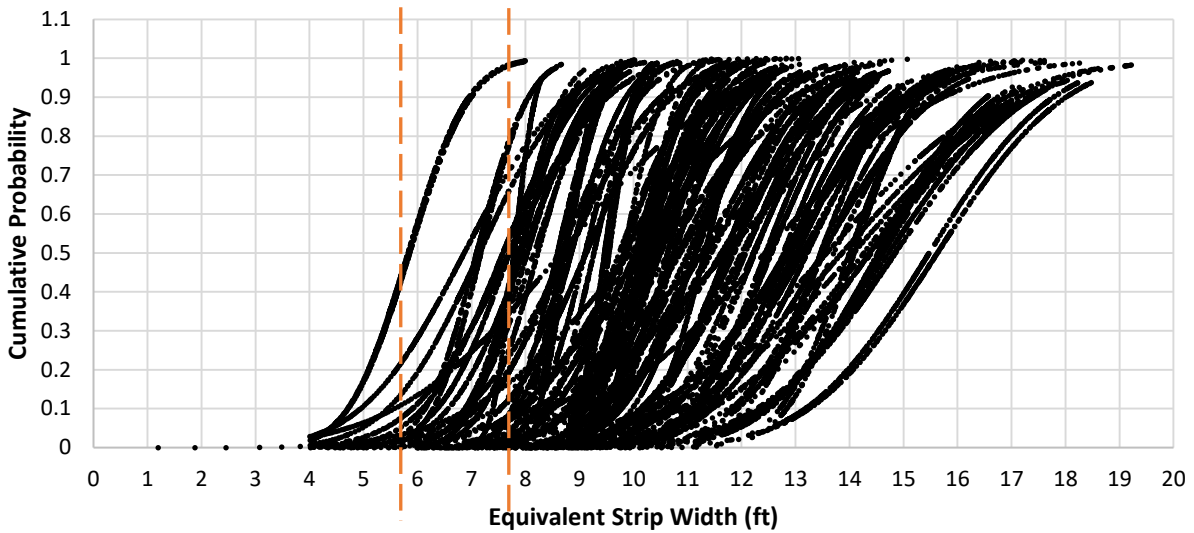


Figure 4-27 Combined CDFs for All Load Cases

This is especially true when considering the transverse position of the vehicle. Figure 4-28 also shows the combined CDFs, but in this case, the load cases are differentiated by color. That is, Load Case 1 for each bridge test is one color, Load Case 2 another, etc. (LC1 = Red, LC2 = Orange, LC3 = Black, LC4 = Green, LC 5 = Blue). It can be observed that the equivalent strip width is generally greater when the truck is positioned closer to the center of the bridge and lower when positioned closer to the curbs.

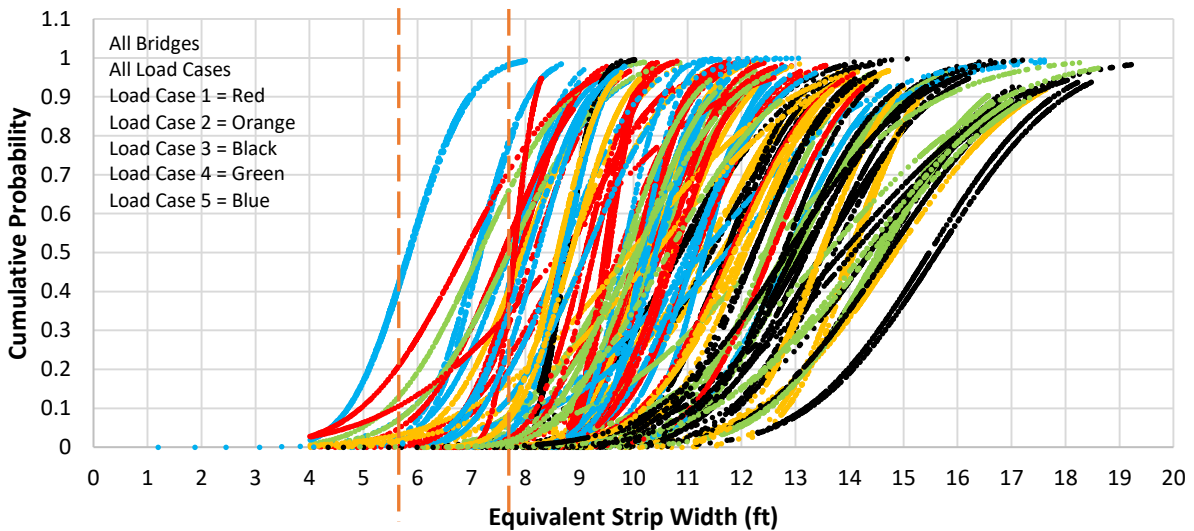


Figure 4-28 Combined CDFs by Load Case

4.2.3 Multiple Lanes Loaded

It is important to recognize the results from above are single-lane-loaded scenarios. The equivalent strip width can be similarly calculated for multiple-lanes-loaded scenarios. This is achieved by combining the strain data for load cases 2 and 4 in the same data set.

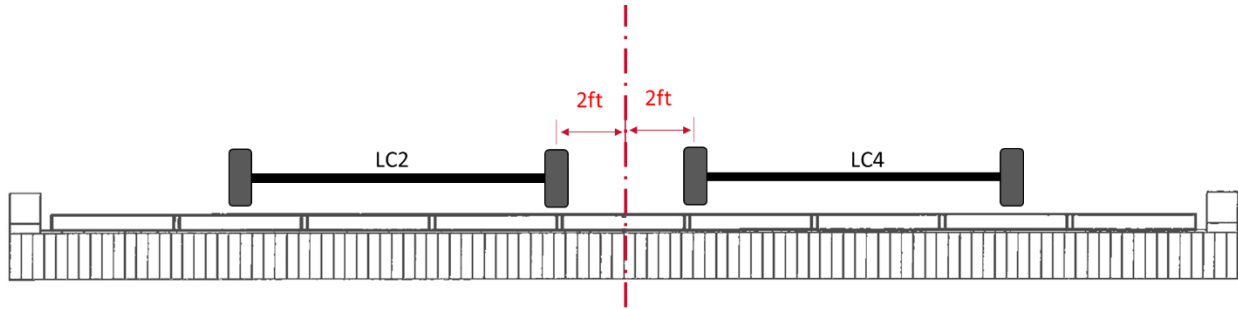


Figure 4-29 Two lanes loaded

An idealized plot of the transverse strain distribution for multiple-lanes-loaded is shown in Figure 4-30. In reality, the magnitude will not decrease at the center of the bridge as much as is shown graphically. However, what is generally true is the overall maximum strain magnitude will not be significantly higher than the maximum strain magnitude observed in a single-lane-loaded scenario. Due to the transverse position of the trucks, the summation of strain imposed by one truck to that of the other tends to be the higher strains from the former to the lower strains from the latter.

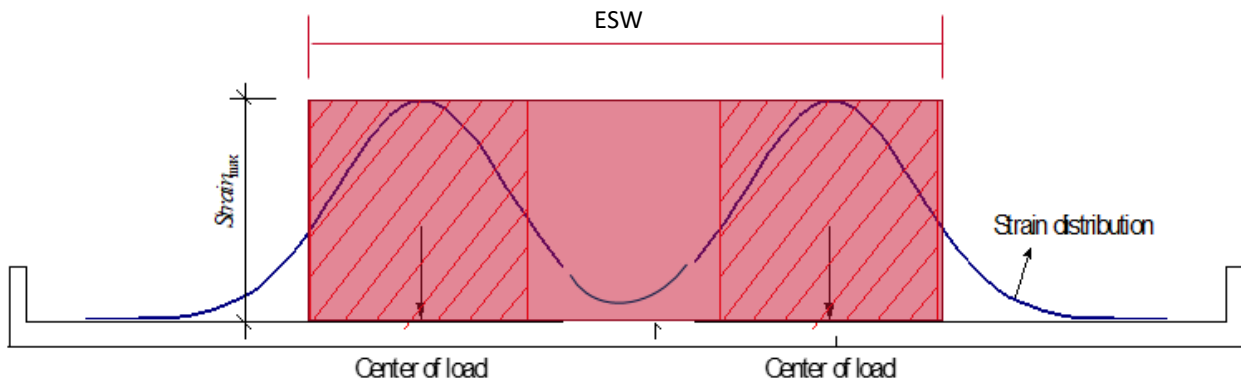


Figure 4-30 Idealized transverse strain distribution for multiple lanes loaded

The ESW for multiple lanes loaded is calculated in the same way as for single lane loaded cases. Several examples of the calculated ESW values are provided in contrast to the single lane loaded cases in Figure 4-31 through Figure 4-33. The ESW for multiple lanes loaded (solid black line) is provided for only approximately 10 data points across the strain time history which provides a good overview of the ESW trend. A full comparison at all truck positions requires a much more extensive calculation process since the truck position with respect to the rate of data acquisition varies for each load pass. Nonetheless, at first look it is observed the multiple-lane ESW exceeds the range of the single-lane ESW. However, since there are two vehicles on the bridge the ESW values must be divided by two. When doing so, the ESW becomes more in line with the lower single-lane ESW range values. The final recommended ESW equation provided in Chapter 6 reflects this relationship.

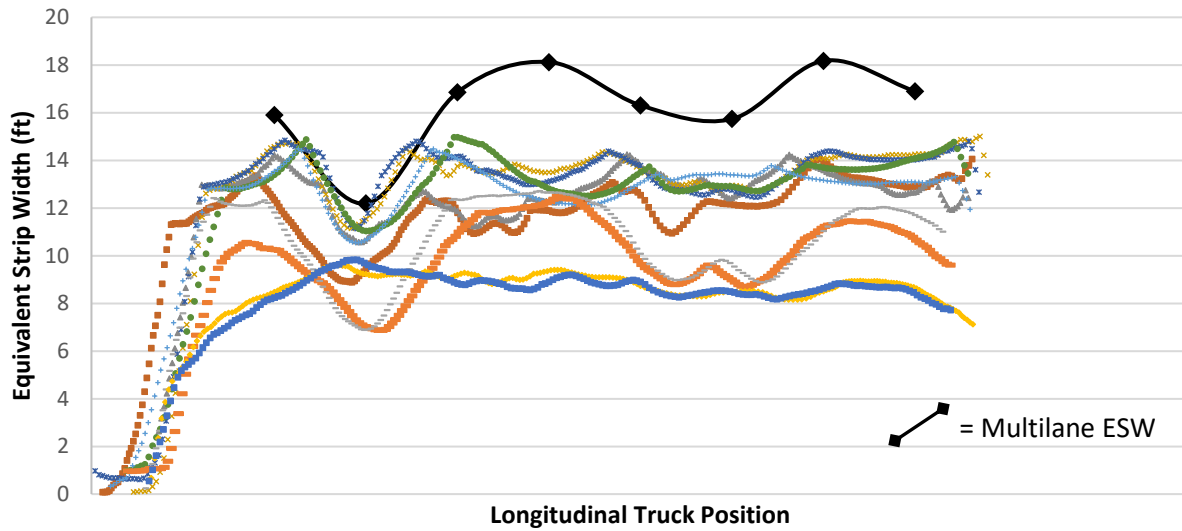


Figure 4-31 ESW Comparison for Combined Load Cases 2 and 4 for Bridge P410948

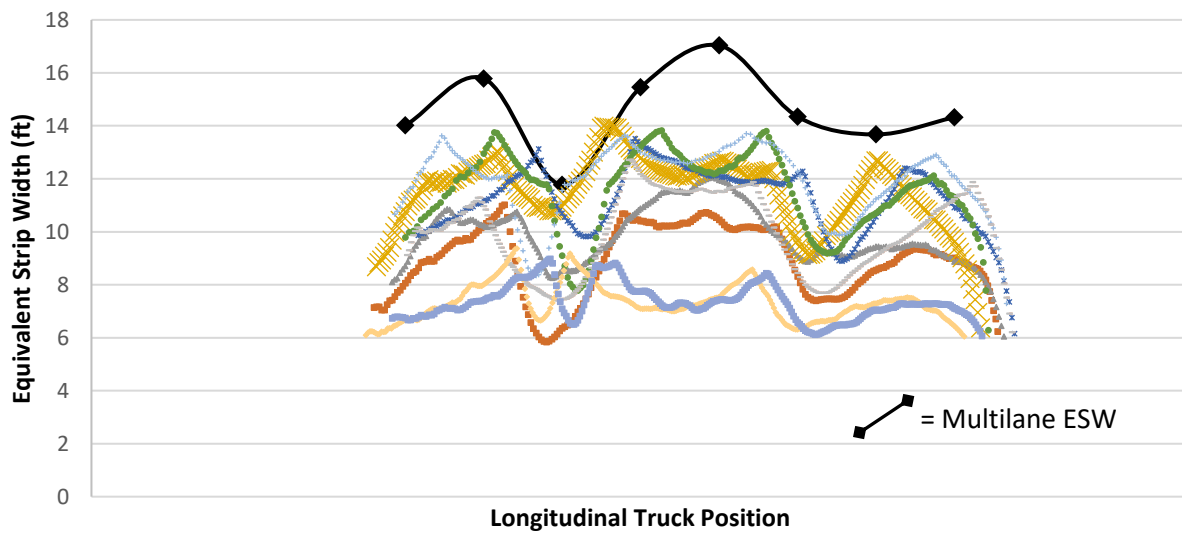


Figure 4-32 ESW Comparison for Combined Load Cases 2 and 4 for Bridge P320064

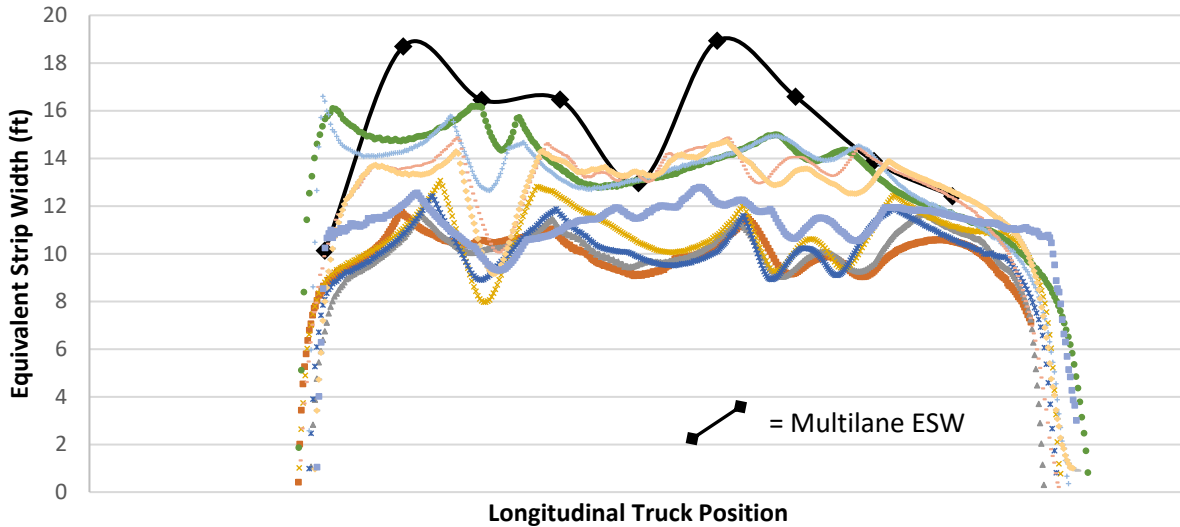


Figure 4-33 ESW Comparison for Combined Load Cases 2 and 4 for Bridge B030174

The variation in equivalent strip width due to number of lanes loaded is similar to current design specifications (AASHTO 2020) for slab-type bridges. Two equivalent widths are calculated, Eq. 3 and Eq. 4, for single and multiple lanes loaded and the smaller equivalent width is to be used.

4.2.4 Retrofit Effectiveness

One opportunity this research project presented was the ability to test three bridges in La Crosse County before and after strengthening retrofits were completed. In each case, 4" thick transverse timber deck panels were fastened to the top of deck with grout injected between the panel and deck to fill any voids. In addition, more spreader beam bolts were added between the deck and spreader beams. Figure 4-34 shows a cross-section plan of the retrofit.

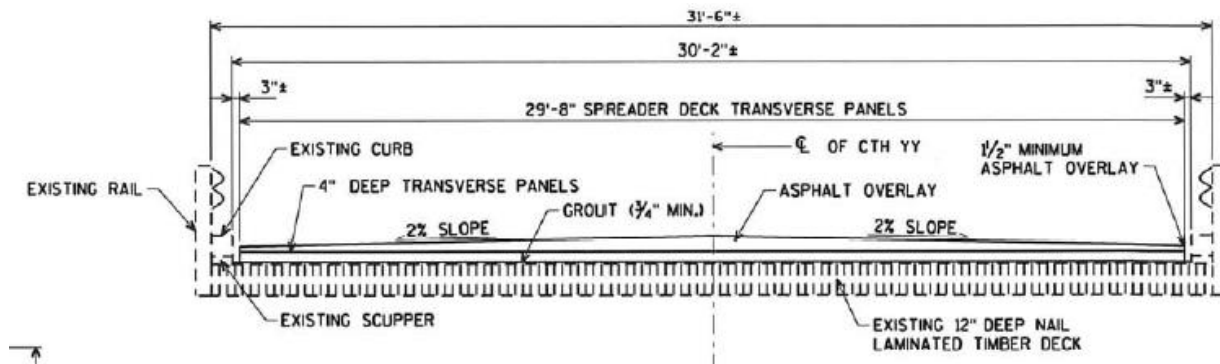


Figure 4-34 La Crosse County Deck Retrofit

Figure 4-35 shows the beginning stages of transverse deck panel placement. The asphalt wearing surface had been removed from the original deck surface and transverse deck panels were being placed, shimmed for proper elevation, and fastened to the deck. After, the void space remaining between the panel and deck was pumped full of grout to ensure continuous load transfer between the panels and deck. The process was completed with a new layer of asphalt placed over the panels.



Figure 4-35 Transverse Timber Slab Retrofit under Construction

Once each La Crosse County bridge was retested and the data analyzed, it was evident the retrofit improved the transverse load distribution and, accordingly, the equivalent strip width. Figure 4-36, Figure 4-37, and Figure 4-38 show the before (black) and after (gray) retrofit ESW plots for Bridges P320064, P320083, and P320110, respectively. In each case the ESW generally improved 2 to 3 ft. As a reminder, the vertical lines represent the equivalent strip width calculated for the bridge for good (right) and poor (left) condition per the Wisconsin bridge manual.

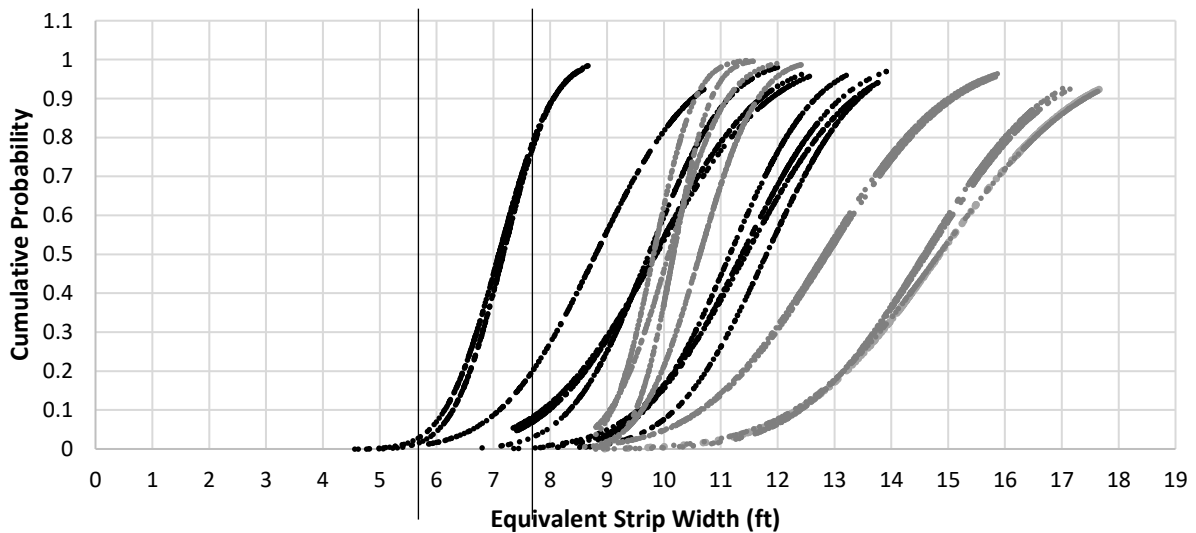


Figure 4-36 CDFs for Bridge P320064 Before and After Retrofit

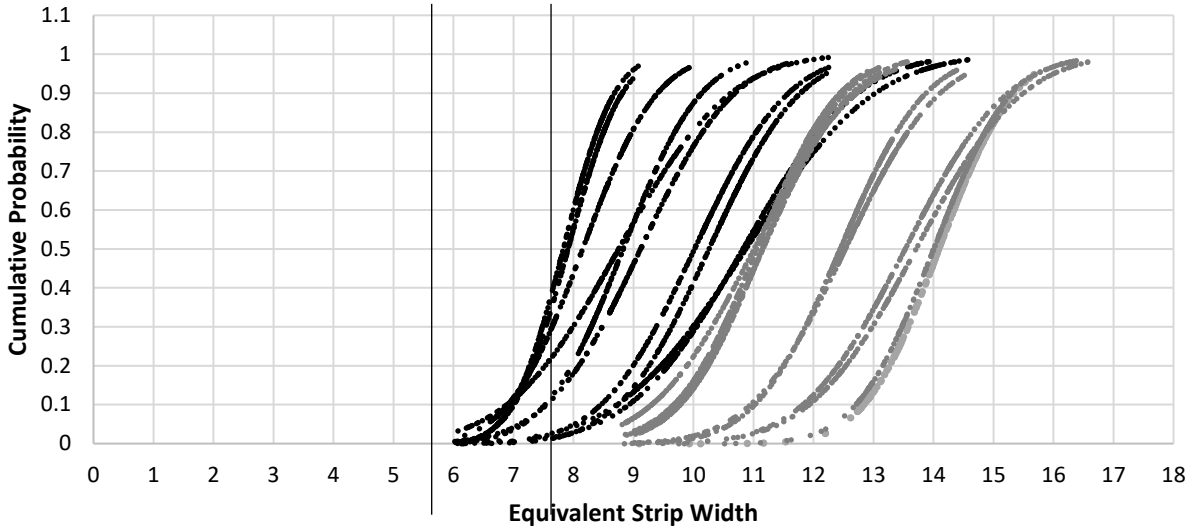


Figure 4-37 CDFs for Bridge P320083 Before and After Retrofit

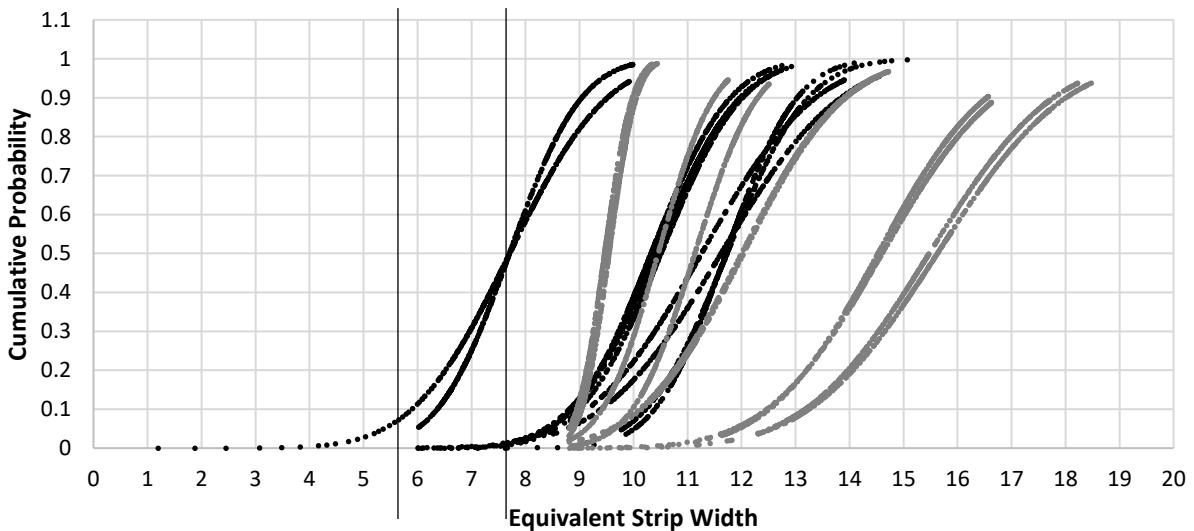


Figure 4-38 CDFs for Bridge P320110 Before and After Retrofit

4.2.5 Bridges Designed by AASHTO LRFD

Monroe County Bridge B410315 shown in Figure 4-39, was selected for testing and evaluation because it was designed using AASHTO LRFD, different than the other bridges. The plan (cross-section shown in Figure 4-40) of the bridge superstructure did not greatly differ from other bridges with the exception of spreader beam number and size. Three spreader beams were used in lieu of the single spreader beam per span used on the other bridges. The beam cross-sectional size was of lesser depth than what was observed on the other bridges, however (8 in. x 6 in. vs. 12 in. x 6 in.), and a closer bolt spacing between the spreader beams and deck was used.



Figure 4-39 Monroe County B410315

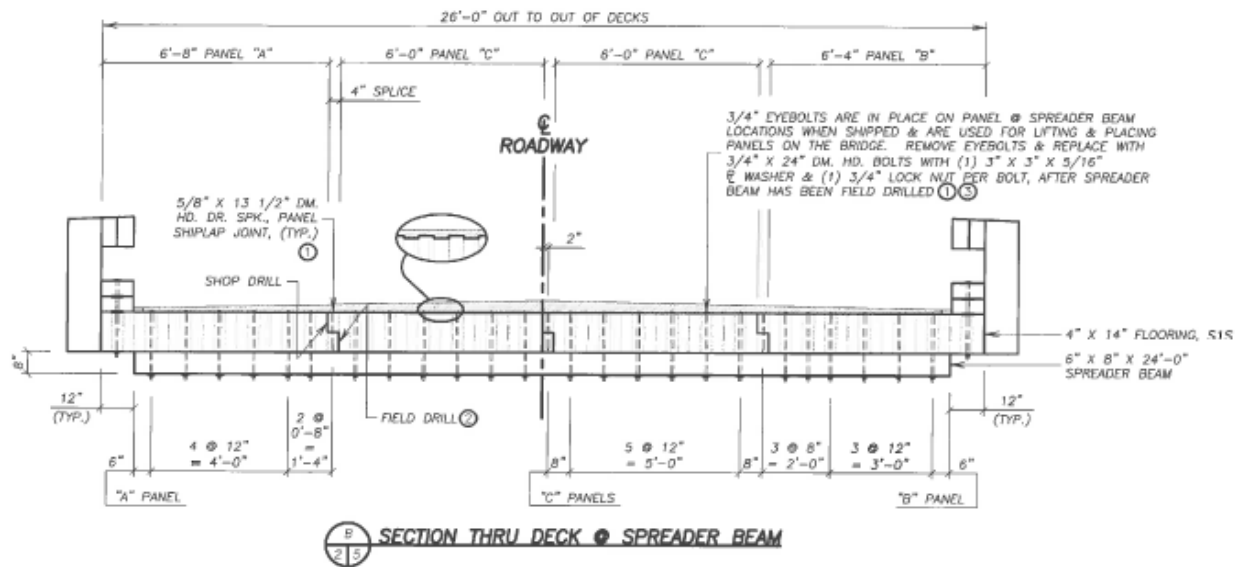


Figure 4-40 AASHTO LRFD Designed Bridge Cross-section

The CDFs of this bridge shown in Figure 4-41 varied from the patterns commonly seen on the other bridges. Though the overall ESWs were within the range of the other bridges, there was a clear distinction between the load cases that positioned the truck wheel lines on one side of the bridge centerline or the other (LC 1, 2, 4, and 5) versus the load case (LC 3) that positioned the truck wheel lines on either side of the centerline. This implies that the load is not being transferred across the bridge centerline as effectively as what is observed on the other bridges. One possible reason for this phenomenon is the stiffness of the spreader beams being approximately one-third that of those on the other bridges. Only one bridge designed using AASHTO LRFD was tested, so it was inconclusive whether this behavior would be observed on similarly designed bridges or if this behavior is unique to this bridge.

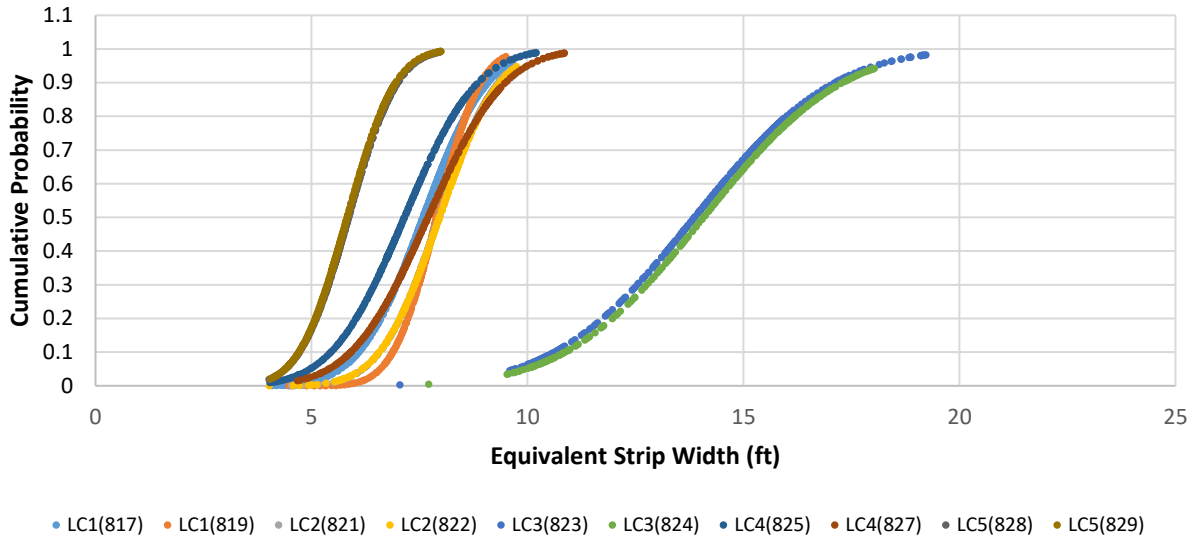


Figure 4-41 CDFs for Bridge B410315

With this information being inconclusive, the oversight committee requested another LRFD-design bridge be field tested. This exercise would provide an opportunity to see similarities or dissimilarities between the two LRFD-designed bridges. No other bridges that closely matched the bridge in question existed in the counties that had already participated in the field tests. However, in Sauk County which neighbors Monroe County, a bridge was identified which had many similarities to the Monroe County Bridge.

Sauk County Bridge B560224 shown in Figure 4-43 has many similarities (materials, connection details, etc.) to the Monroe County Bridge Figure 4-42. As a way of comparison, Figure 4-44 and Figure 4-45 show the plan view and section view, respectively, of the Monroe County Bridge and Figure 4-46 and Figure 4-47 show the plan view and section view of the Sauk County Bridge, respectively. Each bridge has a span length of 28 ft., but a slightly greater width, 30 ft. to 26 ft. The number of longitudinal panels is five, whereas the Monroe County Bridge is four. An odd number of panels results in there not being a longitudinal panel joint at the centerline.

Two noteworthy differences are the depth of laminations, 16 in. to 14 in., and the size and number of spreader beams, each leading to a different structure stiffness. The Monroe County Bridge had three 8 in. deep by 6 in. wide spreader beams located at the quarterspans and midspan (see Figure 4-48), whereas the Sauk County Bridge had a single 12 in. deep by 6 in. wide spreader beam at midspan (see Figure 4-49). The research team believed the reduction in spreader beam stiffness of the Monroe County Bridge resulted in the load transfer across the bridge being less than what would otherwise be expected with a larger spreader beam.



Figure 4-42 Monroe County Bridge B410315



Figure 4-43 Sauk County Bridge B560224

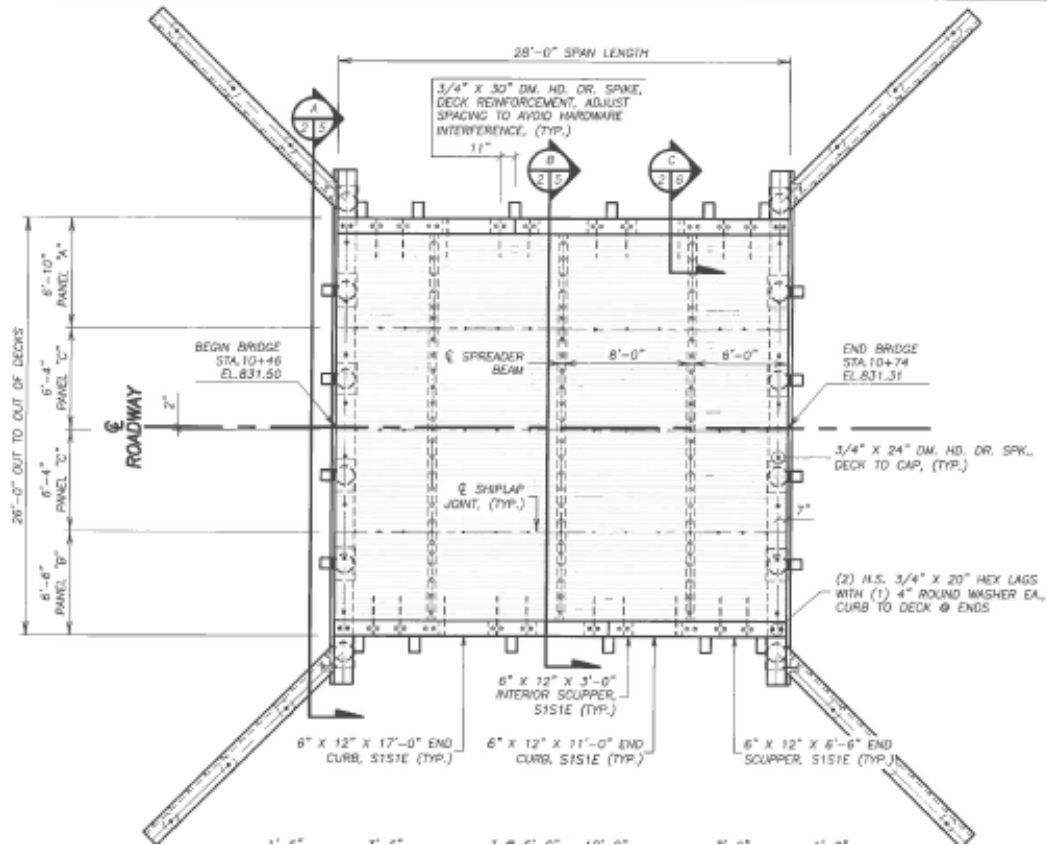


Figure 4-44 Monroe County Bridge B410315 Plan View

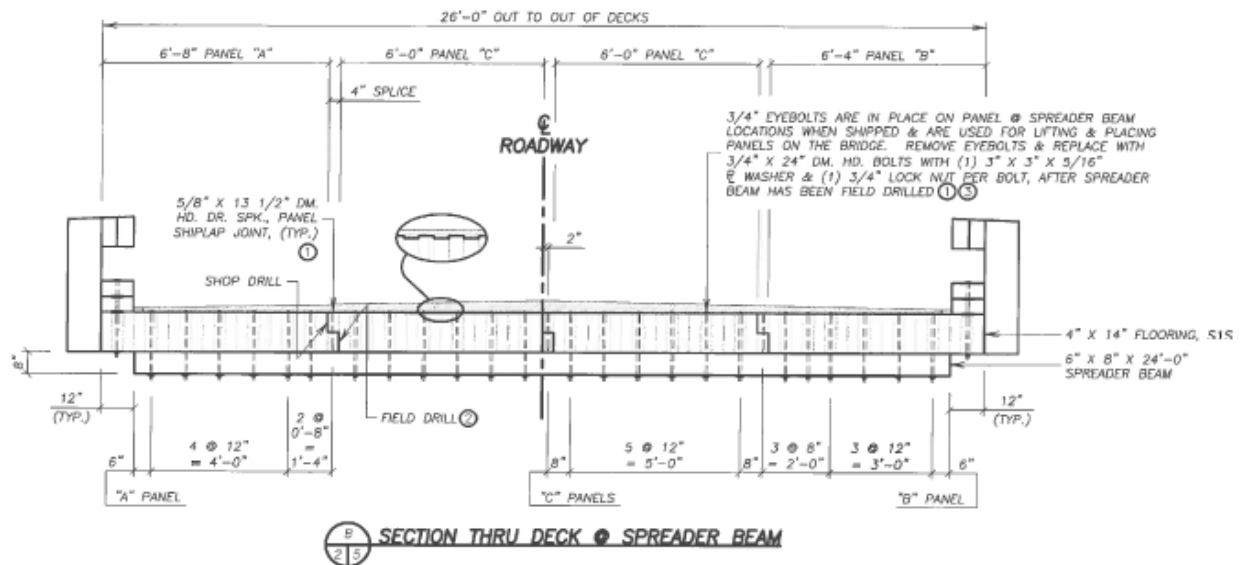


Figure 4-45 Monroe County Bridge B410315 Section View

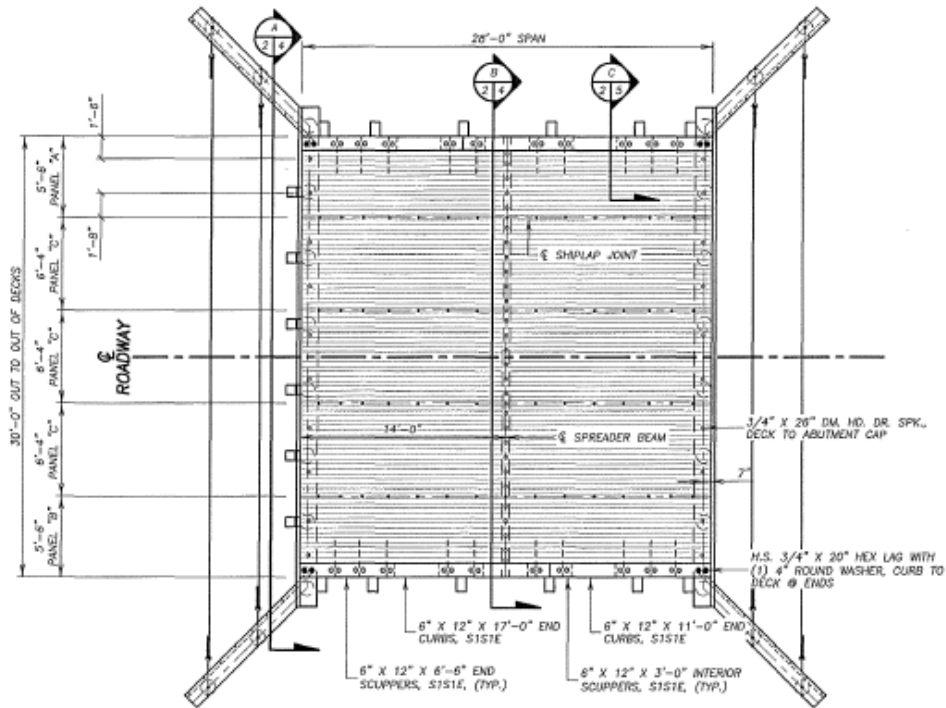


Figure 4-46 Sauk County Bridge B560224 Plan View

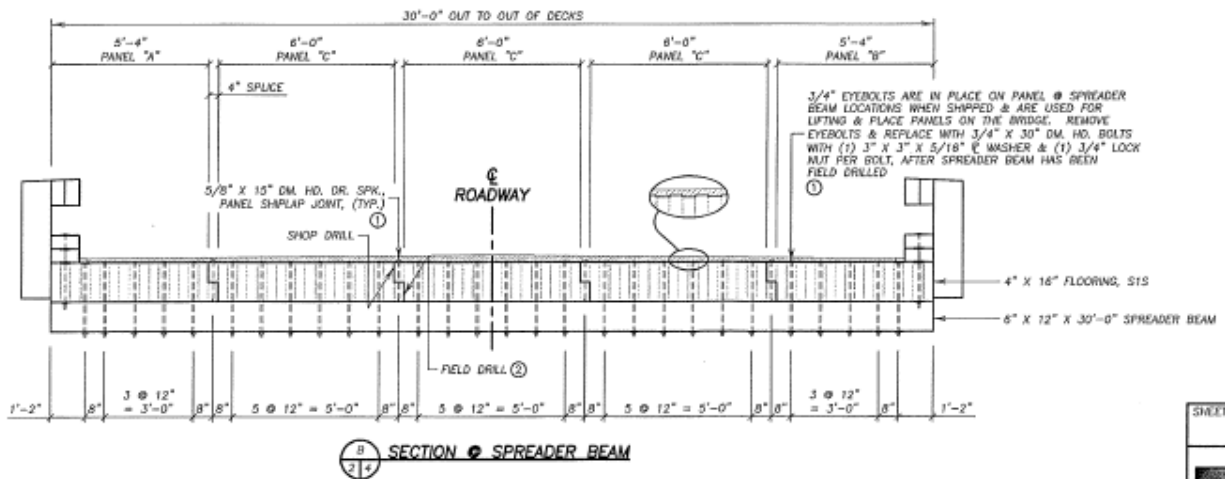


Figure 4-47 Sauk County Bridge B560224 Section View



Figure 4-48 Monroe County Bridge B410315 Spreader Beams

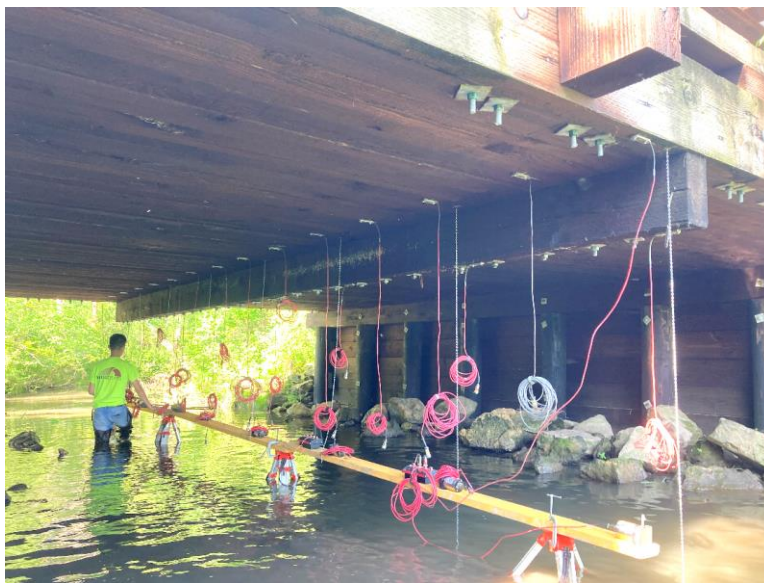


Figure 4-49 Sauk County Bridge B560224 Spreader Beam

The load test vehicles were nearly identical in axle configuration and overall weight which eliminated another variable and helped in the direct comparison.



Figure 4-50 LRFD Bridge Load Vehicles

The load case strain signatures from each bridge were compared and there were no readily apparent deviations in behavior between the two bridges. As the equivalent strip widths and subsequent cumulative distribution functions were calculated, however, there were some differences that became evident. Figure 4-51 shows the CDF groupings of all load cases for both bridges. The grouping of the CDFs of the Sauk County Bridge (black) were much tighter when including all load cases and had an overall greater average magnitude than the Monroe County Bridge (grey). The Sauk County Bridge CDF results proved to be much more alike the results observed from the other timber slab bridge tests. This information leads the researchers to believe the reduced stiffness of the spreader beams on the Monroe County Bridge is less effective in transversely distributing the vehicle load.

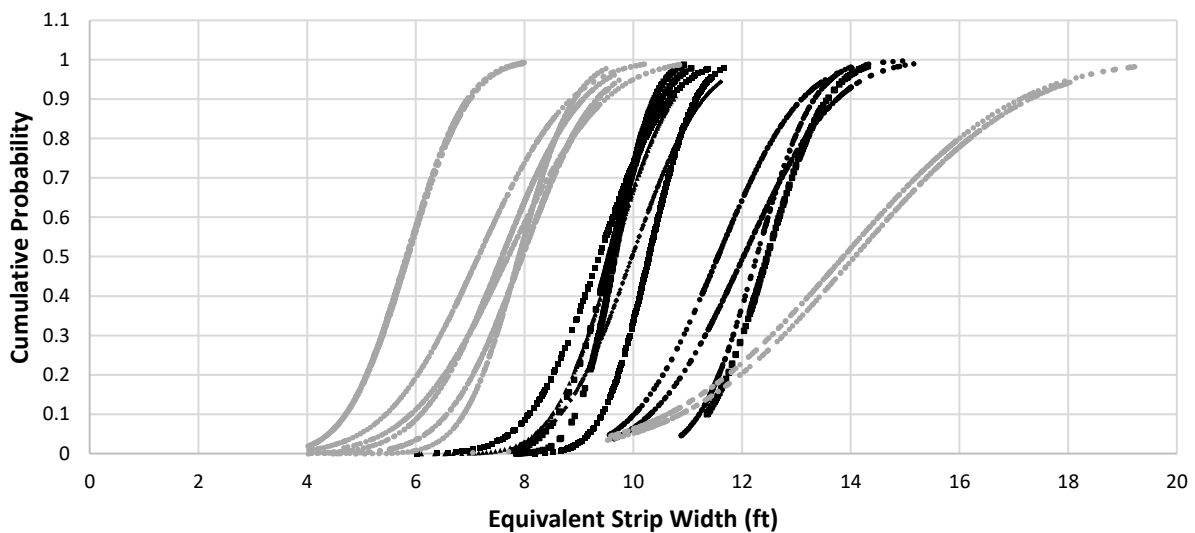


Figure 4-51 CDF Comparison of Monroe (grey) and Sauk County (black) LRFD Bridges

4.3 In-Situ Timber Inspection

In addition to conducting load testing during the field portion of the study, the team conducted an arms-length visual inspection of each bridge tested. This inspection included the use of non-destructive evaluation (NDE) timber inspection tools to assess the in-situ condition of the timber components. Specifically, a Delmhorst RDM3 moisture meter was utilized to collect pertinent moisture content readings from the superstructure members at various locations. These readings were compared to current AASHTO and WisDOT Policy and Procedures regarding moisture adjustment factors to assess if modifications to those factors are deemed necessary. In addition to collecting moisture content data at the time of load testing, the research team returned to the bridges during the winter months to collect below freezing data.

4.3.1 Visual Observation

The timber decks were visually observed for clear areas of degradation, cracking, checking, and loose connections. Generally, the timber deck slabs of each of the bridges were in good condition with few areas of notable poor condition. Examples of the exceptions are shown in Figure 4-52 through Figure 4-56.



Figure 4-52 Missing shims or gapping between spreader beam and bottom side of deck (La Crosse Co. P320083)



Figure 4-53 Cracked Lamination (La Crosse Co. P320083)



Figure 4-54 Cracked Lamination (La Crosse Co. P320083)



Figure 4-55 Vegetation in Curb Gutters (Barron Co. B030174)



Figure 4-56 Delamination near edge of slab (Monroe Co. P410953)

4.3.2 Moisture Results

A means for general assessment of timber quality is to gather moisture level information. Additionally, moisture levels are used to modify the reference design values of timber when elevated moisture levels are present (greater than 19%). For this project, moisture levels were measured at various locations on the tested bridges at depths of 1.5" and 3" from the bottom deck surface. The results varied across all bridges and among the measurements taken on single bridges. Furthermore, the results indicated elevated moisture levels beyond the level in which adjustment factors would be applied. Follow-up measurements were taken during the winter when the bridges were at below-freezing temperatures. The moisture levels at this time similarly varied at elevated levels. Due to the variation, the moisture level data was not used in any appreciable way during the strain data analysis and, rather, was broadly used to

characterize the bridges as being consistently wet while in service. Any effect of moisture levels is inherently included in the test data.

4.3.3 Comparison with AASHTO and WisDOT policy

Chapter 45 of the Wisconsin Bridge Manual includes the use of timber adjustment factors (Chapter 23). Specifically with respect to moisture, a wet service factor is applied to the bending and shear stresses per the guidance of the National Design Specification (NDS) and assumes the timber is wet in service. The exception is if the deck can be considered impervious. Observing the actual conditions of the bridge decks and the extensive research that has been completed with respect to wet service conditions, the authors recommend this practice be continued.

4.3.4 Timber Evaluation using Micro-drill

4.3.5 Micro-drill Procedure

Select locations at the bottom side of the timber deck were identified to add to the condition assessment. The locations were consistently at or near midspan strain gages, with fewer located near an abutment or pier. As shown in Figure 4-57, An IML PD400 micro-drill was used to drill upward through the deck. The drill is able to determine the wood quality by measuring the resistance to penetration. The drill consists of an 18" long, 2 mm diameter drill bit that is rotated at a constant speed. The output consists of a plot showing the resistance versus the depth of penetration. An example plot is shown in Figure 4-58. This plot provides a visual representation of the density of wood. The natural growth patterns of wood are often evident by consistent repetition of peaks and valleys (rings) on the plot and a flattened zone midway (the pith). These patterns are not to be viewed as areas of degradation. Rather, clear inconsistencies in the pattern where a drop in the plot occurs indicates a lesser density and an area where the timber has likely degraded.



Figure 4-57 Micro-drill Assessment (La Crosse Co. P320110)

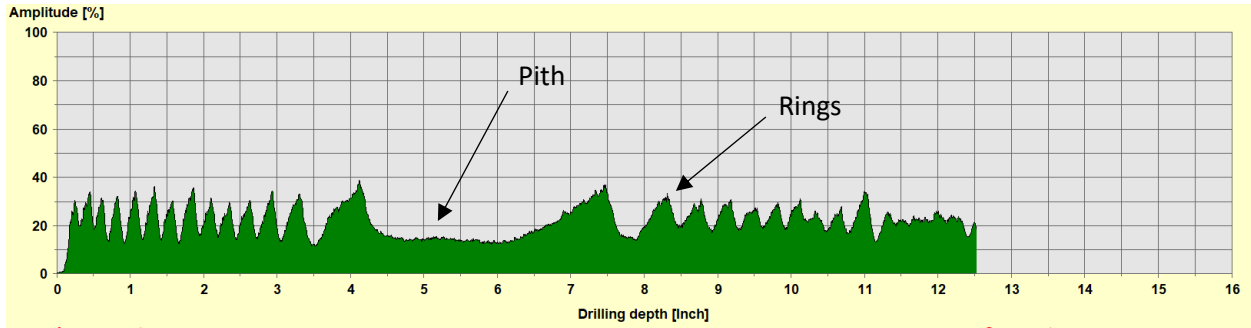
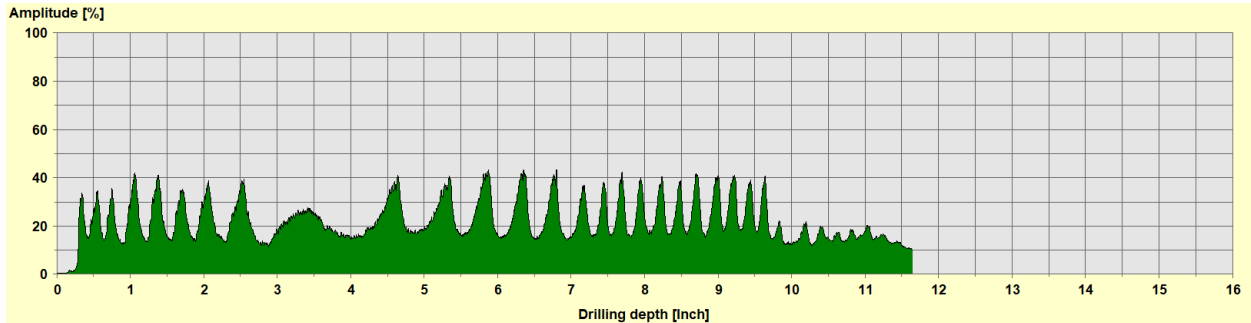
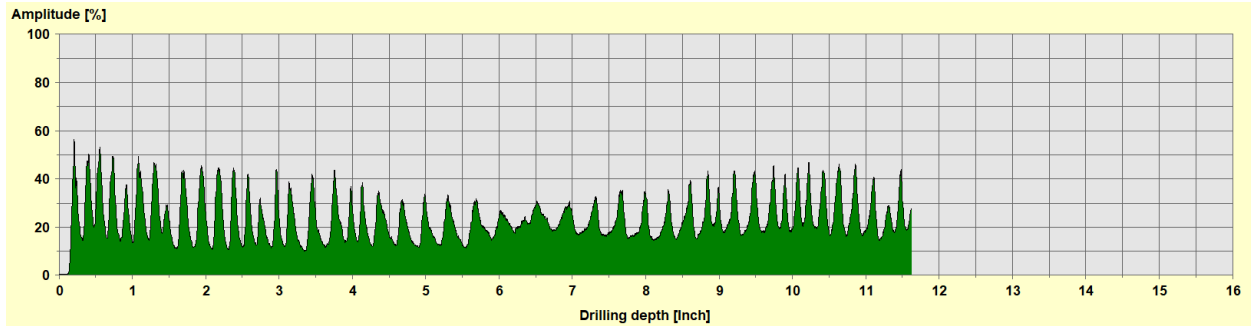
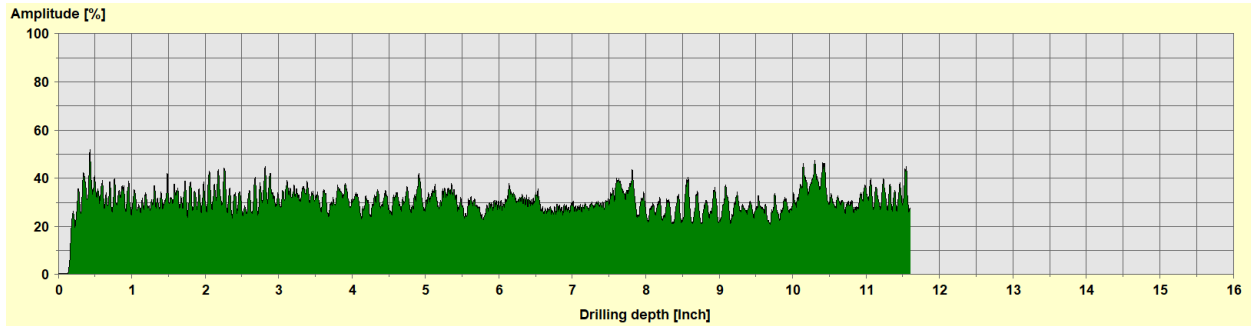


Figure 4-58 Example Plot of Micro-drill Results

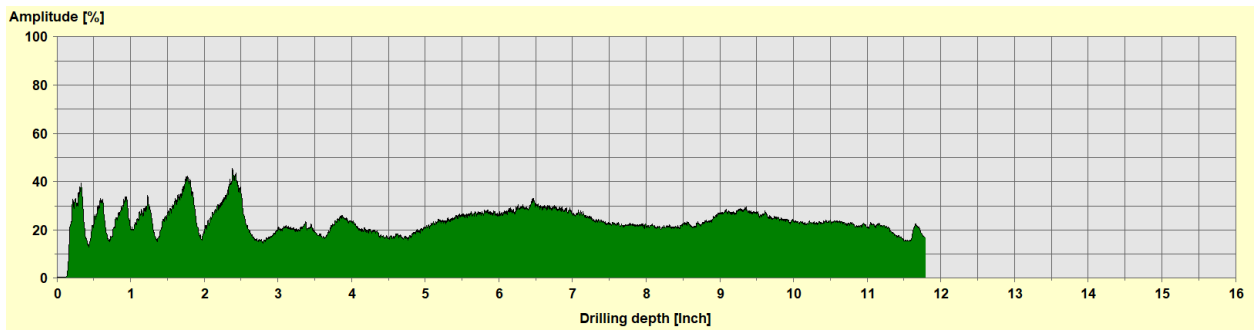
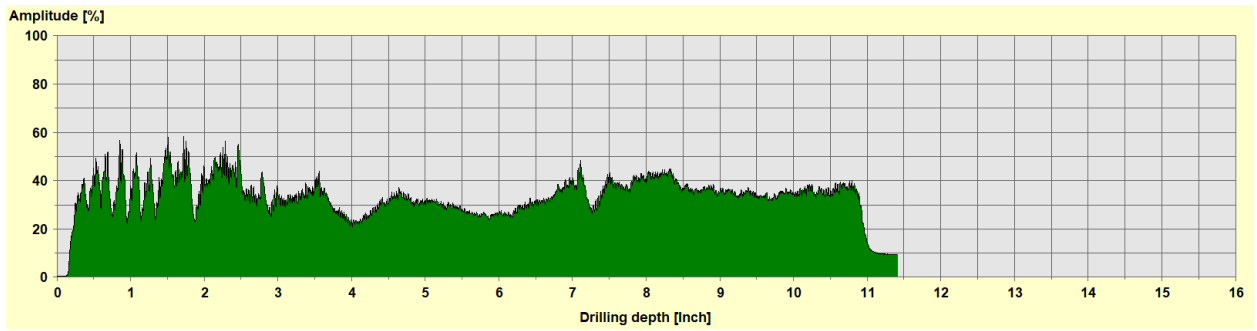
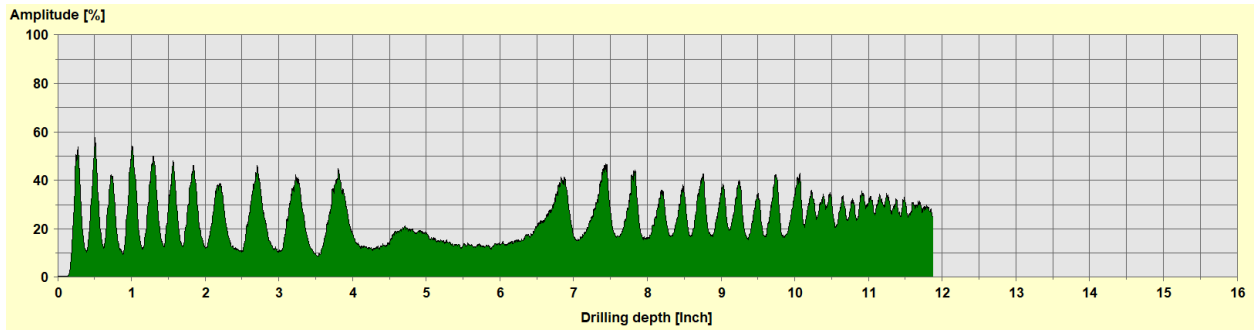
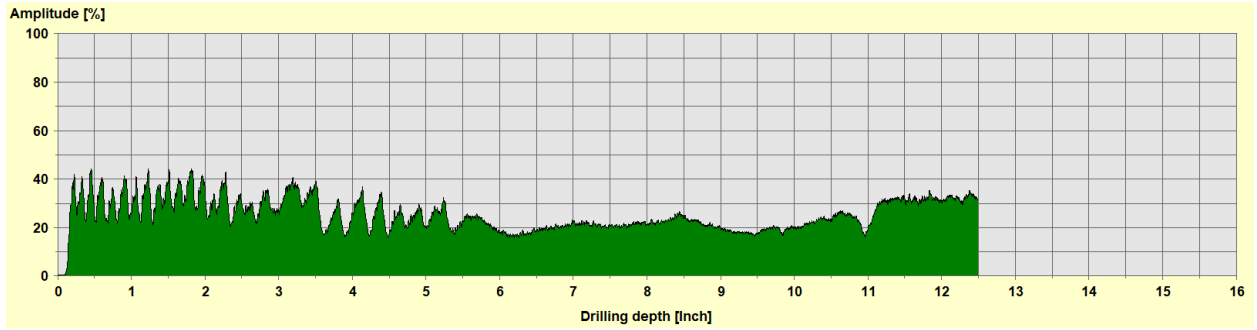
4.3.6 Micro-drill results

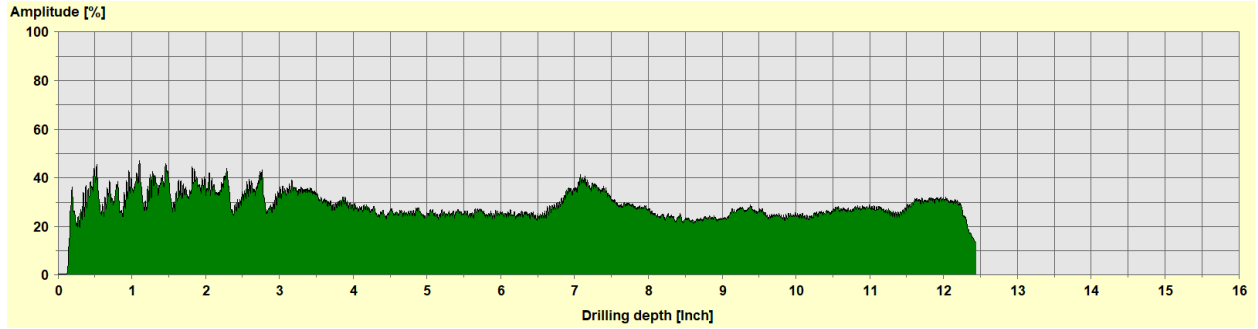
The locations of the micro-drill use were consistent with the locations of the midspan deflection gages. Results for each respective bridge are provided in the following figures along with observations from the drilling log. For all logs, the condition of the wood is consistent with there being no degradation unless noted otherwise on the plot. Overall, the wood was in good condition.

P320083

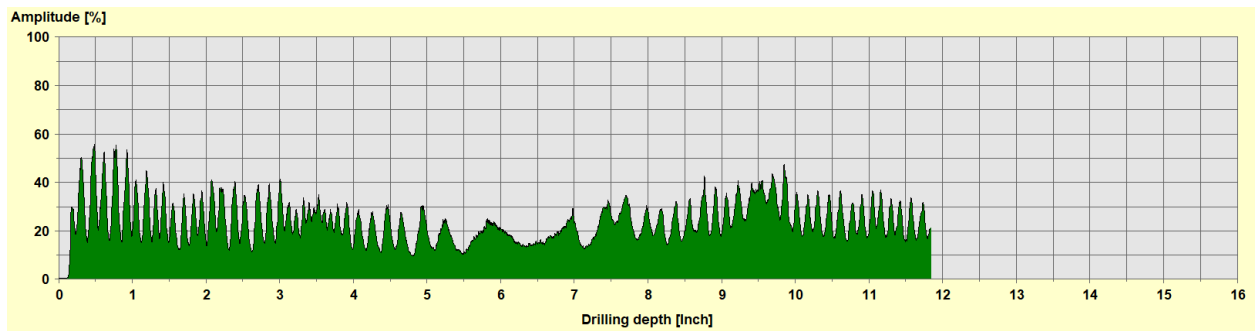
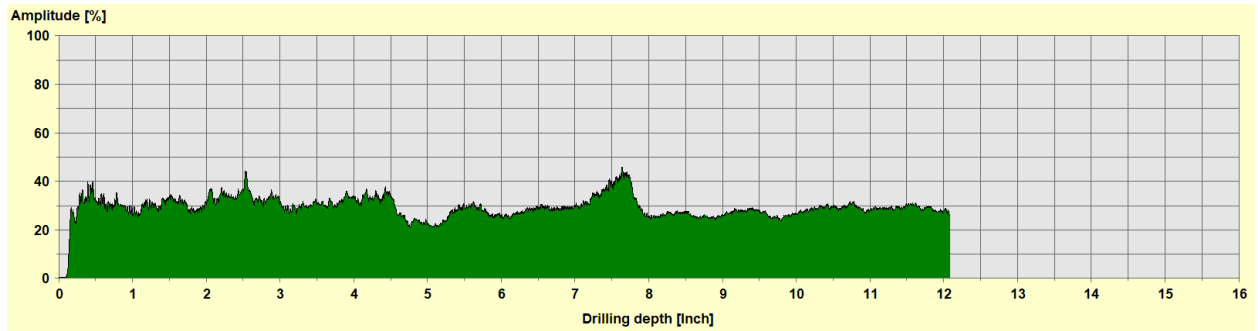
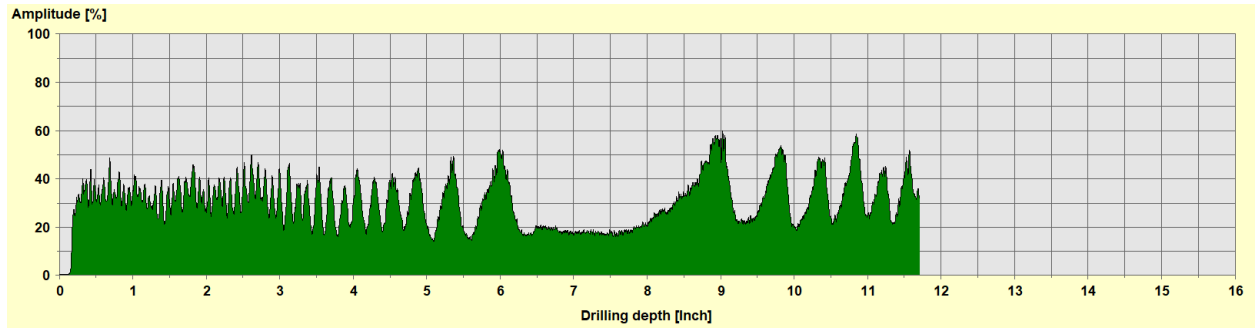


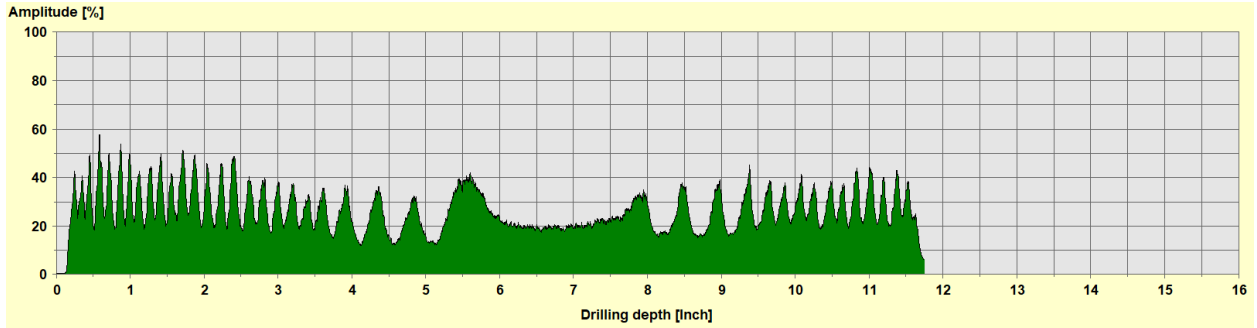
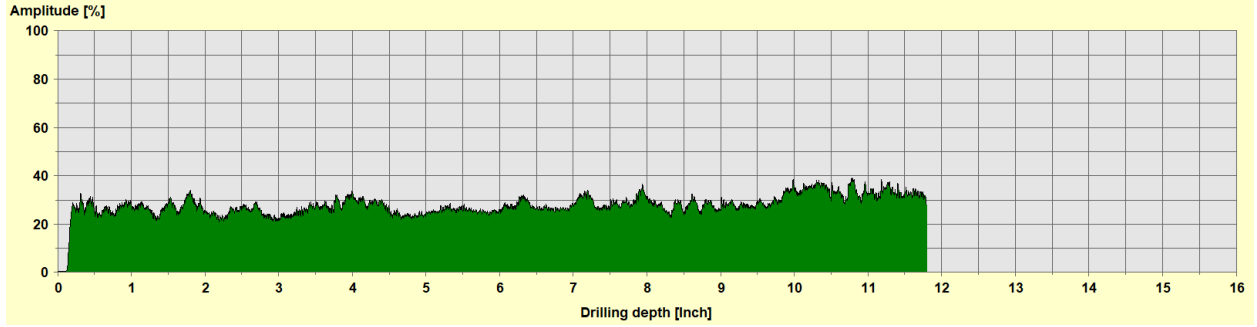
P320110





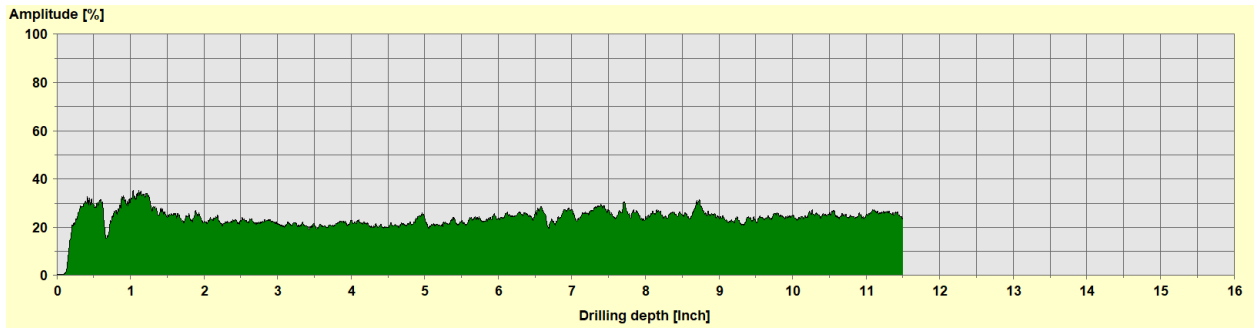
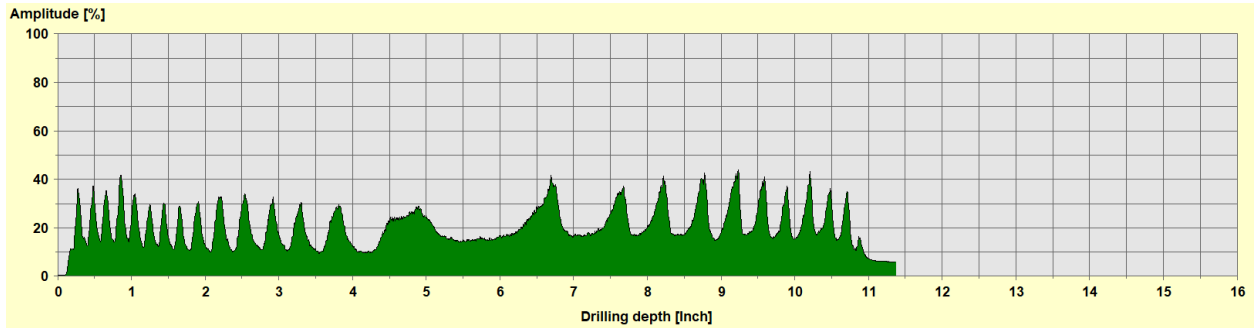
P320064

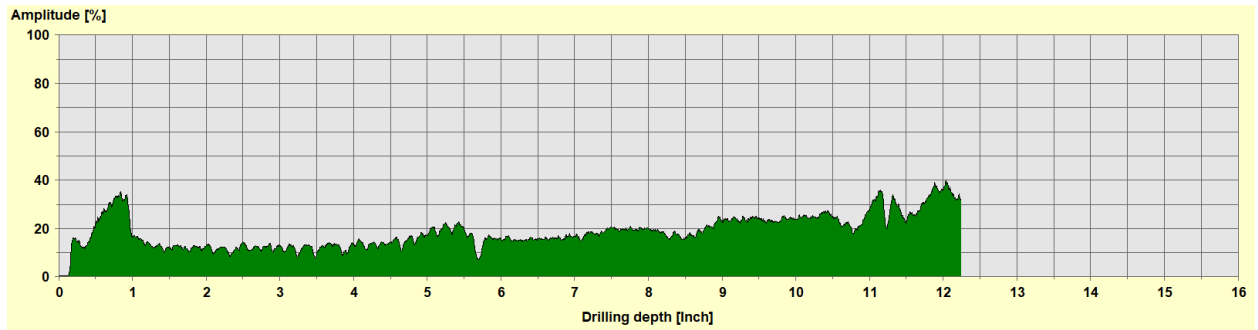
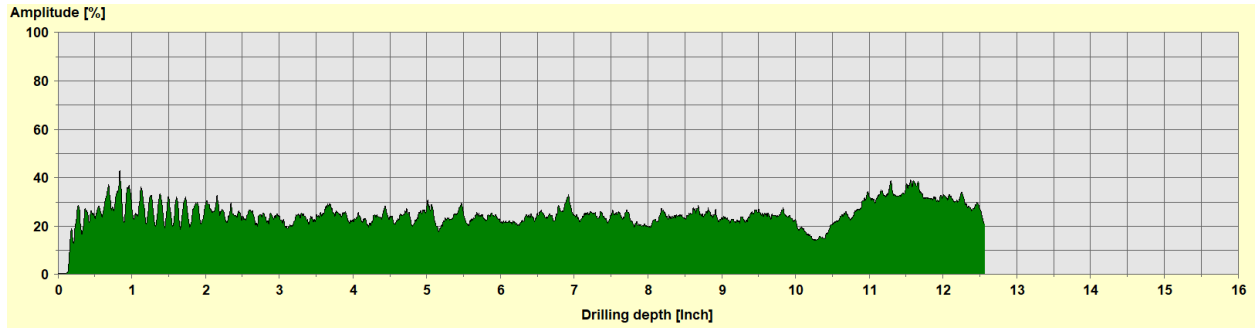
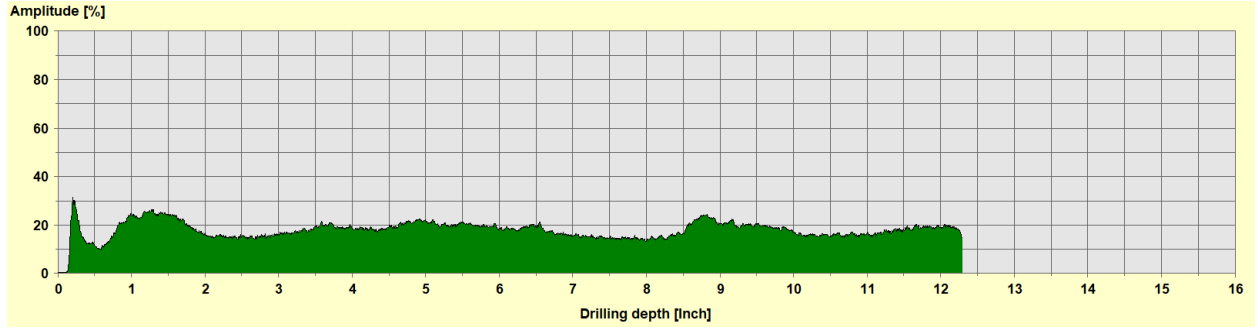




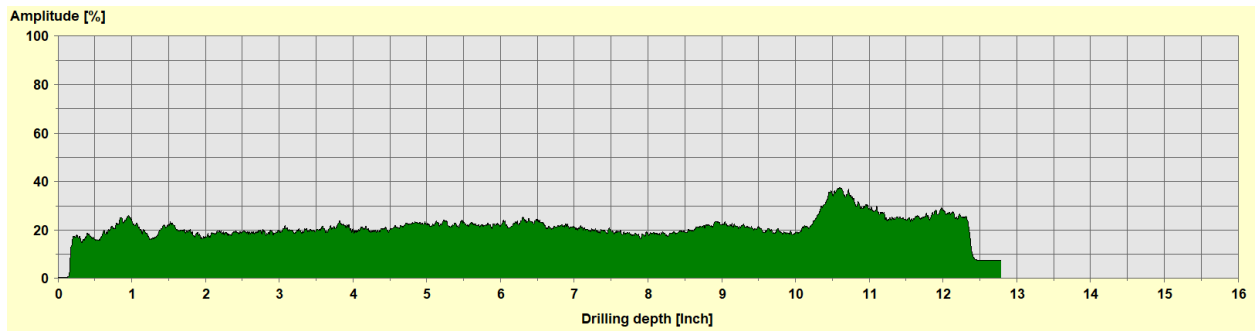
Barron County

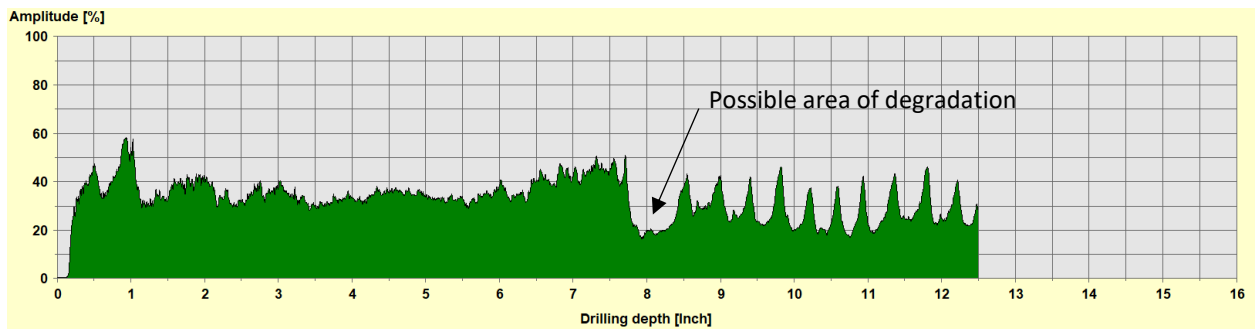
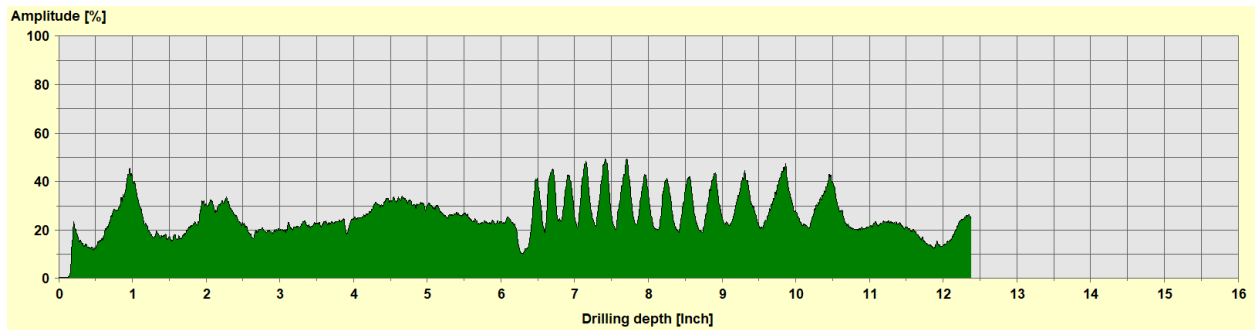
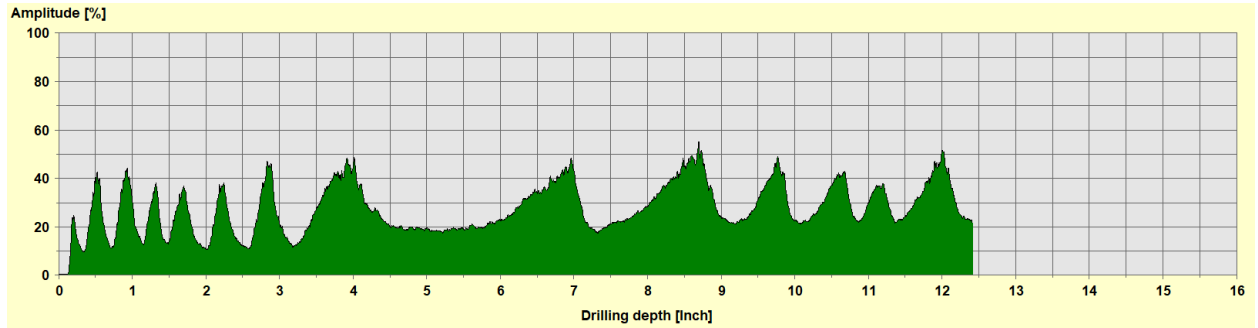
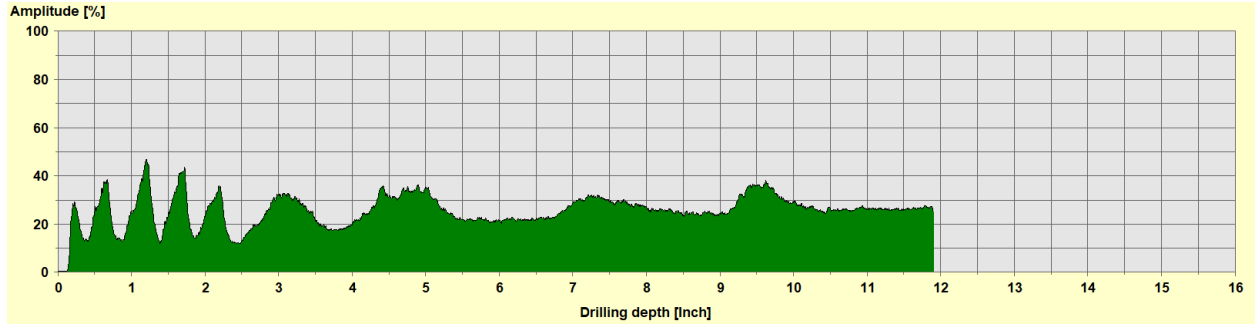
P030079





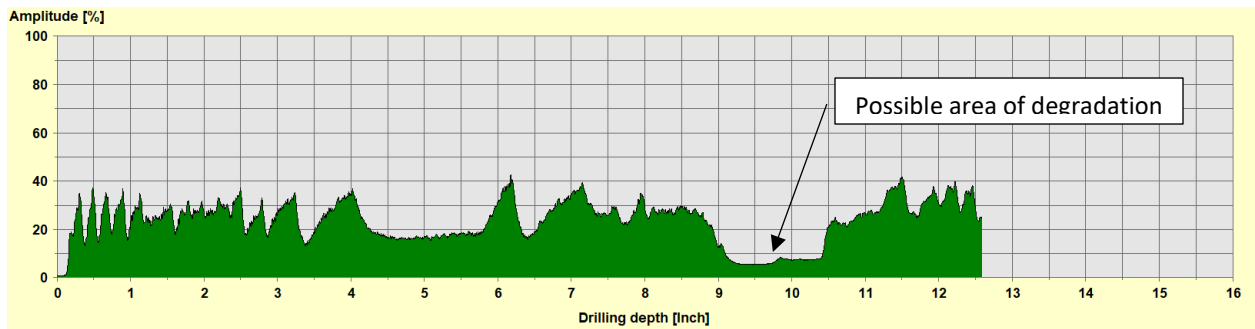
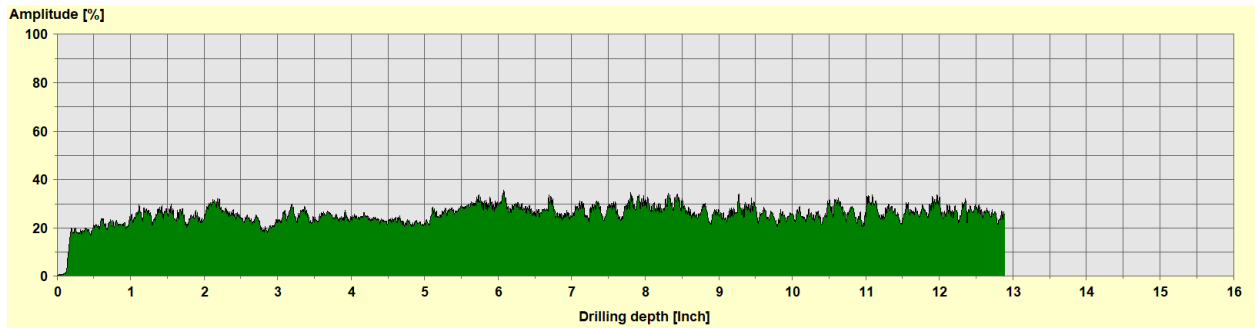
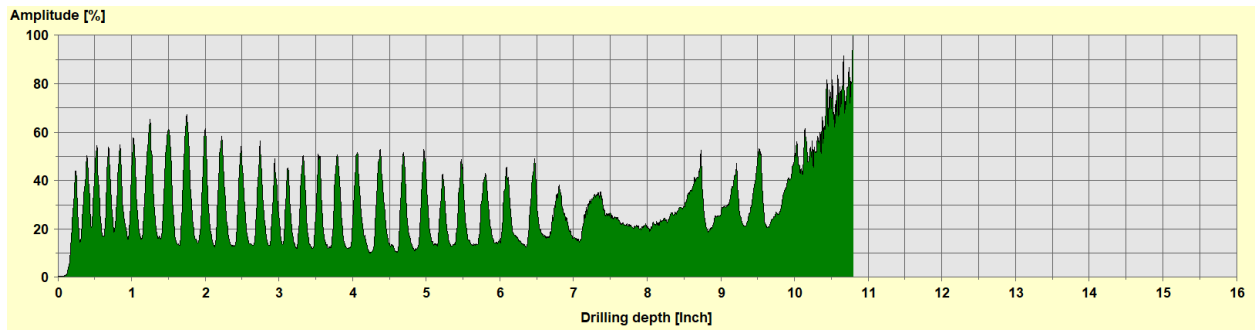
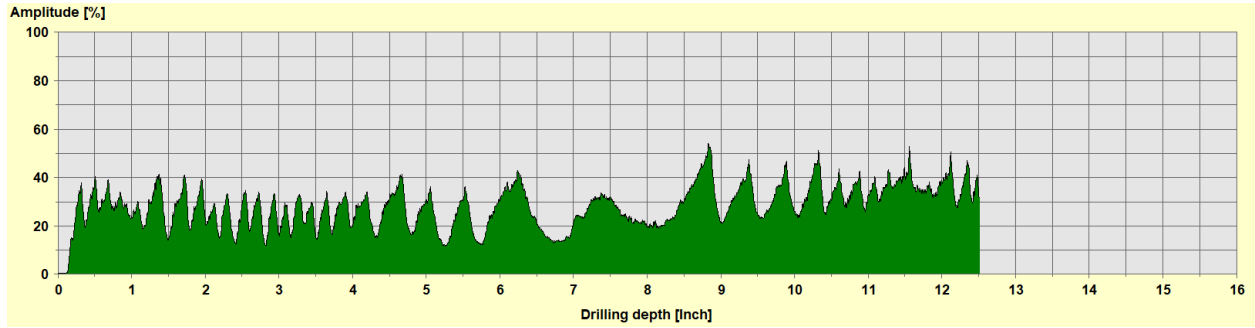
B030174



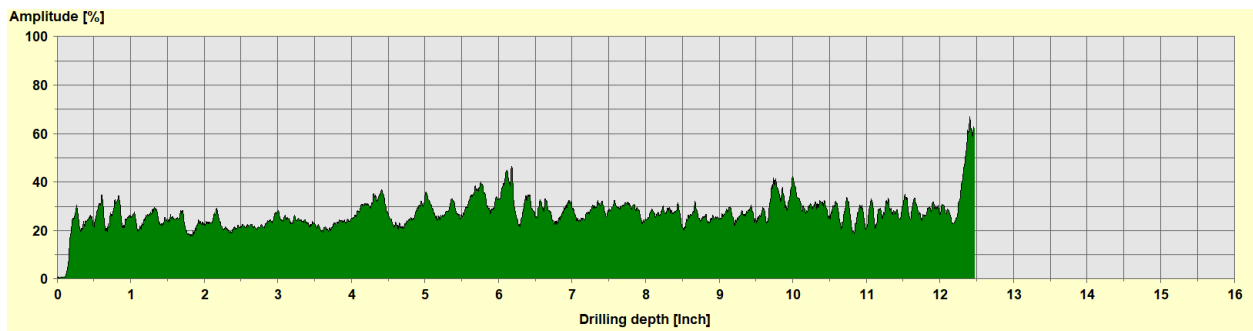
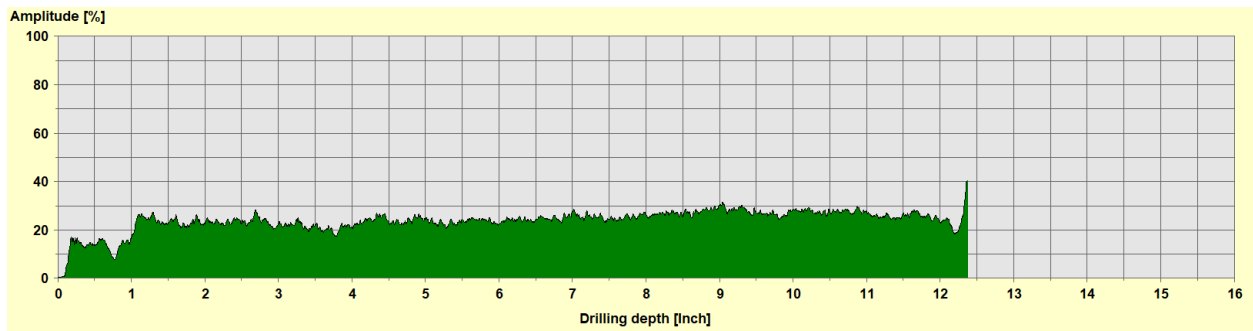
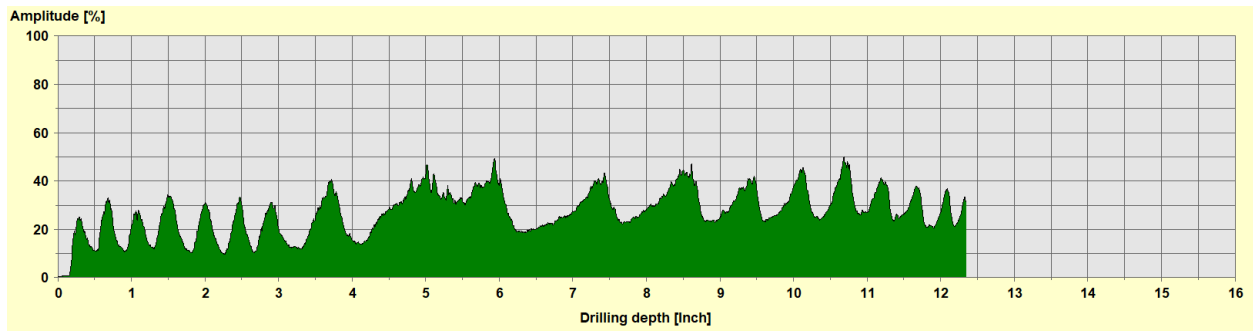
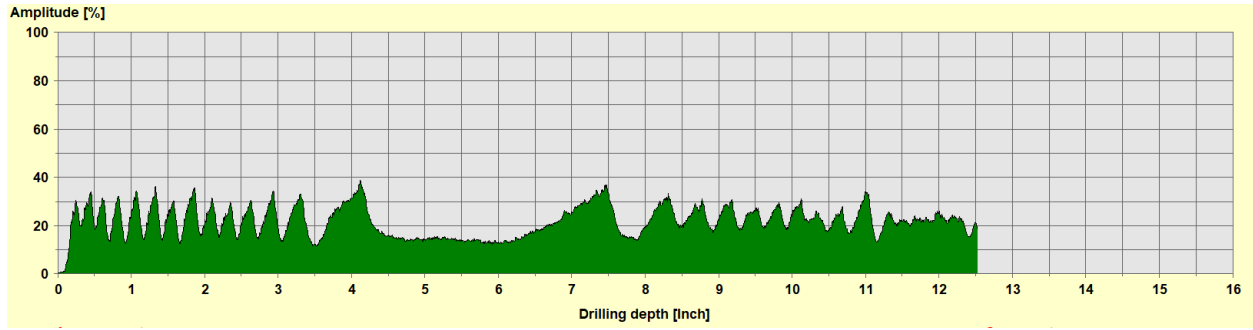


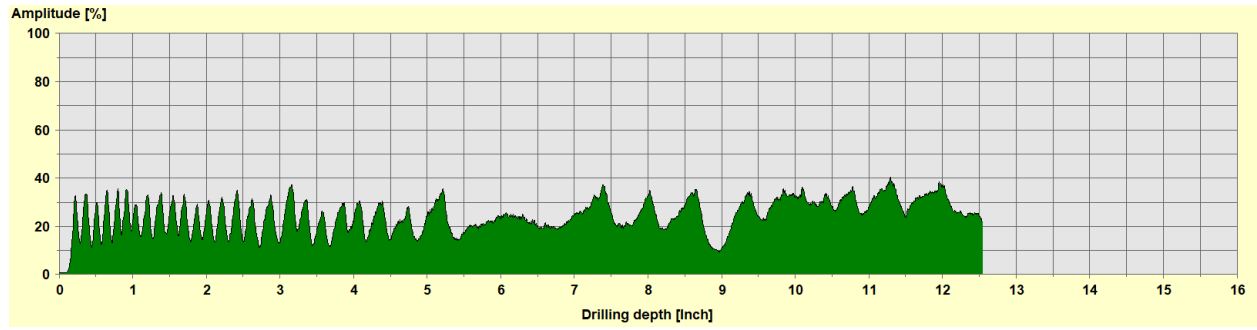
Monroe County

P410140

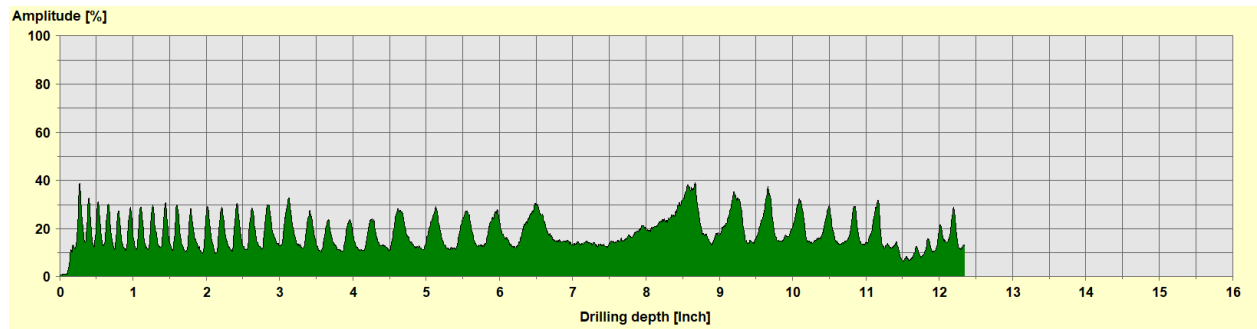
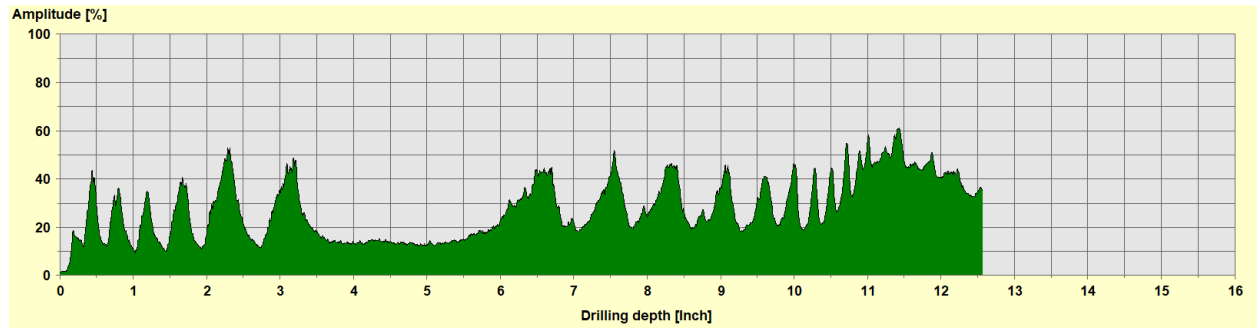
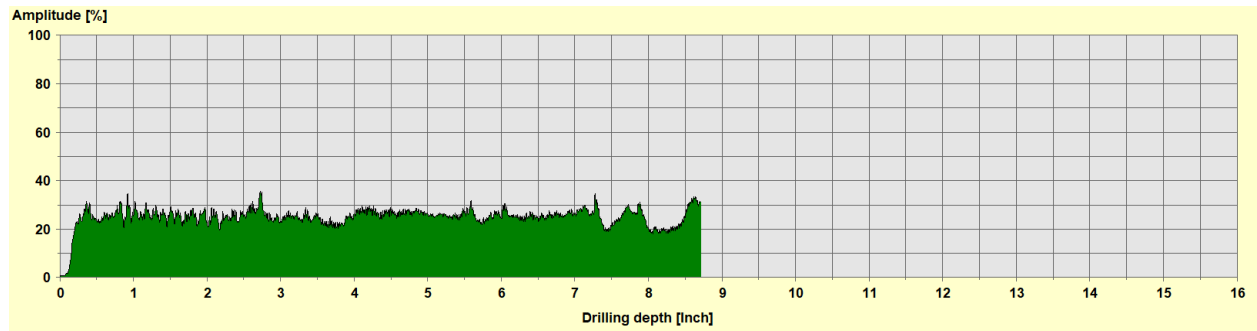


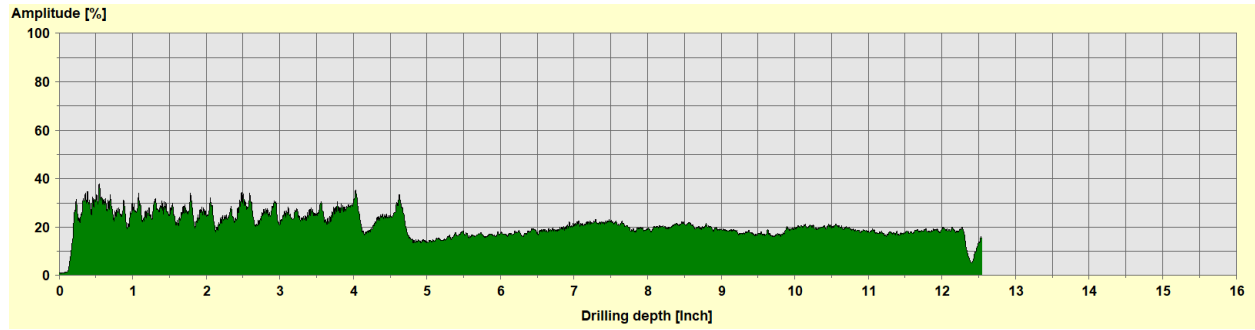
P410953



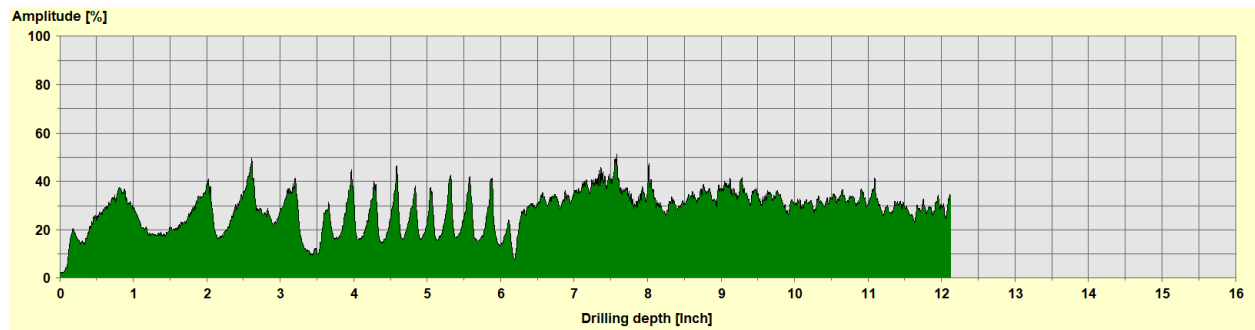
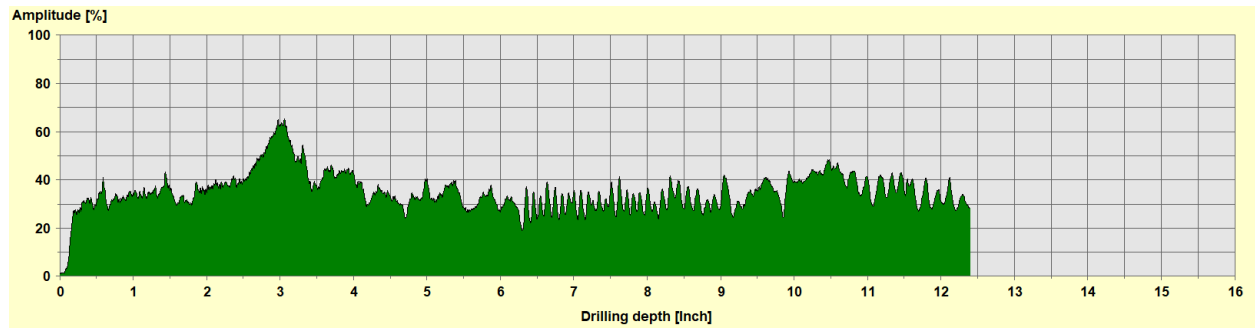
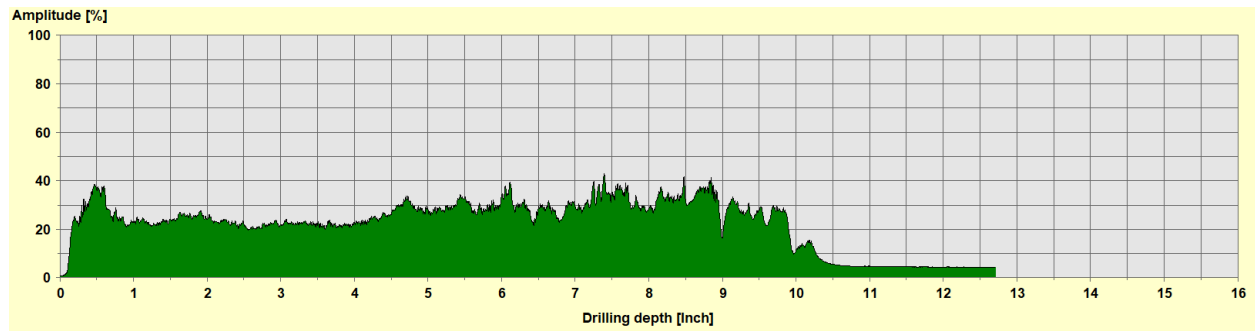


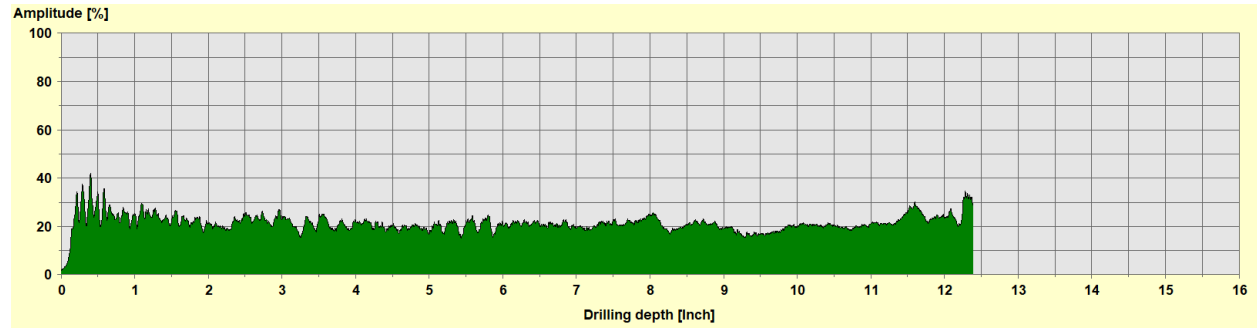
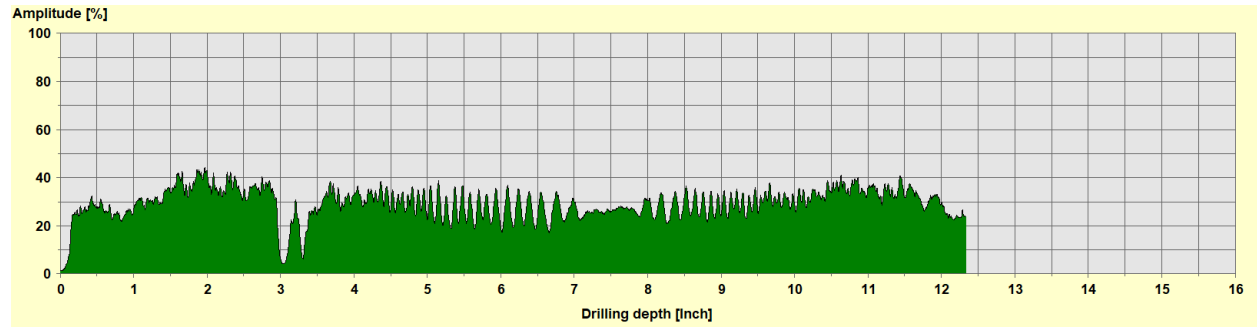
P410948





P410923





5 NUMERICAL MODELING

There are three main objectives in the analytical study: 1) investigate the effective wheel load distribution width on longitudinal timber slab bridges; 2) evaluate the effectiveness of various retrofit options on improving load capacity of these structures and 3) provide information important to the development of guidelines and recommendations for load testing, modeling and calculating wheel distribution width of other longitudinal laminated slab bridges.

In order to achieve these objectives, the analytical study was conducted in three steps: 1) model development, 2) model validation and 3) parametric study. The commercially available software – ANSYS was used to develop the finite element (FE) models.

5.1 Model Development

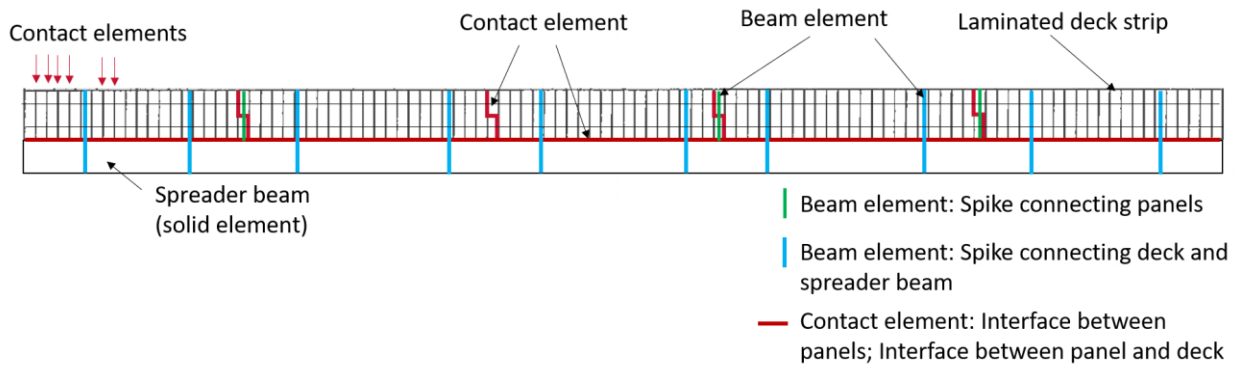
Three dimensional (3D) FE models were developed to simulate various load cases and to calculate the wheel load distribution on the timber slab bridges. In order to achieve that, the modeling work focused on the bridge superstructure.

Each bridge model includes deck laminates, a spreader beam, spikes/through-bolts penetrating the laminates and spreader beam, transverse dowels/spikes in the deck panel, and the spikes connecting the deck panels. Figure 5-1-a shows the element types used in the FE model. 3D solid elements were used to simulate the deck laminates, spreader beam, curbs, pavement and transverse deck (see Figure 5-1-b). Beam elements were used for the spikes and the dowel bars. Since the interaction between the deck panel and stiffener beam varies with transverse location, a contact element allowing only transfer of compression forces will be used at those locations. In order to simulate the separation between the bridge components, the surface contact element was used at the interface between the adjacent laminates, adjacent deck panels, and between the laminates and spreader beam. These contact elements carry compression forces, but no tension. They also allow the sliding behavior between the bridge components, hence, a friction coefficient (0.2) was assigned to the contact elements. A literature search indicated that the friction coefficient between the timber surfaces is between 0.2 and 0.5 (Aira et al., 2014). A value of 0.2 was used for this study which minimizes the influence of interlaminar friction and increases the influence of load transfer through compression contact and the bolt between the deck laminates and spreader beam.

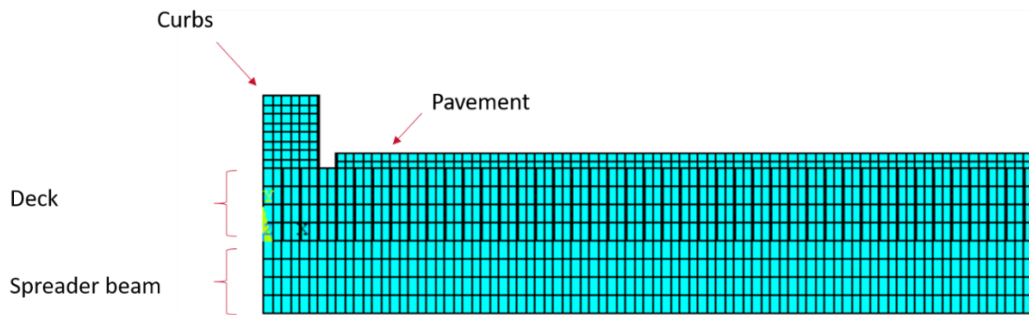
Figure 5-1-c shows a typical full bridge model. Although some bridges have more than one span, only the instrumented span was modeled. Per observation of the collected data and the detailing at the pier, discontinuity at the pier between the adjacent span was assumed.

Table 5-1 presents the modeling details. Orthotropic material properties with a Young's modulus in the longitudinal direction of 1,800 ksi were assigned to the timber components. A Poisson's ratio of 0.4 was input for the timber. For the steel components, a Young's modulus of 29,000 ksi was assigned with a Poisson's ratio of 0.3. The pavement material has a wide range and was calibrated to 100 ksi.

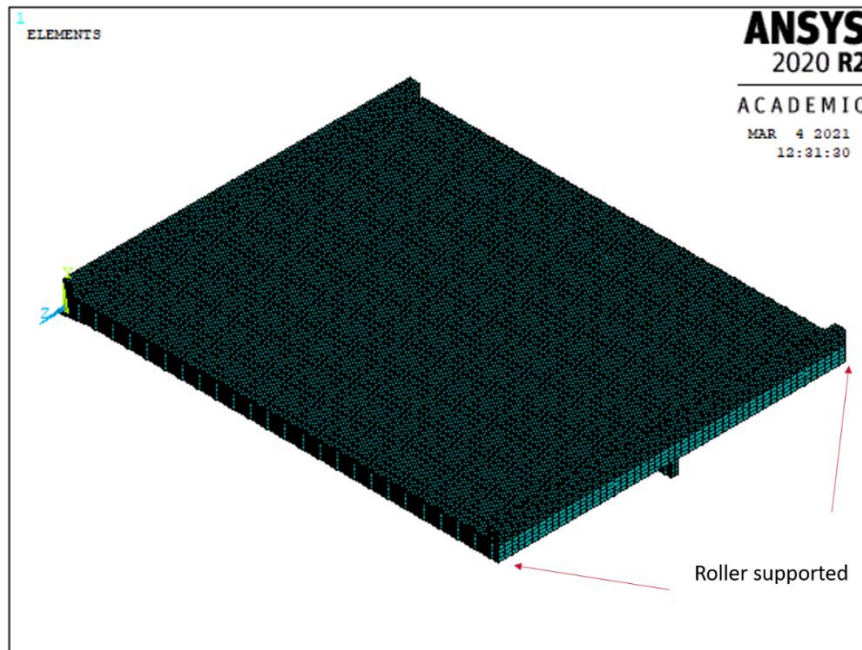
The model was developed for all the field-tested bridges. Two models were developed for each of the three bridges in La Crosse County that were tested twice (one before the retrofit and one after retrofit). The primary difference between these two models is that the model after retrofit work includes a transverse deck on top of the deck laminates.



a) Element types of FE model



b) FE model comments



c) Typical complete FE model

Figure 5-1 FE model detailing

Table 5-1 Modeling details

Bridge Components	Element Types	Material Properties
Deck laminations	Solid	$E_L = 1,800$ ksi
Spreader beam	Solid	$E_L = 1,800$ ksi
Curbs	Solid	$E_L = 1,800$ ksi
Pavement	Solid	$E = 100$ ksi
Spike between the deck panels	Beam	$E = 29,000$ ksi
Spike between the deck and spreader beam	Beam	$E = 29,000$ ksi
Dowel bars	Beam	$E = 29,000$ ksi
Interface between laminations	Contact	Compression only
Interface between deck and beam	Contact	Compression only

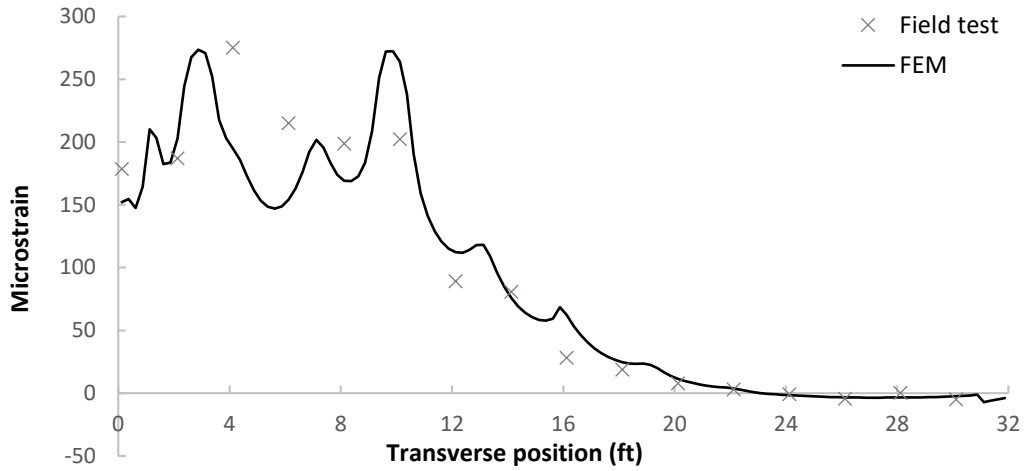
5.2 Model Validation

Following generation of the analytical model, the strain and displacement data collected during the field test were used to compare against the outputs from the FE model.

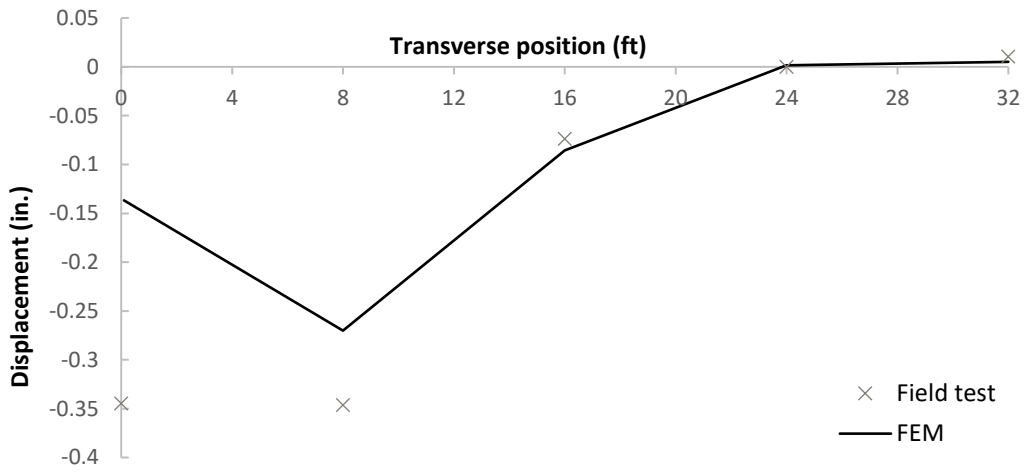
The validation work was conducted for all the tested bridges. For brevity, only the comparison graph for Bridge P320110 was presented in this report as Figure 5-2 and Figure 5-3. The same work was conducted for the other bridges, but only the final results are summarized in Table 5-2.

Figure 5-2-a shows the strain distribution vs. the transverse location at mid-span from LC 1 on bridge P32110. The black line shows the results output from the FE models and the grey "x" shows the field data. Within this graph the strain from the FE model was output from the center of the bottom surface of each laminate, while the field test data comes from strain sensors spaced transversely at 2 ft (see Figure 4-17 for gauge location and labels). Figure 5-2-b shows the displacement at the mid-span. In this picture, both analytical results and field data were output/captured with a spacing of one-quarter bridge width. Figure 5-2-c compares the strain for gauge S-M-3. For LC1, this gauge is close to the driver's side wheel and shows the maximum response.

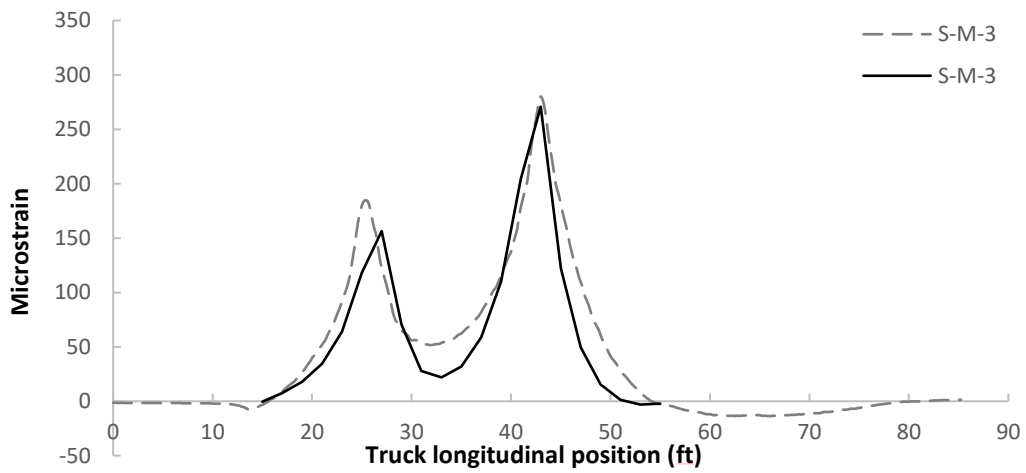
Figure 5-3 was plotted for LC3 in a similar manner. The results from the comparison indicates that the analytical model shows good agreement with the field test data. The model is capable of predicting the strain and displacement values when the bridge is subject to the model live load.



a) Strain distribution at the middle span

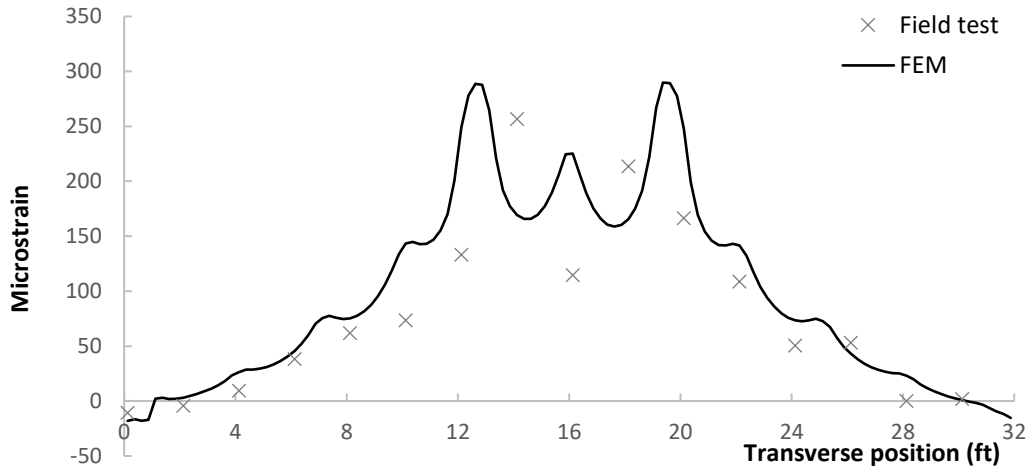


b) Displacement distribution at the middle span

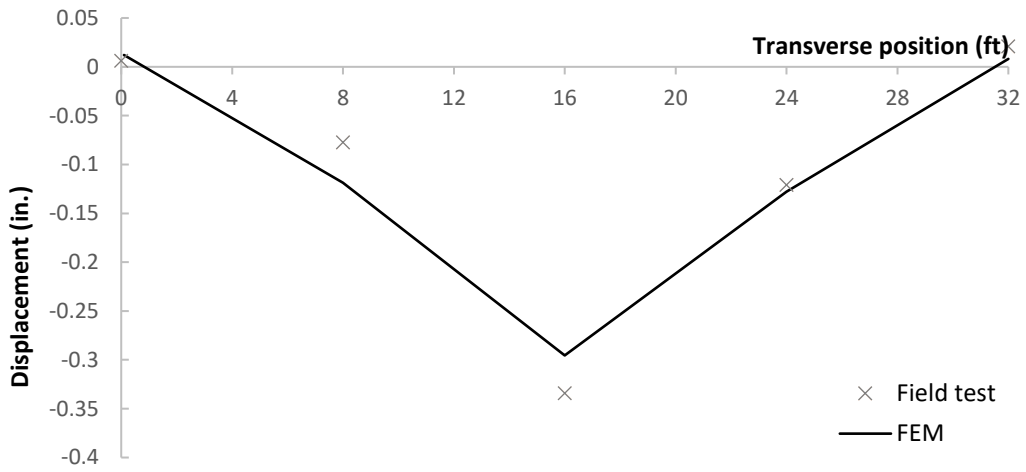


c) Strain distribution along the longitudinal direction

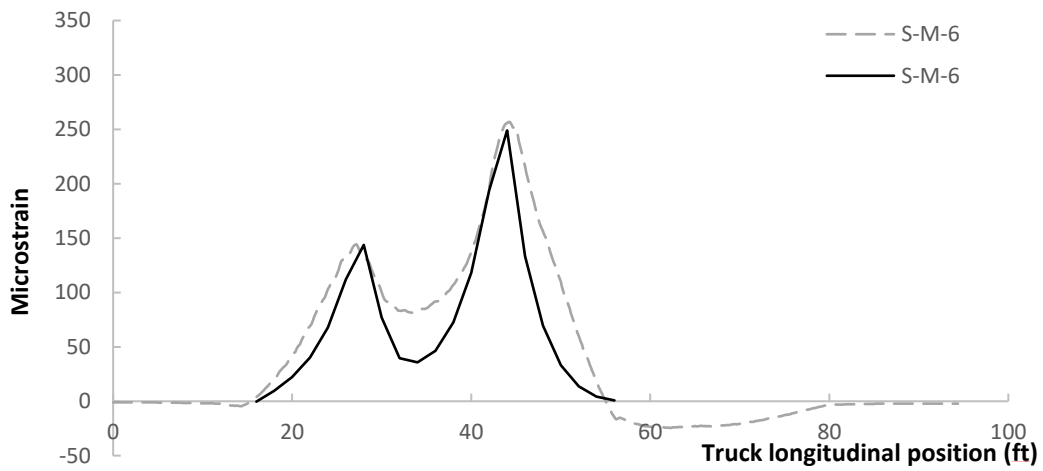
Figure 5-2 Model calibration results from LC1 (La Crosse Co. P320110)



a) Strain distribution at the middle span



b) Displacement distribution at the middle span



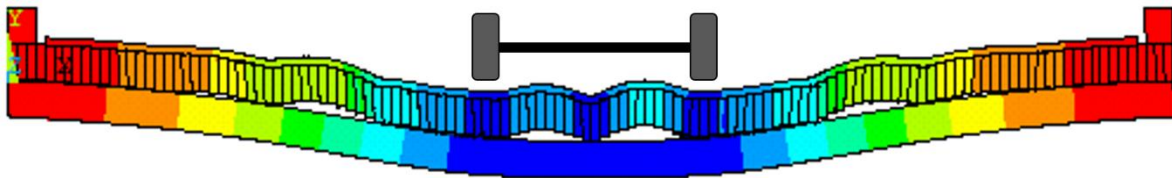
c) Strain distribution along the longitudinal direction

Figure 5-3 Model calibration results from LC3 (La Crosse Co. P320110)

Figure 5-4 shows the exaggerated deformed shape at the mid-span of the bridge for both LC1 and LC3. The red color indicates no/minimum vertical displacement and the blue indicates a negative deflection. The results indicate that the deck laminates and spreader beam keep in contact at the locations under the wheels and where spikes (penetrating deck laminates and spreader beam) exists. This is where the compression-only contact element works. At the other locations, a gap exists and no tensile forces occur at the interface elements.



a) Exaggerated deformed shape (LC1)



b) Exaggerated deformed shape (LC3)

Figure 5-4 Exaggerated deformed shape (La Crosse Co. P320110)

The same validation work was conducted for the other bridges. Table 5-2 lists the results for all. The equivalent wheel load distribution width for the FE models was calculated utilizing Eq. 9 with strain data output from every laminate at the middle span. The difference between the analytical and field results was calculated by Eq. 10.

$$\text{Rate of difference} = \frac{(E_{field} - E_{FE})}{E_{field}} * 100\% \quad \text{Eq. 10}$$

where, E_{field} is the equivalent wheel load width calculated based on field collected data; and E_{FE} is the equivalent wheel load width calculated based on FE model results.

The results show an agreement with the findings from field data that higher E values exist when the truck is near the center of the bridge and lower E values occur when the truck is near the curb lines. For most LCs and bridges, the analytical and field results show a difference no greater than 20%, which is generally considered reasonable for timber modeling. Considering the inherent variation of timber material, this result was regarded as acceptable and the modeling approach was hence validated for the use in the subsequent parametric study.

Table 5-2 Model calibration results

Bridge #	Bridge status	County	Year	Main feature	Span length	Width	Deck strip	Truck (Kips)	Results Type	LC1	LC2	LC3	LC4	LC5
P320064	Before strengthening	LA CROSSE	1973	Single spreader beam	26'	32'	3"x12"	15+25	Field test	8.0	9.2	9.2	7.5	6.3
									FEM	9.5	10.5	11.2	10.5	9.5
									Difference (%)	18.6	13.8	21.2	39.6	50.6
	After strengthening	LA CROSSE	2021	Single spreader beam; Transverse deck;	26'	32'	3"x12"	15+25	Field test	10.6	12.2	11.7	10.2	9.8
									FEM	10.2	12.2	13.0	12.2	10.2
									Difference (%)	-4.0	0.1	11.3	19.8	3.9
P320083	Before strengthening	LA CROSSE	1976	Single spreader beam	26'	31'-6"	3"x12"	15+25	Field test	7.6	9.5	9.5	9.1	6.8
									FEM	10.2	10.9	12.0	10.9	10.2
									Difference (%)	33.9	14.5	26.1	19.5	49.7
	After strengthening	LA CROSSE	2021	Single spreader beam; Transverse deck;	26'	31'-6"	3"x12"	15+25	Field test	9.7	13.4	11.7	9.9	11.8
									FEM	10.8	12.2	13.2	12.2	10.8
									Difference (%)	11.3	-8.8	13.0	23.4	-8.5
P320110	Before strengthening	LA CROSSE	1971	Single spreader beam	25'-6"	32'	3"x12"	15+25	Field test	10.0	9.6	9.8	8.8	9.5
									FEM	9.9	10.6	11.3	10.6	9.9
									Difference (%)	-1.2	10.1	14.8	20.1	4.0
	After strengthening	LA CROSSE	2021	Single spreader beam; Transverse deck;	25'-6"	32'	3"x12"	15+25	Field test	12.4	13.5	14.3	11.7	12.0
									FEM	11.6	12.2	12.8	12.2	11.6
									Difference (%)	-6.3	-9.5	-10.4	4.4	-3.2
P410140	Without strengthening	MONROE	1991	Single spreader beam; Skewed	31'	25'-4"	4"x14"	15.7+34.4	Field test	9.2	12.0	13.7	10.0	10.0
									FEM	11.1	11.1	11.0	11.9	11.8
									Difference (%)	20.3	-7.7	-19.9	19.0	18.0
P410923	Without strengthening	MONROE	1945	Single spreader beam;	23'	25'-4"	4"x12"	15.7+34.4	Field test		9.3	8.4	10.0	
									FEM		10.5	11.9	10.5	
									Difference (%)		13.1	41.6	5.2	
P410953	Without strengthening	MONROE	1990	Single spreader beam;	25'	31'-4"	4"x12"	15.7+34.4	Field test	8.9	11.2	12.2	12.0	8.0
									FEM	10.6	11.3	11.3	11.3	10.6
									Difference (%)	19.3	0.5	-7.0	-6.2	32.7
B410315	Without strengthening	MONROE	2018	Three spreader beams; 24 deck-spreader beam spikes	28'	26'	4"x14"	15.7+34.4	Field test	9.0	9.5	11.0	9.5	9.0
									FEM	13.0	13.5	14.0	13.5	13.0
									Difference (%)	44.4	42.1	27.3	42.1	44.4
P410948	Without strengthening	MONROE	1970	Single spreader beam;	25'	26'	3"x12"	15.7+34.4	Field test	11.0	12.7	12.8	8.7	8.2
									FEM	10.7	11.0	13.5	11.0	10.7
									Difference (%)	-2.7	-13.5	5.1	26.2	30.6
B030174	Without strengthening	BARRON	2001	Single spreader beam;	24'	25'-9"	3"*x12"	23+50	Field test	9.0	9.5	14.0	13.3	12.5
									FEM	9.4	9.6	10.6	9.6	9.4
									Difference (%)	4.7	1.1	-24.2	-27.8	-24.6
P030079	Without strengthening	BARRON	1969	Single spreader beam; Transverse deck;	25'-6"	26'	3"x12"	23+50	Field test	7.6	8.9	11.7	10.3	8.8
									FEM	10.6	11.0	12.5	11.0	10.6
									Difference (%)	39.7	23.4	7.1	6.6	20.6

5.3 Parametric Study

The objective of the parametric study is to provide the analytical support to the evaluation of the wheel load distribution and the performance of various retrofit methods on the bridges with different configurations. In order to achieve this objective, one of the calibrated models (P320110) was selected as the base model while individual parameters were changed. Bridge P320110 was tested twice: once before the retrofit and once after retrofit. The retrofit installed is a 4 in. thick transverse deck placed on top of the existing deck laminates with grout injection of void spaces between. The result is an increased transverse stiffness. The models in the parametric study were created utilizing the modeling approach developed and validated in Section 5.1 and 5.2, respectively.

5.3.1 Parameters of interests

The parameters that may affect the wheel load distributions were identified from three categories: truck loading, bridge geometry, and retrofit approach. The truck related parameters include the number of traffic lanes, number of axels, gauge spacing, and tire width. The bridge parameters include bridge length and width, and lamination size. The retrofit method related parameters include spacing and cross-section size of the spreader beam, deck-to-beam spike spacing, and transverse spreader deck thickness. These parameters were determined based on the results from literature review (Fanous et al., 2010; Wipf et al., 1986), state practice review (see Sections 2 and 3), researcher's experience, and input from the oversight committee members.

Table 5-3 lists the parameters for the models that were established during the study. The calibrated models were developed using the same configuration and loading as the load test truck. It was determined the rear, more heavily loaded axle, was the primary contributor to the load effects. Model 1 was developed accordingly, and the parametric models 2 through 14, with the exception of 13, used only the rear axle loading of 26 kips. Model 13 was loaded with the same loading as the calibrated model and the result was compared with the calibrated model (after retrofit).

Models 2, 3 and 4 were created to study the effect of gauge spacing and tire width. The gauge spacing was arbitrarily increased/decreased by 2 ft. and the tire width was reduced to half. Models 5 to 8 were developed to study the bridge geometry parameters. A review of the timber slab bridge data in Wisconsin indicated that the maximum span length is approximately 50 ft and the maximum bridge width is approximately 50 ft. Although all the bridges to be tested were approximately 30 ft in length and width, the parametric study was performed on bridge lengths and widths up to 50 ft. A review of the 10 field-tested bridges showed two laminate cross-section sizes, 12 in. by 4 in. and 14 in. by 4 in. These cross-section size were studied in Models 7 and 8. Models 9 to 13 were developed to investigate the effect of the retrofit methods. Bridge P320110 is constructed with a single spreader beam placed at mid-span, while the parametric study incorporates three spreader beams (one at mid-span and one at each quarter span) and no spreader beams. Based on the bridge drawings reviewed during the research, the cross-section size for spreader beam is as small as 8 in. tall by 6 in. wide and the spacing of deck-beam spike is 1 ft. On Model 13, the thickness of the transverse deck was increased arbitrarily to 6 in. to investigate the effect. Per the request by the oversight committee members, Model 14 was performed with two lanes loaded.

Table 5-3 Model matrix for parametric study of La Crosse Co. P320110

Model	Enhancement	Truck				Bridge geometry			Spreader beam			Transverse deck
		# of lanes	Axle (kips)	Gauge spacing (ft)	Tire width (in.)	Length (ft)	Width (ft)	Lamination size (in.xin.)	# of spreader beams	Cross-section	Deck-beam spike spacing (ft)	Thickness (in.)
P320110 (before)	Spreader beam	1	Front (15)+Back(26)	6	24	26	32	12x3	1	12x6	3.25	-
P320110 (after)	Spreader beam + transverse deck	1	Front (15)+Back(26)	6	24	26	32	12x3	1	12x6	3.25	4
1	Single beam	1	Single(26)	6	24	26	32	12x3	1	12x6	3.25	-
2	Single beam	1	Single(26)	4	24	26	32	12x3	1	12x6	3.25	-
3	Single beam	1	Single(26)	10	24	26	32	12x3	1	12x6	3.25	-
4	Single beam	1	Single(26)	6	12	26	32	12x3	1	12x6	3.25	-
5	Single beam	1	Single(26)	6	24	50	32	12x3	1	12x6	3.25	-
6	Single beam	1	Single(26)	6	24	26	50	12x3	1	12x6	3.25	-
7	Single beam	1	Single(26)	6	24	26	32	12x4	1	12x6	3.25	-
8	Single beam	1	Single(26)	6	24	26	32	14x4	1	12x6	3.25	-
9	Spreader beam	1	Single(26)	6	24	26	32	12x3	3	12x6	3.25	-
10	Spreader beam	1	Single(26)	6	24	26	32	12x3	0	12x6	3.25	-
11	Spreader beam	1	Single(26)	6	24	26	32	12x3	1	8x6	3.25	-
12	Spreader beam	1	Single(26)	6	24	26	32	12x3	1	12x6	1	4
13	Spreader beam + transverse deck	1	Front (15)+Back(26)	6	24	26	32	12x3	1	12x6	3.25	6
14	Spreader beam	2	Single(26)	6	24	26	32	12x3	1	12x6	3.25	4

 = Single variable change in model

5.3.2 Parametric study results

After the completion of all the models, the ESW was calculated in the same way as during the model validation; the strain from every laminate at the mid-span was used for the calculation.

Since both field data and the model validation results indicated that the lesser ESW occurs in LC1 and greater ESW occurs in LC3, with the results from LC2 always between LC1 and LC3, the model was limited to only LC1 and LC3 loading. The results from the parametric study are presented in Table 5-4.

Table 5-4 Parametric study results

Model	ESW Results			
	LC1		LC3	
	ESW (ft)	Rate of change (%)	ESW (ft)	Rate of change (%)
P320110 (before)	9.9	---	11.2	---
P320110 (after)	11.6	---	12.8	---
1	9.9	0	11.2	0
2	8.7	-12	10.3	-8
3	11.3	14	12.7	13
4	8.6	-13	9.5	-16
5	9.5	-4	15.5	38
6	9.8	-1	11.1	-1
7	9.5	-3	11.5	2
8	9.0	-9	10.8	-4
9	9.9	0	11.3	1
10	6.3	-37	6.8	-39
11	8.3	-16	9.3	-17
12	10.4	5	11.9	6
13	12.0	3	13.4	5
14	9.0	-9		

The results from the table are summarized as following:

- Comparing the results from the calibrated model before retrofit and Model 1, it was found that both models resulted in the same ESW. This indicated that the wheel load distribution was dominated by the rear heavy axle.
- Comparing results from Model 1 to Model 2 and 3, as the gauge spacing decreases, the load distribution width decreases and vice versa.
- Comparing results from Model 1 to Model 4, as the tire width decreases, the load distribution width decreases.
- Comparing results from Model 1 to Model 5, as bridge length increases, the load distribution width from LC3 increases dramatically. With other parameters unchanged, increasing the bridge length decreases the bridge longitudinal stiffness.
- Comparing results from Model 1 to Model 6 and 7, the bridge width and lamination thickness has minimum effect on the load distribution width.
- Comparing results from Model 1 to Model 8, deeper deck laminations decrease the load distribution width. With other parameters unchanged, deeper deck laminations increase the bridge longitudinal stiffness. This contradicts the wheel load distribution equation in AASHTO 2002 and thus the Wisconsin Bridge Manual (Eq. 6), where deeper deck lamination results in a greater distribution width.
- Comparing results from Model 1 to Model 9, adding more spreader beams at quarter span will increase ESW only minimally.
- Comparing results from Model 1 to Model 10 and 11, the spreader beam at the middle span shows a significant effect on the ESW. Cross-section reduction or removal of the spreader beam (at middle) span results in a significant reduction on ESW. Cross-section reduction or removal of the spreader beam reduced the transverse stiffness.
- Comparing results from Model 1 to Model 12, increasing the number of spikes between the deck and spreader beam will slightly increase ESW.
- Comparing results from the calibrated model after retrofit work to Model 13, increasing the thickness of transverse spreader deck from 4 in. to 6 in. will increase ESW, although the effect is not significant. However, comparing the results from calibrated model before and after retrofit work, there is a greater increase of the wheel load distribution with utilizing of a 4 in. transverse deck panel.
- Comparing results from Model 1 to Model 14, the results indicated that the two lane traffic loading results in a lower ESW than that from single lane traffic.

Based on the results from the parametric study, two primary aspects control the wheel load distribution, truck configuration and bridge geometry. The following conclusions could be made:

Vehicle: The transverse load distribution on a timber slab bridge varies with gauge spacing, number of traffic lanes, and wheel tire width. Hence, non-standard vehicle configurations should be evaluated differently for purposes of load rating.

Bridge: The transverse load distribution is affected by the longitudinal and transverse stiffness. All else being the same, an increase of longitudinal stiffness reduces the transverse load distribution and an increase of the transverse stiffness increases the transverse load distribution. This can be restated as the ratio of longitudinal-stiffness to transverse-stiffness (K_L/K_T) has an effect on the wheel load distribution. For example, when the bridge length increases or deck depth decreases, the longitudinal stiffness decreases. With transverse-stiffness unchanged (number of spreader beam=1; nailing pattern unchanged), the K_L/K_T ratio decreases, which increases the wheel load distribution width. Therefore, the

selection of bridge retrofit/enhancement methods should be considered with the goal of decreasing the ratio of longitudinal-stiffness to transverse-stiffness.

These findings and conclusions were used to develop the recommendations and guidelines for Wisconsin DOT in Chapter 6.

6 DEVELOPMENT OF RECOMMENDATIONS

The field test results in Chapter 4 and analytical study results in Chapter 5 provide important information used to develop the recommendations and guidelines for the Wisconsin DOT. In particular, the analytical parametric study results provide significant data for the evaluation of the wheel load distribution and the performance of different retrofit methods on various bridge configurations. These data are used to develop the equivalent strip width equation in this task. The recommendations are given with a focus on prediction of wheel load distribution during design and load rating, and proposing retrofit methods.

In this section, the wheel load distribution width calculated based on the field and analytical results are compared with calculated values according to the current AASHTO LRFD code and Wisconsin Bridge Manual. The difference between the field, analytical and design values is discussed and the recommendations for the revision to the design equation is proposed.

6.1 Comparison with Current AASHTO Code and Wisconsin Specification

The current AASHTO LRFD design specification calculates the wheel load distribution width utilizing Eq. 3 and Eq. 4 for both timber slab bridges as well as reinforced concrete slab bridges (Section 2.1). Fanous (2010) indicated these equations were developed based on the study of 130 reinforced concrete slab bridges; longitudinal glued/spike-laminated timber deck bridges were not included in the test. Both Eq. 3 and Eq. 4 considers only the bridge length and width. The number of traffic lanes was considered only in the limitation criteria.

In Chapter 45 of the Wisconsin Bridge Manual (45.6.4.1), the wheel load distribution for a nailed laminated timber deck bridge is calculated utilizing Eq. 6 and Eq. 7 for bridge load rating (Section 3.1). These equations were included in USFS (1990) for the design of three types of timber slab bridges: glue-laminated deck panels, nail-laminated lumber deck, and longitudinal glulam deck on transverse floor beams. These equations predict strip width with respect to the wheel width and the deck thickness.

Based on both methods, the codified wheel distribution width was calculated for each tested bridge and compared with the results from the field tests as shown in Figure 6-1. Note the field test results in Figure 6-1 show the range calculated based on the point in time when the maximum strain value was collected at the mid-span from each load case; typically the maximum strain occurs when the center of gravity of the truck is positioned over the bridge mid-span. The Wisconsin codified results in Figure 6-1 consider only a single lane situation. In addition, the probability of the ESW being less than the strip width calculated per the Wisconsin Bridge manual is presented as a bar chart in Figure 6-1.

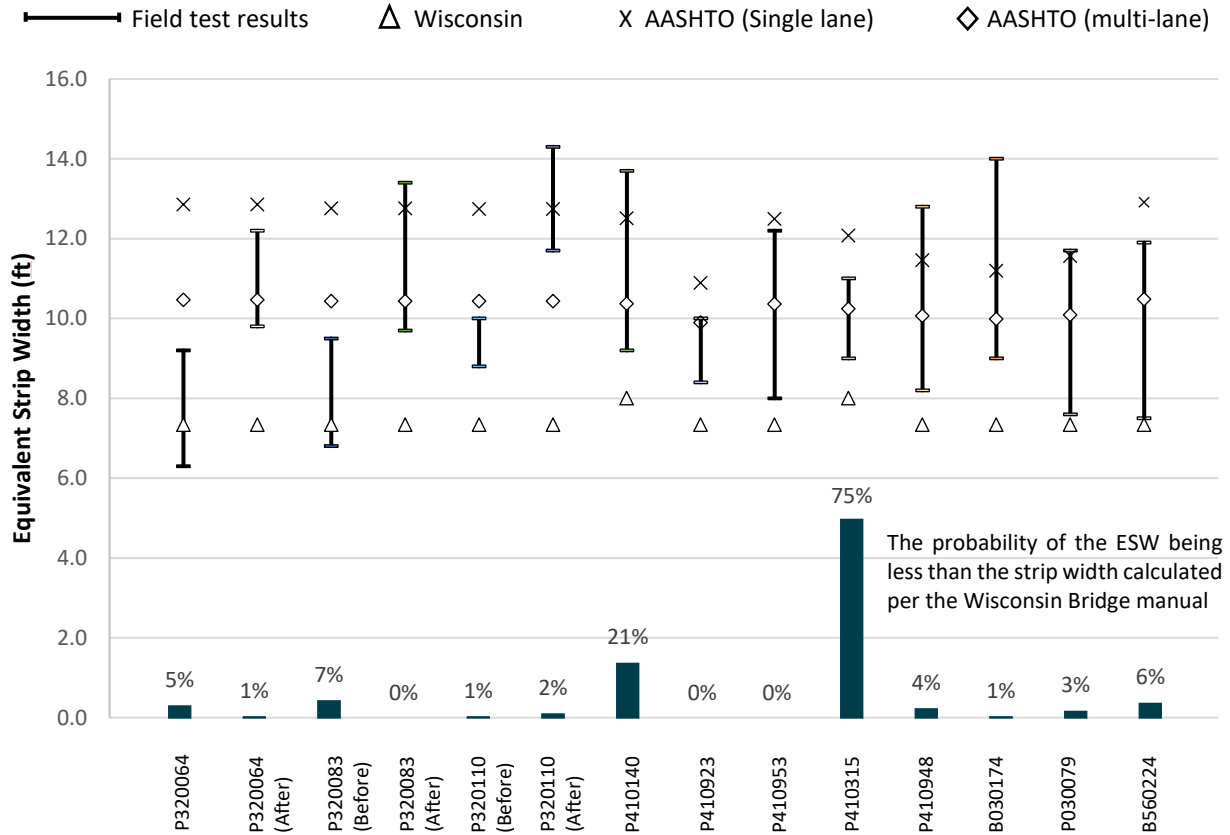


Figure 6-1 Comparison between the field data and codified values

The results indicate that a large difference exists between the calculated design values from AASHTO LRFD and Wisconsin DOT load rating values. The AASHTO LRFD code results in design wheel load distribution width ranging from 11 to 13 ft which is, in most cases, greater than the field results. This indicates that the AASHTO prediction is not conservative. The equation in the Load Rating Chapter in the Wisconsin Bridge Manual results in a lower lane load distribution width for bridges in good condition of about 8 to 8.7 ft for all bridges which is generally conservative when compared to the field test results. It should be noted the equation only considers the deck thickness and wheel tire width as variables.

6.2 Development of the ESW Equation

As a subsequent result of the field and analytical studies, an equation to more accurately calculate the ESW was developed which is inclusive of several variables. The project oversight committee stressed that although many parameters investigated during the parametric study may affect the wheel distribution width, it is unrealistic to have access to all variables. Hence, the ESW equation was developed with a few baseline assumptions: 1) truck with 6 ft gauge spacing; 2) 20 in. tire width; 3) at least one spreader beam; 4) No transverse spreader deck.

To date, methods used to improve load distribution on timber slab bridges include tightening existing spreader beams, adding spreader beams, using transverse post-tensioning, and using 4 in. thick laminated spreader deck panels placed transversely on top of the existing slab. These retrofit techniques have typically aimed to increase load capacity by increasing the effective wheel load distribution width. Based on the results from the load testing and the analytical parametric study, the effectiveness of utilizing a

spreader beam and transverse deck is discussed in Section 6.2.1 and 6.2.2, respectively. The recommendations for utilizing both retrofit methods are provided.

6.2.1 Spreader Beam

The parametric study results indicated that the transverse load distribution is affected by the longitudinal and transverse stiffness. All else being the same, an increase of longitudinal stiffness reduces the transverse load distribution and an increase of the transverse stiffness increases the transverse load distribution. This can be restated as the ratio of longitudinal-stiffness to transverse-stiffness (K_L/K_T) has an effect on the wheel load distribution. For example, when the bridge length increases or deck depth decreases, the longitudinal stiffness decreases. With transverse-stiffness unchanged (number of spreader beam=1; nailing pattern unchanged), the K_L/K_T ratio decreases, which increases the wheel load distribution width.

Based on the parametric study, deeper deck laminations decrease the load distribution width. With other parameters unchanged, deeper deck laminations increase the bridge longitudinal stiffness. The spreader beam at the middle span shows a significant effect on the ESW. Cross-section reduction or removal of the spreader beam at middle span reduces the transverse stiffness, and eventually results in a significant reduction on ESW. In order to quantitatively investigate the effect of lamination depth and spreader beam cross-section, additional FE models were created with various combinations of lamination depth and spreader beam depth.

Table 6-1 shows specific information of these models (Model 15-1 to Model 15-9) with the changing parameters highlighted. These models were developed based on Model 1 with 3 in. wide laminations and a single 6 in. wide timber spreader beam. The lamination rigidity ($E_L I_L$, longitudinal rigidity) per 3 in. and the spreader beam rigidity ($E_S I_S$, transverse rigidity) per 6 in. were calculated and presented in Table 6-1. Initial models indicated that LC1 governs the distribution width, therefore the distribution results from LC1 were listed in Table 6-1.

The ESW results from Model 15-1 to Model 15-9 were plotted in Figure 6-2 with respect to the ratio of longitudinal to transverse rigidity ($E_L I_L / E_S I_S$). It was found that the ESW is not linearly related to $E_L I_L / E_S I_S$, and a logarithmic curve could be used to fit the data in Figure 6-2. A detailed investigation indicated that the ESW shows a linear relationship with respect to $E_L I_L / E_S I_S \times H_L / H_S$, adding the ratio of the lamination depth to spreader beam depth to the equation as is shown in Figure 6-3

Table 6-1 Model calibration results of spreader beam variations

Model	Enhancement	Truck				Bridge geometry					Spreader beam					Transverse deck	ESW Results (ft)
		No. of lanes	Axle (kips)	Gauge spacing (ft)	Tire width (in.)	Length (ft)	Width (ft)	Lamination Width (in.)	Depth H_L (in.)	Rigidity $E_L I_L$ (k-in ²)/3in	No. of spreader beams	Width (in.)	Depth H_S (in.)	Rigidity $E_S I_S$ (kip-in ²)/6in	Deck-beam spike spacing (ft)		
1	Spreader beam	1	Single(26)	6	24	26	32	3	12	777600	1	6	12	1555200	3.25	0	9.9
10	No spreader beam	1	Single(26)	6	24	26	32	3	12	777600	0	0	0	0	0	0	6.3
15-1	Spreader beam	1	Single(26)	6	24	26	32	3	9	328050	1	6	9	656100	3.25	0	10.1
15-2	Spreader beam	1	Single(26)	6	24	26	32	3	9	328050	1	6	12	1555200	3.25	0	10.9
15-3	Spreader beam	1	Single(26)	6	24	26	32	3	9	328050	1	6	15	3037500	3.25	0	11.0
15-4	Spreader beam	1	Single(26)	6	24	26	32	3	12	777600	1	6	9	656100	3.25	0	9.4
15-5	Spreader beam	1	Single(26)	6	24	26	32	3	12	777600	1	6	12	1555200	3.25	0	9.9
15-6	Spreader beam	1	Single(26)	6	24	26	32	3	12	777600	1	6	15	3037500	3.25	0	10.0
15-7	Spreader beam	1	Single(26)	6	24	26	32	3	15	1518750	1	6	9	656100	3.25	0	8.5
15-8	Spreader beam	1	Single(26)	6	24	26	32	3	15	1518750	1	6	12	1555200	3.25	0	9.0
15-9	Spreader beam	1	Single(26)	6	24	26	32	3	15	1518750	1	6	15	3037500	3.25	0	9.1
16-1	Spreader beam-W6*25	1	Single(26)	6	24	26	32	3	12	777600	1	6.08	6.28	1548600	3.25	0	10.0
16-2	Spreader beam-W8*31	1	Single(26)	6	24	26	32	3	12	777600	1	8	8	3190000	3.25	0	10.1

= Modified variables in model

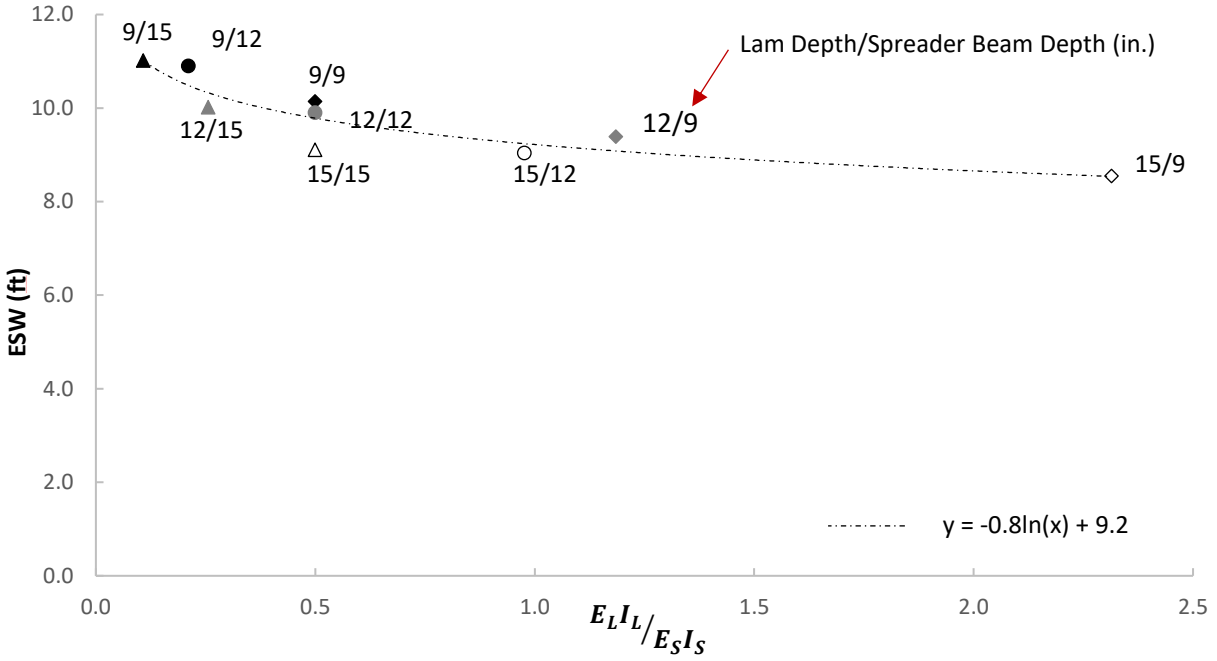


Figure 6-2 ESW with respect to $E_L I_L / E_S I_S$

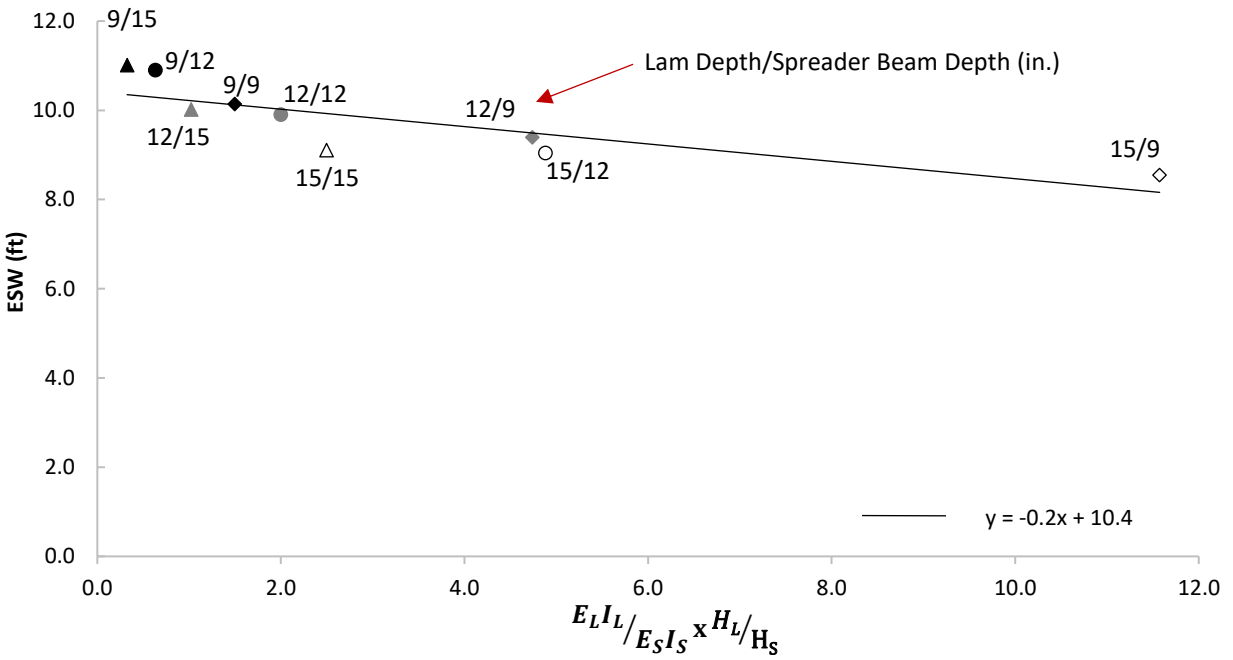


Figure 6-3 ESW with respect to $E_L I_L / E_S I_S \times H_L / H_S$

The relationship between the ESW (E_1) and $E_L I_L / E_S I_S \times H_L / H_S$ is established utilizing Eq. 11.

$$E_1(ft) = \left[-0.2 \times \left(\frac{E_L I_L}{E_S I_S} \times \frac{H_L}{H_S} \right) + 10.4 \right] > 6ft \quad \text{Eq. 11}$$

where, $E_L I_L$ is the rigidity of laminate per 3 in. of deck width, $E_S I_S$ is the rigidity of spreader beam (if multiple, use the spreader beam closest to midspan), H_L is the depth of laminate and H_S is the depth of spreader beam.

In the case where no spreader beam is present, the term $-0.2 \times E_L I_L / E_S I_S \times H_L / H_S$ becomes an infinitely negative number. Based on the field test and the FE model results, the calculated ESW does not need to be less than 6 ft. Note this equation is developed for the typical Wisconsin timber slab bridge configuration with a thru-bolt spacing connecting the spreader beam and deck of about 3.5 ft. Based on the parametric study results, increasing the number of connectors between the deck and spreader beam will slightly increase the ESW.

6.2.2 Spreader Beam Material

In addition, another type of spreader beam was also evaluated using FE models. Model 16-1 and Model 16-2 in Table 6-1 were developed based on Model 1 with the spreader beam replaced by a W-shape steel beam W6x25 and W8x21, respectively. These two beams were selected for evaluation since their rigidities are close to 12 in. x 6 in. and 15 in. x 6 in. timber spreader beam. Comparing the ESW from Model 15-5 and Model 15-6 to Model 16-1 and Model 16-2, the results indicated that the ESW is rather unaffected by the spreader beam material and the bridge model performs nearly equally with spreader beams of equivalent rigidity.

6.2.3 Transverse Spreader Deck

Both analytical and field test results indicated that the use of a 4 in. deep transverse spreader deck increases the load distribution and wheel load distribution width by about 16%. The parametric study results indicate that a further increase of the transverse deck panel depth from 4 in. to 6 in. does provide a benefit, but not to the extent of the benefit seen going from no spreader deck to 2 or 4 in. There are diminishing returns with incrementally deeper spreader deck panels. It should be noted the material properties of the spreader deck panels were assumed to be similar to those of the timber slab.

To account for the influence of a transverse spreader deck, Eq. 11 is factored by α_T resulting in Eq. 12.

$$E_{m1}(ft) = \alpha_T \times E_1 \quad \text{Eq. 12}$$

where α_T accounts for the presence of a transverse spreader deck. Table 6-2 shows the values of α_T based on the spreader deck depth.

Table 6-2 Value of α_T

Spreader deck thickness (in.)	α_T
0	1
4	1.16
6	1.22

6.2.4 Multiple Lanes Loaded

Further analytical study investigated the potential change in the ESW due to multiple lanes loaded. It was found that the ESW generally decreased by 10% with two vehicles simultaneously on the bridge in the load case 1 and load case 5 transverse positions (see Figure 4-14). Accordingly, an additional modifier of Eq. 11 was introduced for when a load rating engineer would anticipate the load positions of the crossing vehicles to be near to the deck edge and guard rail (≤ 2 ft). Despite evidence of decreased ESW when vehicles are positioned at the outermost transverse positions, it is more common and likely for vehicles to cross at a position nearer the centerline. For this case, a change of the equation is not required and thus the modifier is equal to 1.0.

$$E_{m2}(ft) = \alpha_l \times E_1 \quad \text{Eq. 13}$$

where

$\alpha_l = 1.0$ when the number of vehicles is equal to 1 or the number of vehicles is greater than 1 and the transverse position of each vehicle is such that the outermost wheel line is greater than 2 ft from the guardrail/curb

$\alpha_l = 0.9$ when the number of vehicles is greater than 1 and the transverse position of each vehicle is such that the outermost wheel line is within 2 ft of the guardrail/curb

6.3 Validation of Proposed Equation

In order to evaluate the value of the proposed equation (Eq. 11, with modifiers Eq. 12 and Eq. 13), the results from the field tests and parametric study were used to compare with the calculated values from Eq. 11 with applicable modifiers as shown in Figure 6-4 and Figure 6-5.

The field results in Figure 6-4 were presented as a range inclusive of the ESW calculated at the point of maximum strain for each load case (see Table 5-2). The predicted ESW values are close to the lower bound of field test results, which indicates that the prediction equation provides a conservative estimation of the wheel load distribution. Conservatism would be reduced by any modification (> 0.80) to the factor of safety.

The parametric study results in Figure 6-5 were presented as a range with the maximum and minimum values for each bridge reflecting the results from Table 5-4. The results from Figure 6-5 show that the prediction values are lower than all the parametric study results and the prediction equation provides a conservative estimation.

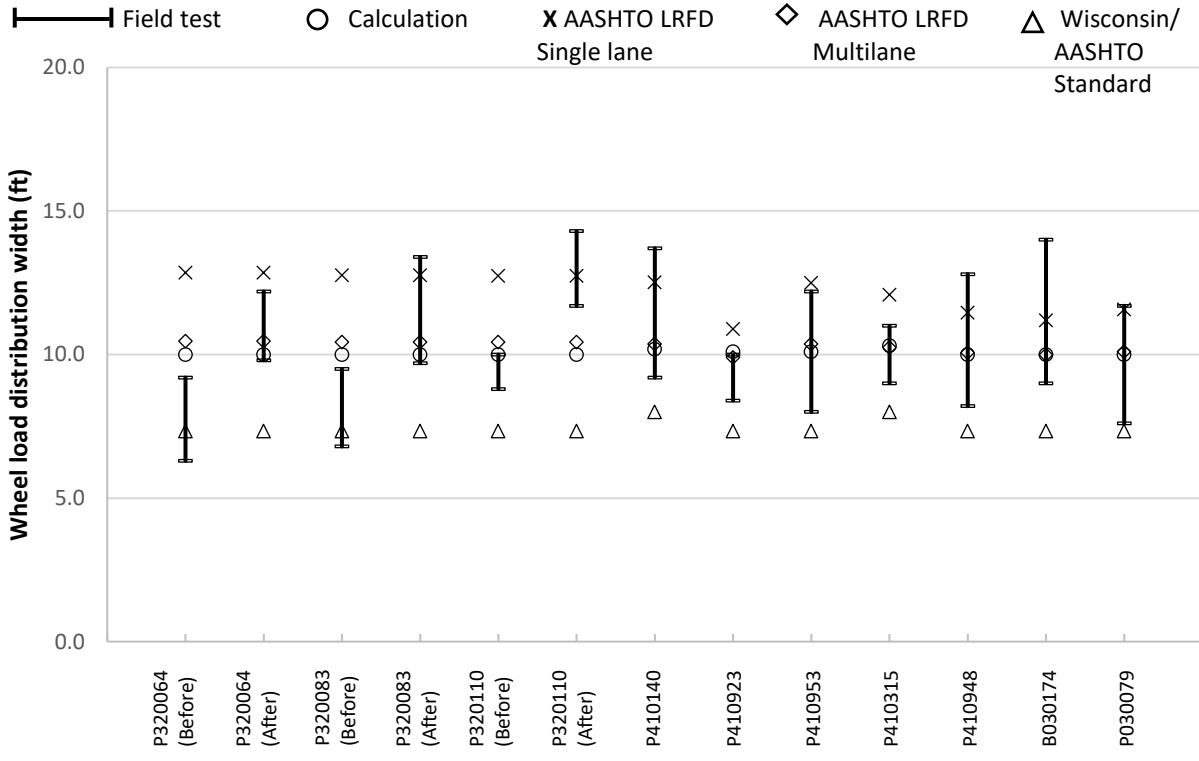


Figure 6-4 Validation of equation by field test data

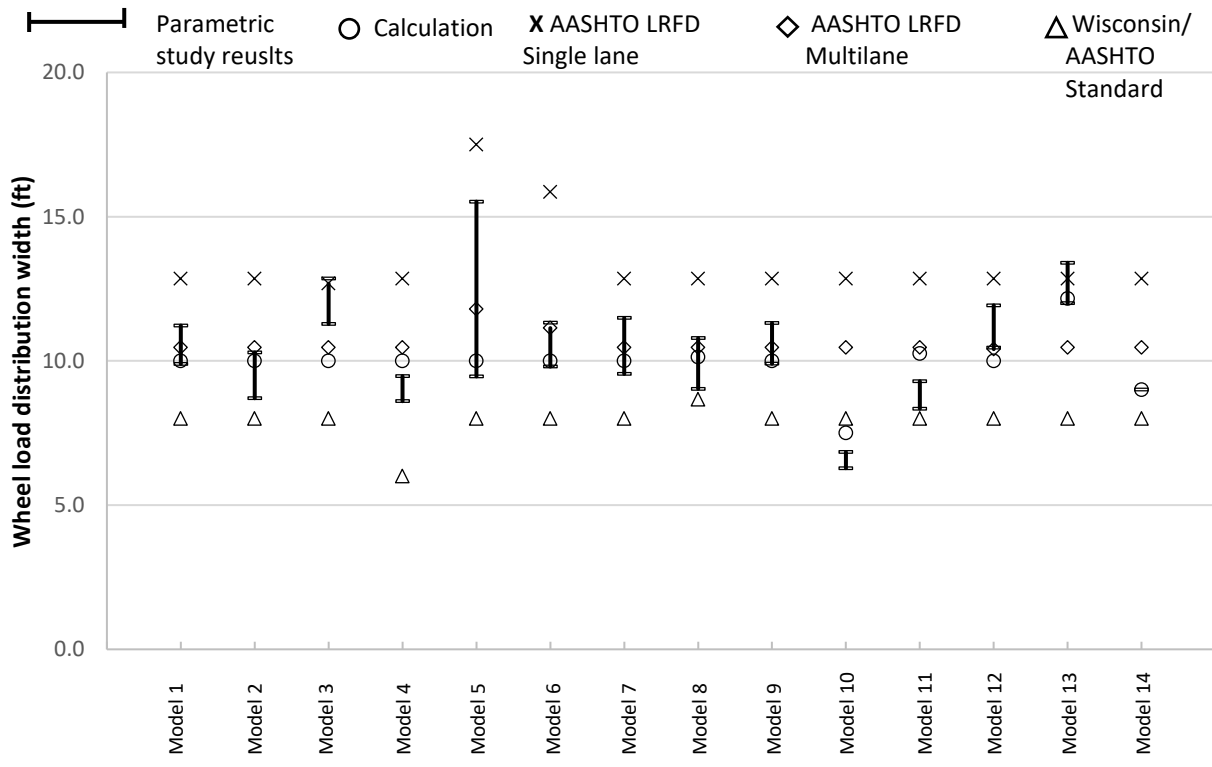


Figure 6-5 Validation of equation by parametric study results

6.4 Recommendations

As a result of the completed field testing and analysis of wheel load distribution width and viable retrofit techniques, it is recommended the WisDOT Bridge Manual Chapters 45 be revised according to the recommendations and guidelines in this section.

6.4.1 Summary

- The ESW can be calculated utilizing Eq.11 and applicable modifiers for a vehicle with standard gauge spacing (6 ft gauge spacing with 20 in. tire width).
- The transverse load distribution is affected by the longitudinal and transverse stiffness of the bridge deck. Solely increasing the longitudinal stiffness decreases the ESW, while solely increasing the transverse stiffness (e.g., increased spreader beam size, use of spreader deck) increases the ESW. Therefore, the selection of bridge retrofit/enhancement methods should be considered with the goal of decreasing the ratio of longitudinal stiffness to transverse stiffness.
- A spreader beam, or lack thereof, at mid-span is a key contributor to the ESW. Cross-section reduction or removal of the spreader beam will reduce the transverse stiffness, resulting in a significant reduction of ESW. Conversely, spreader beams with greater stiffness increases the ESW. The use of the spreader beam at the quarter span does not provide a significant effect on the wheel load distribution, especially at locations of maximum load effect.
- The use of a 4 in. thick transverse deck increases the load distribution and wheel load distribution width by about 16%. However, further increases of spreader deck depth provides benefit with diminishing returns.

6.4.2 Limitations

- The transverse load distribution on a timber slab bridge varies with gauge spacing. The developed ESW equation does not account for non-standard vehicles. Hence, non-standard vehicle configurations should be evaluated differently for purposes of load rating.

7 LOAD TESTING PROCESS

7.1.1 Introduction

The development of recommendations within this study is predicated upon the extensive amount of strain data collected via a data acquisition system. It was proposed to use deflection data to similarly define the transverse load distribution, knowing deflection data can be more easily acquired with non-specialized tools. Accordingly, deflection data were collected during the field tests in two ways: 1) Linear variable deflection transducers (LVDTs) and 2) Surveying total station, shown in Figure 7-1 and Figure 7-2, respectively. The intent was to compare the data to see if the deflection measurements from the LVDTs could be replicated by the surveying total station. Using a total station would allow a simpler method of determining the transverse load distribution by defining the deformed shape in the transverse direction. Also, this method could likely be completed with local labor forces. This exercise showed some promise of working well but did not provide the accuracy or consistency the authors believe would be necessary to accurately define the transverse load distribution. It is also noteworthy that the field test results and subsequent finite element models provided a lot of clarity regarding the actual structural behavior of longitudinal timber slabs. The equations developed within this research better define the behavior of longitudinal timber slab bridges and can be used with confidence. It is recommended for bridges whose structural behavior is believed to be different than the bridges evaluated in this study that a load test be completed in the same way as was completed during this research. The following sections outline the process by which the data necessary to assess the structural behavior can be collected.

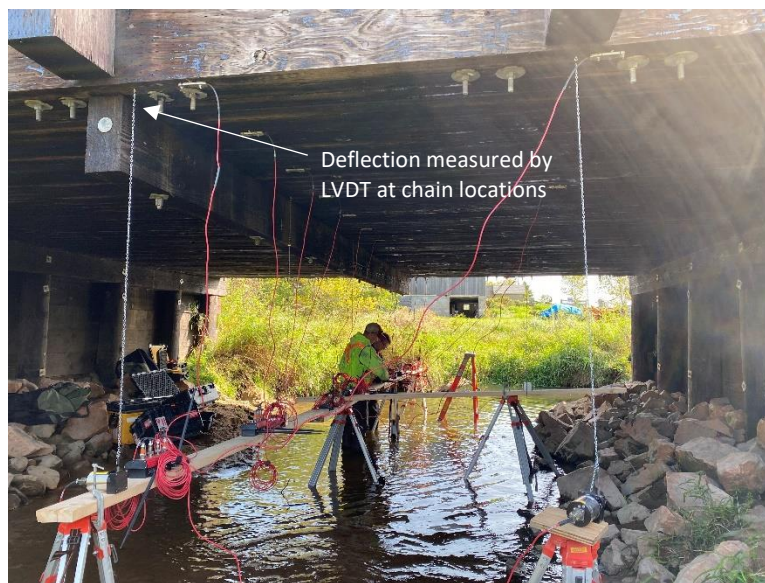


Figure 7-1 Deflection data collected via LVDTs



Figure 7-2 Deflection data collected via total station

7.1.2 Load Testing Procedure

Based on the load testing of the candidate bridges for this work, along with the analytical analysis and recommendations that follow, a step-by-step process for conducting load testing on similar longitudinal laminated timber slab bridges is described below.

7.1.2.1 General Load Testing Preparation/Considerations

- 1) Prior to the day of testing, determine how strain gages and data acquisition equipment can best be installed under the bridge (e.g., ladders, snoopers).
- 2) Prior to the day of testing, identify traffic control needs
- 3) Prior to the day of testing, arrange for a load vehicle (e.g., loaded dump truck) and for the load vehicle to be weighed (gross, front axle, rear tandem axles)
- 4) Review plan set and/or previous inspection records for unique features or condition abnormalities
- 5) The day of testing, ensure worker safety by using traffic control and/or traffic signs as necessary dependent on the bridge location and anticipated traffic volumes

7.1.2.2 Instrumentation Selection/Placement

- 1) Layout and mark strain gage locations. Place strain gages longitudinally at 2 ft on center located a distance equal to the spreader beam depth away from the spreader beam face. Strain gages used on timber most typically will require screws to fasten the gage to the bottom of the deck
- 2) Connect strain gages to data acquisition equipment
- 3) Note strain gage numbers and locations on bridge plan
- 4) Ensure strain gages and data acquisition equipment is operational and ready for data collection

7.1.2.3 Load Weight Considerations

- 1) Provide a load vehicle with a weight of greatest legal magnitude to induce well-defined structural behavior. A fully-loaded standard, 3-axle dump truck typically weighs between 50,000 and 55,000 lbs.

7.1.2.4 Load Test Preparation

- 1) Mark load paths on the bridge deck using spray paint or other marking means.
- 2) Mark longitudinal distance at 10 ft spacing on the bridge deck to define the vehicle location in the data. Begin marks 10 ft before the bridge entrance and continue marks a minimum of 20 ft beyond the bridge exit to ensure a sufficient amount of data is collected prior to the load vehicle entering and after the load vehicle exits the bridge.

7.1.2.5 Load Placement Considerations

Strain data should be acquired during multiple transverse placements of the load vehicle. The recommended load cases are as follows:

- 1) Center the passenger-side, front axle tire 2 ft from bridge curbline.
- 2) Center driver's side, front axle tire 2 ft from bridge centerline on same side of centerline as previous load case.
- 3) Center the load vehicle on the centerline of bridge.
- 4) Center the passenger side, front axle tire 2 ft from bridge centerline on opposite side of centerline as load cases 1 and 2.
- 5) Center the driver's side, front axle tire 2 ft from bridge curbline.

7.1.2.6 Conducting Load Test

- 1) Ensure the load vehicle operator crosses the bridge on the designated load path at a consistent walking-pace speed (<5 mph) and does not impose unnecessary dynamic loading by braking while on the bridge. The test is pseudo-static in nature and continuously collects data at every longitudinal position.
It is beneficial to place someone within view of the load vehicle operator to direct the operator left or right as necessary to stay on the designated load path.
- 2) Initiate data collection via the data acquisition system prior to the truck being on the bridge. As the vehicle crosses the bridge, mark the data as the front axle crosses the distance marks (every 10 ft). Stop data collection once the vehicle is entirely off the bridge and has passed the last distance mark. Ensure data collection is complete prior to allowing the vehicle to back across the bridge.
- 3) Collect strain data at each load path a minimum of two times to ensure repeatability of the data. Position the load vehicle on the next designated load path and repeat the process until each load path has been completed.

7.1.2.7 Data Reduction and Analysis

- 1) Upon completion of the load test, reduce the strain data to only the data acquired while the load vehicle was on the bridge
- 2) Ensure the data is "zeroed" by subtracting the initial strain reading from the individual strain gage data set
- 3) Multiply each strain data value by the tributary width of the respective strain gage (e.g., strain x 2 ft or strain x 1ft for edge-of-deck gages).
- 4) Calculate the equivalent strip width by summing the multiplied strain values for all points in time and divide by the maximum strain value for that same point in time. An equivalent strip width can be calculated for each point in time. See Equation 9.

$$E (\text{Equivalent strip width}) = \frac{\sum_{i=1}^n (\text{strain}_i \times d_i)}{\text{strain}_{\max}}$$

- 5) Repeat for the data sets from each load path.

7.1.2.8 Interpretation of Load Test Results and Load Rating Considerations

- 1) Plot the equivalent strip width data set versus the truck position for each load path on a combined plot. A visible band will become apparent with respect to the low and high values of equivalent strip width. See Figure 4-23 . The values can be compared to the equivalent strip width values calculated in Equation 11 with applicable modifiers in Equations 12 and 13. Engineering judgment should be applied when comparing the field test data to the equivalent strip width equation in order to determine the best equivalent strip width to use for the individual bridge.
- 2) Once the strip width is determined and used in the load rating process, the remaining steps that are typical to the load rating process per the Wisconsin Bridge Manual are continued without modification.

8 SUMMARY

The Wisconsin Department of Transportation recognizes the importance of accurately assessing the timber deck slab bridge inventory within the state. Of the 571 timber bridges in Wisconsin, 450 bridges are timber slab bridges. Current methods of load rating employ equations first developed in the later 1980s and early 1990s for determining the equivalent strip width. These equations often produce results that unnecessarily penalize the bridge by requiring a posted weight limit.

Through a program of bridge live load tests and analytical modeling, the researchers in this study have both measured and modeled the bridge behavior with more accuracy and have shown the current equivalent strip width calculation methodologies to be conservative, as was originally speculated. Ten unique bridges were tested a part of this study. Three of them were tested twice; once before and once after bridge strengthening measures were employed. An equation to calculate the equivalent strip width was developed with numerous variables in mind.

The equivalent strip width is shown to be a function of the ratio of longitudinal and transverse stiffness of the timber slab deck. Accordingly, where bridge strengthening or rehabilitation methods are being considered, it is to the benefit of the structural capacity to be mindful of this relationship. Ways to increase the transverse stiffness are provided within this report.

Load testing has proven to be extremely beneficial in developing the models and recommendations. The resulting equation for calculating the equivalent strip width is considered to be a good representation of actual structural behavior.

An initial objective of the project was to develop a process to easily load test and proof rate legal load capacity timber slab bridges by using deflection data obtained using a survey total station. The researchers determined the accuracy and variability of the data obtained by this method were not to the level that would accurately depict the true live load behavior of the timber slab bridge subjected to live loads. For this reason, the method is not fully described in this report. Nonetheless, the steps required to complete additional live load testing as the research team did are provided so other bridges can be tested in the future if deemed necessary.

9 REFERENCES

- Aira, J. R., Arriaga, F., Íñiguez-González, G., & Crespo, J. (2014). Static and kinetic friction coefficients of Scots pine (*Pinus sylvestris* L.), parallel and perpendicular to grain direction. *Materiales de Construcción*, 64(315), e030-e030.
- AASHTO. 1996. AASHTO Standard Specification for Highway Bridges, 16th Edition. Washington, DC: AASHTO.
- AASHTO. 2002. AASHTO Standard Specification for Highway Bridges, 17th Edition. Washington, DC: AASHTO.
- AASHTO. 2004. AASHTO LRFD bridge design specifications. Washington, DC: AASHTO.
- AASHTO. 2010. AASHTO LRFD bridge design specifications. Washington, DC: AASHTO.
- AASHTO. 2018. AASHTO LRFD bridge design specifications. Washington, DC: AASHTO.
- AASHTO. 2020. AASHTO LRFD bridge design specifications. Washington, DC: AASHTO.
- Brashaw, B., Wacker, J., Hosteng, T., Dahlberg, J. “Development and Integration of Advanced Timber Bridge Inspection Techniques for NBIS”, Minnesota Department of Transportation, Final Report, Research Project MN/RC 2015-01, 2015.
- Ekholm, K., Kliger, R., & Crocetti, R. (2011). Full-scale ultimate-load test of a stress-laminated-timber bridge deck. *Journal of Bridge Engineering*, 17(4), 691-699.
- Fanous, F., J. May and T. Wipf, “Development of Live Load Distribution Factors for Glued-Laminated Timber Girder Bridges”, *American Society of Civil Engineers (ASCE) Journal of Bridge Engineering*, March/April 2011, Volume 16, Number 2, ISSN1084-0702, p. 179-187.
- Fanous, F., May J., Wipf, T. and Ritter, M., “Live Load Distribution on Longitudinal Glued-Laminated Deck Bridges”, Final Report: Conclusions and Recommendations, General Technical Report FPL-GTR-194, USDA Forest Service, Forest Products Laboratory, 14 pp., July 2010
- Funke, R.W. 1986. Behavior of longitudinal glued-laminated timber deck bridges. Ames, IA: Iowa State University. M.S. thesis.
- Hosteng, T.K., D.L. Wood, B.M. Phares and T.J. Wipf, “Test and Evaluation Report”, Iowa Department of Transportation, Office of Bridges and Structures, Embargo Bridge Test Series, 2009 (count as 1 report):
- 5-Span Concrete Slab Ramp Bridge off Hwy 20 Near Wellsburg, IA, July 2009, 12 pp
 - IA-92 Bridge West of Massena, IA, Aug 2009, 7 pp
 - IA-31 Bridge West of Quimby, IA, Aug 2009, 10 pp
 - IA-18 Bridge East of Hartley, IA, Sept 2009, 10 pp
 - IA-183 Bridge North of Pisgah, IA, Sept 2009, 8 pp
 - IA-136 Bridge in Dubuque County, IA, Sept 2009, 12 pp
 - IA-5 Bridge in Appanoose County, IA, Oct 2009, 11 pp

- IA-57 Bridge in Butler County, IA, Oct 2009, 11 pp
- Hosteng, T., B. M. Phares, T. J. Wipf and D. L. Wood, "Laboratory Evaluation of Design Details for Minimizing Differential Panel Deflection on Glued-Laminated Timber Girder Bridges", Final Report, Project No: 04-JV-11111105-076 U. S. Forest Service, Forest Products Laboratory, 32 pp., 2005
- Iowa, DOT "Bridge design manual." Office of Bridges and Structures, Ames, IA (2000).
- Kurian, A.V. 2001. Finite-element analysis of longitudinal glued-laminated timber deck and glued-laminated timber girder bridges. Ames, IA: Iowa State University. M.S. thesis.
- Michigan Manual, Bridge Design. Michigan Department of Transportation, Lansing, 2020.
- Indiana, DOT. "Bridge design manual." Office of Bridges and Structures, Ames, IA (2020).
- Oregon, DOT. "Bridge Design and Drafting Manual." (2020)
- New York Manual, Bridge Design. "New York State Department of Transportation." (2020).
- Delaware Manual, DelDOT Bridge Design. "State of Delaware Department of Transportation. (2020)
- New Jersey Manual, Bridge Design. "New York State Department of Transportation." (2020).
- Wisconsin Manual, Bridge Design. "New York State Department of Transportation." (2020).
- Minnesota, DOT "LRFD Bridge Design Manual." (2020).
- Oliva, M. G., Dimakis, A. G., Ritter, M. A., and Tuomi, R. L. (1990). "Stress-laminated wood bridge decks: Experimental and analytical evaluations." Research Paper FPL-RP-495, U.S. Dept. of Agriculture, Forest Service, Forest Products Laboratory, Madison, WI.
- Phares, B.M., C. T. Kilaru, L.F. Greimann, J. Seo, and K. Freeseaman, "Study of the Impacts of Implements of Husbandry on Bridges Volume I: Live Load Distribution Factors and Dynamic Load Allowances", Iowa Highway Research Board, IHRB Project TR-613 and TPF-5(232), August 2017.
- Phares, B. and Hosteng, T., "Demonstration of Load Rating Capabilities through Physical Load Testing: Ida County Bridge Case Study, Final Report, 25 pp., August 2013.
- Ritter, M.A. "Timber Bridges: Design, Construction, Inspection and Maintenance". EM 7700-8 USDA Forest Service, 1990.
- Sanders, W. W., Jr., Klaiber, F. W., and Wipf, T. J., "Load Distribution in Glued Laminated Longitudinal Timber Deck Highway Bridges", Contract Report, American Institute of Timber Construction, ERI-85441, Project 1716, April 1985.
- Sarisley, J. E. F. and Accorsi, M. L. (1990). "Prestress Level in Stress-Laminated Timber Bridges." Journal of Structural Engineering 116 (11): 3003-3019.

- Wipf, T. J., Funke, R. W., Klaiber, F. W., and Sanders, W. W., Jr., "Experimental and Analytical Load Distribution Behavior of Glued Laminated Timber Deck Bridges", Proceedings of the 2nd International Conference on Short and Medium Span Bridges, Vol. 2, pp. 63-78, Aug. 1986.
- Wipf, Terry J., F. Wayne Klaiber, and Wallace W. Sanders Jr. Load distribution criteria for glued-laminated longitudinal timber deck highway bridges. No. 1053. 1986.
- Wipf, T. J., Klaiber, F. W., & Funke, R. W. (1990). Longitudinal glued laminated timber bridge modeling. *Journal of Structural Engineering*, 116(4), 1121-1134.
- Zokaie, T.; Osterkamp, T.A.; Imbsen, R.A. 1991. Distribution of Wheel Loads on Highway Bridges. Washington, DC.: NCHRP Research Results Digest 187. TRB, National Research Council.
- May, Jeremy James. "Live load distribution factors for glued-laminated timber bridges." (2008). Master thesis, Iowa State University.

10 APPENDIX

10.1 Appendix A: Bridge Information

10.1.1 Appendix A.1 B030174 BARRON COUNTY



Figure A. 1 Bridge photos for B030174

10.1.2 Appendix A.2 P030079 BARRON COUNTY



Figure A. 2 Bridge photos for P320079

10.1.3 Appendix A.3 P320064 LA CROSSE COUNTY



Figure A. 3 Bridge photos for P320064

10.1.4 Appendix A.4 P320083 LA CROSSE COUNTY



Figure A. 4 Bridge photos for P320083

10.1.5 Appendix A.5 P320110 LA CROSSE COUNTY



Figure A. 5 Bridge photos for P320110

10.1.6 Appendix A.6 P410140 MONROE COUNTY



Figure A. 6 Bridge photos for P410140

10.1.7 Appendix A.7 P410923 MONROE COUNTY



Figure A. 7 Bridge photos for P410923

10.1.8 Appendix A.8 P410953 MONROE COUNTY



Figure A. 8 Bridge photos for P410953

10.1.9 Appendix A.9 B410315 MONROE COUNTY



Figure A. 9 Bridge photos for B410315

10.1.10 Appendix A.10 P410948 MONROE COUNTY

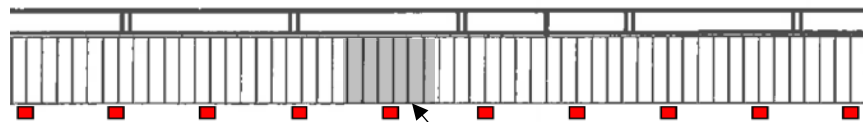


Figure A. 10 Bridge photos for P410948

10.2 Appendix B: ESW Calculation Example

The equivalent strip width (ESW) can be calculated for any unique data record; that is, at any point in time while the data is being collected. (e.g., time = 20.05 sec). Using the output from each strain gage and the known attributable width the ESW is quickly determined.

The data below shows a hypothetical example of an ESW calculation using 10 equally spaced gages at 2 ft and the outermost gages at the deck edge.



	Strain Gage 1	Strain Gage 2	Strain Gage 3	Strain Gage 4	Strain Gage 5	Strain Gage 6	Strain Gage 7	Strain Gage 8	Strain Gage 9	Strain Gage 10
Attributable Width (ft)	1	2	2	2	2	2	2	2	2	1
	x	x	x	x	x	x	x	x	x	x
Strain Data Record	5	30	70	120	150	135	105	75	50	40
	=	=	=	=	=	=	=	=	=	=
Width x Strain	5	60	140	240	300	270	210	150	100	40

Max Strain

Sum Values = 1515

$$\begin{aligned} \text{ESW} &= \text{Sum Values} / \text{Max Strain} \\ \text{ESW} &= 1515 / 150 \\ \text{ESW} &= 10.1 \text{ ft} \end{aligned}$$